



**NEAR EAST UNIVERSITY  
INSTITUTE OF GRADUATE STUDIES  
DEPARTMENT OF CIVIL ENGINEERING**

**SEISMIC PERFORMANCE RISK ANALYSIS OF MOMENT RESISTING  
RC FRAME STRUCTURE**

**MSc.THESIS**

**Hama Issa MOCTAR**

**Nicosia  
June, 2023**

**HAMA ISSA MOCTAR**

**SEISMIC PERFORMANCE RISK ANALYSIS OF MOMENT  
RESISTING RC FRAME STRUCTURE**

**NEU  
2023**

**NEAR EAST UNIVERSITY  
INSTITUTE OF GRADUATE STUDIES  
DEPARTMENT OF CIVIL ENGINEERING**

**SEISMIC PERFORMANCE RISK ANALYSIS OF MOMENT RESISTING  
RC FRAME STRUCTURE**

**M.Sc. THESIS**

**Hama Issa MOCTAR**

**Supervisor**

**Prof. Kabir SADEGHI**

**Co-Supervisor**

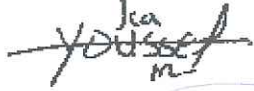


**Dr. Mahdi Azizi**

**Nicosia**

**June, 2023**


## Approval

We certify that we have read the thesis submitted by **Hama Issa Moctar** titled **“SEISMIC PERFORMANCE RISK ANALYSIS OF MOMENT RESISTING RC FRAME STRUCTURE”** and that in our combined opinion it is fully adequate, in scope and in quality, as a thesis for the degree of Master of Educational Sciences.

Examining Committee	Name-Surname	Signature
Head of the Committee:	Assoc. Prof. Dr Youssef Kassem	
Committee Member:	Assoc. Prof. Fatemeh Nouban	
Supervisor:	Prof. Dr. Kabir Sadeghi	
Co-Supervisor:	Dr. Mahdi Azizi	

Approved by the Head of the Department

24/07/2023

  
Prof. Dr. Kabir Sadeghi  
Head of Civil Engineering Department.

Approved by the Institute of Graduate Studies

  
Prof. Dr. Kemal Hüsnü Can Başer

Head of the Institute of Graduate Studies.

**Declaration**

I hereby declare that all information, documents, analysis and results in this thesis have been collected and presented according to the academic rules and ethical guidelines of the institute of graduate studies, Near East University. I also declare that as required by these rules and conduct, I have fully cited and referenced information and data that are not original to this study.

**Hama Issa Moctar**

.../.../2023

### **Acknowledgments**

I want to express my sincere gratitude to both my co-supervisor, Dr. MAHDI AZIZI, and my supervisor, PROF. KABIR SADEGHI. This thesis has benefited much from your knowledge, persistence, and persistent commitment. Your sage advice, helpful criticism, and unceasing support have helped me realize my full potential. I genuinely appreciate the endless hours you spent editing and revising my work, as well as the stimulating conversations that have extended my perspective on academic subjects.

I want to thank all the professors and lecturers at Near East University, especially Assoc. Dr. Rifat Reşatoğlu for sharing their knowledge and providing genuine and helpful support during the course.

I would want to convey my sincere gratitude to my parents for their constant support and inspiration in helping me successfully complete my master's degree, both via their direct involvement and their indirect contributions.

Furthermore,

I want to extend my appreciation to my siblings, as well as my mates with whom we have been supporting each other in order to fulfil our purpose.

**Abstract****SEISMIC PERFORMANCE RISK ANALYSIS OF MOMENT RESISTING  
RC FRAME STRUCTURE.****Hama Issa MOCTAR****Prof. Kabir SADEGHI****Dr. Mahdi AZIZI****MSc., Civil Engineering Department****June 2023, 125 Pages**

One of the most important assets that any structural engineer must be able to guarantee in any circumstance is the safety of the buildings. The greatest significance of aseismic structures has been demonstrated throughout history while dealing with the risk of earthquakes. Researchers are constantly searching for the best and most effective method of evaluating pre- or post-earthquake structures to forecast the structural behavior of buildings during seismic motion due to the casualties that seismic hazard events have caused. This theory of performance analysis shed light on a structure's responsiveness during an earthquake to prevent a sudden collapse. This study focused on the 3D analysis of 9-moment resisting reinforced concrete frames with different system configurations using incremental dynamic analysis to achieve a better and thorough understanding of the behavior of the structure under different ground motion scenarios. The Peak Ground Acceleration as Intensity Measure and Inter Storey Drift as Engineering Demand Parameter are used to address the fragility curve. Using SAP2000 software, three different framing systems have been analyzed with a variation of the span length according to the following regulations: ACI 318-08, ASCE 7-10, UBC 97 and FEMA 365 regulations. It is found that the yielding and collapse PGA vary with the framing system and the use of shear wall has a significant effect on the enhancement of the structure performance against lateral forces. The results shown also that the increase of the span length induce the structure to become more flexible.

**Keywords:** RC Structure, Incremental Dynamic Analysis (IDA), Federal Emergency Management Agency (FEMA), SAP2000, Fragility Curve.

## ÖZET

Herhangi bir yapı mühendisinin her koşulda garanti etmesi gereken en önemli varlıklardan biri binaların güvenliğidir. Sismik yapıların en büyük önemi, tarih boyunca deprem riskiyle uğraşırken gösterilmiştir. Araştırmacılar, sismik tehlike olaylarının neden olduğu kayıplar nedeniyle sismik hareket sırasında binaların yapısal davranışını tahmin etmek için deprem öncesi veya sonrası yapıları değerlendirmenin en iyi ve en etkili yöntemini sürekli olarak araştırıyorlar. Bu performans analizi teorisi, bir yapının bir deprem sırasında ani bir çökmeyi önlemek için tepki verebilirliğine ışık tutuyor. Bu çalışma, farklı yer hareketi senaryoları altında yapının davranışını daha iyi ve kapsamlı bir şekilde anlamak için artımlı dinamik analiz kullanarak farklı sistem konfigürasyonlarına sahip 9-moment dayanımlı betonarme çerçevelerin 3B analizine odaklanmıştır. Şiddet Ölçüsü olarak Tepe Yer İvmesi ve Mühendislik Talebi Parametresi olarak Katlar Arası Kayma, kırılma eğrisini ele almak için kullanılır. SAP2000 programı kullanılarak, ACI 318-08, ASCE 7-10, UBC 97 ve FEMA 365 yönetmeliklerine göre açıklık uzunluklarının değişimi ile üç farklı çerçeveleme sistemi analiz edilmiştir. Akma ve göçme PGA'nın çerçeve sistemine göre değiştiği ve perde duvar kullanımının yanıl kuvvetlere karşı yapı performansının artırılmasında önemli bir etkiye sahip olduğu bulunmuştur. Sonuçlar, açıklık uzunluğunun artmasının yapının daha esnek hale gelmesine neden olduğunu da göstermiştir.

Anahtar Kelimeler: RC Yapısı, Artımlı Dinamik Analiz (IDA), Federal Acil Durum Yönetim Ajansı (FEMA), SAP2000, Kırılma Eğrisi.

## Table of contents

Approval.....	I
Declaration .....	II
Acknowledgments.....	III
Abstract .....	IV
ÖZET.....	V
Table of contents .....	VI
List of figures .....	X
List of tables.....	XIV
List of abbreviations.....	XVI
CHAPTER I .....	1
Introduction .....	1
1.1 Problem statement.....	1
1.2 Goals of the research.....	3
1.3 Generic earthquake idea.....	4
1.4 Seismic Performance Analysis.....	4
1.5 Seismic performance analysis relevance.....	5
1.6 Seismic resistant structures .....	5
1.7 Organization and scope .....	6
CHAPTER II.....	7
Literature Review.....	7
2.1 Overview .....	7
2.2 Moment resisting frames (MRF).....	12
2.3 Moment resisting frame using shear wall (MRFSW) .....	13
2.4 Moment resisting frame with bracing (MRFB) .....	14
2.5 Seismic performance analysis and design code .....	15
2.5.1 Nonlinear static procedure .....	17
2.5.2 Generic of incremental dynamic analysis (IDA) .....	17
2.6 Regulations base on the federal emergency management agency (FEMA) ...	18
2.7 Friction dampers.....	20
CHAPTER III .....	22
Methodology .....	22



3.1	Overview .....	22
3.2	Analysis strategy .....	22
3.3	Location of the case study .....	23
3.3.1	Cyprus seismic activity .....	23
3.4	Peer records .....	25
3.5	Scale factor .....	29
3.6	Intensity measure (IM) .....	29
3.7	Damage measure (DM) .....	30
3.8	Inter-story drift ratio or ISDR .....	30
3.9	Damage state (DS) .....	31
3.10	Fragility curve .....	32
3.11	Frames configuration .....	34
3.11.1	<i>Material properties</i> .....	34
3.12	Applied loads .....	35
3.13	Dead load .....	35
3.14	Live load .....	35
3.15	Super dead load .....	35
3.16	Seismic lateral load .....	36
3.17	Gravity loads .....	36
3.17.1	<i>Plastic hinges</i> .....	36
3.18	Shear wall .....	37
3.19	Bracing .....	38
3.20	Slab design .....	38
3.21	Geometry of frames .....	39
3.21.1	<i>Reinforcement Details</i> .....	39
3.21.2	<i>Models description</i> .....	41
CHAPTER IV .....		46
Results and discussions .....		46
4.1	Introduction .....	46
4.2	Moment resisting frame .....	46
4.2.1	<i>Discussion of the results</i> .....	48
a)	<i>IDA Curve for all MRFs</i> .....	48
□	<i>Comparison among the MRFs models with respect to IDA curve results</i> .....	50

b) Fragility curve for all MRFs .....	51
□ <i>Comparison Among the MRFs models with respect to fragility curve results ...</i>	56
C) Inter-Story Drift Ratio of all the MRFs models .....	57
d) Fundamental time period effect of all the MRFs models .....	60
4.3 Moment resisting frame with bracing (MRFB) .....	61
4.3.1 Discussion of the results.....	62
a) IDA curve for all MRFB .....	62
□ <i>Comparison among the MRFB models with respect to IDA curve results .....</i>	64
b) Fragility curve for all MRFB.....	65
□ <i>Comparison among the MRFB models with respect to fragility curve results ...</i>	70
C) Inter-story drift ratio of all the MRFs models.....	71
d) Fundamental time period effect of all the MRFB models.....	74
4.4 Moment resisting frame with shear wall (MRFSW).....	75
4.4.1 Discussion of the results.....	76
a) IDA curve for all MRFSW .....	76
□ <i>Comparison among the MRFSW models with respect to IDA curve results .....</i>	78
b) Fragility curve for all MRFSW.....	79
□ <i>Comparison among the MRFSW models with respect to fragility curve results</i>	84
C) Inter-Story drift ratio of all the MRFSW models.....	84
d) Fundamental time period effect of all the MRFSW models.....	88
4.5 Comparison among all the 3 different framing systems .....	88
4.5.1 Comparison based on the fragility curve with respect to the CP limit state ....	88
4.5.2 Comparison based on the fundamental time period of all the models .....	89
CHAPTER V.....	91
Discussion .....	91
5.1 Overview .....	91
CHAPTER VI .....	92
Conclusion and recommendations .....	93
6.1 Conclusion .....	93
6.2 Recommendations .....	95
Références .....	95
APPENDICES .....	99
Appendix A.....	99

Input tables for fragility curve of remaining moment resisting frames .....	100
Appendix B .....	109
Roof displacement of the remaining frames .....	109
Appendix C .....	122
Uniform and concentrated loads from UBC-1997 code .....	122
Appendix D .....	123
Similarity check report .....	123
Appendix E .....	124
Ethical approval letter .....	124

## List of figures

Figure 1 .....	13
Moment resisting frame .....	13
Figure 2 .....	14
Moment resisting frame using shear wall .....	14
Figure 3 .....	15
Type of bracing used in moment resisting frames .....	15
Figure 4 .....	18
Seismic analysis methods.....	18
Figure 5 .....	23
Study process .....	23
Figure 6 .....	24
a) Seismicity of Cyprus, b) Earthquake map of Cyprus.....	24
Figure 7 .....	27
a): Spectra axe loglog, b): Spectra axe semilog X, c): Spectra axe linear .....	27
Figure 8 .....	28
Selected earthquake ground acceleration: a): Humbolt Bay, b): Northwest Calif- 01, c): Northwest Calif-02, d): Tabas_ Iran, e): Borah Peak_ ID-01, f): Taiwan SMART1 (45), g): San -Fernando .....	28
Figure 9 .....	30
Drift measurement.....	30
Different damage states.....	31
Figure 11 .....	33
Fragility curve process .....	33
Figure 12 .....	37
Plastic hinge chart according to FEMA .....	37
Figure 13 .....	38
Shear wall layer definition in SAP2000.....	38
Figure 14 .....	41
Number of spans .....	41
Figure 15 .....	42
Typical story height.....	42

Span length of the frames; a) 5m, b) 6m, c) 7m.....	42
Figure 17 .....	43
MRF model with 10-story different views; a) Elevation; b) 3D.....	43
Figure 18 .....	44
MRFSW model with 10-story different views; a) Elevation; b) 3D.....	44
Figure 19 .....	44
MRFB model with 10-story views ; a) Elevation; b) 3D.....	44
Plan view .....	45
Figure 21 .....	49
a) IDA Curve for moment resisting frame with 5m span length.....	49
b) IDA Curve for moment resisting frame with 6m span length .....	49
	49
c) IDA Curve for moment resisting frame with 7m span length.....	50
Figure 22 .....	51
Different limit state values according to: a) GM3 with MRFs, b) GM4 with .....	51
MRFs.....	51
Figure 23 .....	55
a) Fragility curve for MRFs with 5m span length.....	55
b) Fragility curve for MRFs with 6m span length.....	55
c) Fragility curve for MRFs with 7m span length.....	56
Figure 24 .....	56
Probability of exceeding the CP limit state graph for all the MRFs models .....	56
Figure 25 .....	57
Roof displacement for MRFs with 5m span length: a) GM2, b) GM3, c) GM4 .....	57
Figure 26 .....	58
Roof displacement for MRFs with 6m span length: a) GM2, b) GM3, c) GM4 .....	58
Figure 27 .....	59
Roof displacement for MRFs with 7m span length: a) GM2, b) GM3, c) GM4 .....	59
Figure 28 .....	60
The fundamental time period of all the MRFs models .....	60
Figure 29 .....	63
a) IDA curve for moment resisting frame with bracing with 5m span length .....	63
b) IDA curve for moment resisting frame with bracing with 6m span length .....	63

.....	64
c) IDA curve for moment resisting frame with bracing with 7m span length .....	64
Figure 30 .....	65
Different limit state values according to: a) GM3 with MRFB, b) GM5 with MRFB	
.....	65
Figure 31 .....	69
a) Fragility curve for MRFB with 5m span length.....	69
b) Fragility curve for MRFB with 6m span length .....	69
c) Fragility curve for MRFB with 7m span length.....	70
Figure 32 .....	70
Probability of exceeding the CP limit state graph for all the MRFB models .....	70
Figure 33 .....	71
Roof displacement for MRFB with 5m span Length: a) GM2, b) GM3, c) GM4.....	71
Figure 34 .....	72
Roof displacement for MRFB with 6m span length: a) GM2, b) GM3, c) GM4 .....	72
Figure 35 .....	73
Roof displacement for MRFB with 7m span length: a) GM2, b) GM3, c) GM4 .....	73
Figure 36 .....	74
The fundamental time period of all the MRFB models .....	74
Figure 37 .....	77
a) IDA curve for moment resisting frame with shear wall with 5m span length.....	77
b) IDA Curve for moment resisting frame with shear wall with 6m span length.....	77
c) IDA curve for moment resisting frame with shear wall with 7m span length.....	78
Figure 38 .....	79
Different limit state values according to: a) GM3 with MRFSW b) GM5 with	
MRFSW .....	79
Figure 38 .....	82
a) Fragility curve for MRFSW with 5m span length .....	82
b) Fragility curve for MRFSW with 6m span length .....	83
c) Fragility curve for MRFSW with 7m span length .....	83
Figure 39 .....	84
Probability of exceeding the CP limit state graph for all the MRFSW models.....	84
Figure 40 .....	85

Roof displacement for MRFSW with 5m span length: a) GM2, b) GM3, c) GM4... 85	
Figure 41 .....	86
Roof displacement for MRFSW with 6m span length: a) GM2, b) GM3, c) GM4... 86	
Figure 42 .....	87
Roof displacement for MRFSW with 7m span length: a) GM2, b) GM3, c) GM4... 87	
Figure 43 .....	88
The fundamental time period of all the MRFSW models .....	88
Figure 41 .....	89
All models CP limit state percentages .....	89
Figure 42 .....	90
All Models fundamental time period values .....	90

### List of tables

CP: Collapse Prevention .....	XVI
Design code used in the USA.....	16
Table 2.....	25
The largest past 5 years earthquakes in Cyprus .....	25
Table 3.....	26
Properties of the GM used for this investigation .....	26
Table 4.....	32
Different Limit state.....	32
Table 5.....	34
Material Properties .....	34
Table 6.....	36
Wind loads assigned.....	36
Table 7.....	39
Details of the frame's configuration .....	39
Table 8.....	40
Reinforcement details of beams for 10-story models .....	40
Table 9.....	40
Reinforcement details of columns for 10-story models .....	40
Table 10.....	47
a) Inter-story drift ratio of the MRFs with 5m span length.....	47
b) Inter-story drift ratio of the MRFs with 6m span length .....	47
c) Inter-story drift ratio of the MRFs with 7m span length.....	47
Table 11.....	51
a) Fragility function data for the MRFs with 5m span length.....	51
b) Fragility function data for the MRFs with 6m span length.....	52
c) Fragility function data for the MRFs with 7m span length.....	53
Table 12.....	61
a) Inter-story drift ratio of the MRFB with 5m span length.....	61
b) Inter-story drift ratio of the MRFB with 6m span length .....	62
c) Inter-story drift ratio of the MRFB with 7m span length.....	62
Table 13.....	65



a) Fragility function data for the MRFB with a 5m span length.....	66
b) Fragility function data for the MRFB with a 6m span length.....	67
c) Fragility function data for the MRFB with a 7m span length.....	68
Table 14.....	75
a) Inter-story drift ratio of the MRFSW with 5m span length .....	75
b) Inter-story drift ratio of the MRFSW with 6m span length .....	75
c) Inter-story drift ratio of the MRFSW with 7m span length .....	76
Table 15.....	79
a) Fragility function data for the MRFSW with a 5m span length.....	79
b) Fragility function data for the MRFSW with a 6m span length .....	80
c) Fragility function data for the MRFSW with a 7m span length.....	81
Table 16.....	89
Percentage of the CP limit state of all the models .....	89
Table 16.....	90
The fundamental time period for all the analyzed models .....	90

**List of abbreviations**

FEMA: Federal Emergency Management Agency  
MRFs: Moment Resisting Frames  
MRFB: Moment Resisting Frame with Bracing  
MRFSW: Moment Resisting Frame with Shear Wall  
PEER: Pacific Earthquake Engineering Research Center  
Km: Kilometre  
m/s<sup>2</sup>: Meter per Second Square  
GM: Ground Motion  
g: Gravitational Acceleration  
SF: Scale Factor  
IM: Intensity Measure  
PGA: Peak Ground Acceleration  
PGV: Peak ground velocity  
PGD: Peak ground displacement  
DM: Damage Measure  
EDPs: Engineering Demand Parameters  
ISDR: Inter-story Drift Ratio  
 $\Phi$ : Standard Normal Cumulative Distribution Function (CDF)  
 $\lambda$ : Median of the Fragility Function  
 $\zeta$ : Standard Deviation  
DL: Dead Load  
LL: Live Load  
SD: Super Dead Load  
GL: Gravity Load  
EX: Earthquake Load  
IO: Immediate Occupancy  
LS: Life Safety  
CP: Collapse Prevention

## **CHAPTER I**

### **Introduction**

The issues, objectives, significance, restrictions, and associated explanations of the research are all included in this chapter.

#### **1.1 Problem statement**

Earthquakes are a common occurrence in many parts of the world. When they occur close to congested areas, strong earthquakes have resulted in significant loss of life and property. Although there has been significant growth in the discipline of seismic prediction, earthquakes cannot be precisely predicted in terms of timing, magnitude, or location. A powerful seismic event can have an enormous socioeconomic impact not solely on nearby neighbourhoods but on the nation as a whole, as witnessed in the 2010 Chilean disaster, the 2011 earthquake that hit Tohoku in the nation of Japan, the 2012 Quake in Christchurch, New Zealand, and the temblors in Turkey in 2023.

Due to the rapidly growing urbanization and connectivity, an earthquake occurrence may cause significant socioeconomic damage. Regarding this instance in terms of human life and property prevention and mitigation of loss, developing comprehensive knowledge on pre- and post-quake became crucial. As a result, much recent study has been devoted to analysing adaptability, or the tendency to limit harm via reliability, and resiliency in the event of such catastrophic occurrences. Undoubtedly, such efforts are required for assessing regional damage while taking earthquake-related risks and quake demands on structures into thoughtfulness.

The term "seismic Risk evaluation" refers to a recognized procedure or approach for assessing architectural deficiencies that prevent the structure from meeting a chosen performance target. Researchers have given particular focus to the seismic evaluation of current structures and infrastructure due to the tendency to collapse alongside insufficiency of reliability of facilities throughout the world during the last decade. Because of advancements in seismic assessment tools, the prospective seismic risk of buildings has become a major concern. In general, several factors are considered in the assessment processes of each construction. The key areas of interest for these qualities are the framework, seismic capabilities, site circumstances, level

and elevations regularity, and small-field data collection. These variables provide a realistic description of the structural system's behaviour. In essence, the risks connected with a seismic hazard comprise the possibility of high losses occurring during a given time span. Buildings may not have been built to withstand seismic forces or may have been built before the current seismic codes were published. Additionally, buildings may be in poor condition or have deteriorated over time due to changes in their intended use or because the soil has a high liquefaction potential. The conclusions of this study are very important in the understanding of structural element behaviour under a particular ground motion.

A configuration may be altered to reduce its seismic demand, improve its capacity, or be removed depending on the results of the seismic evaluation. Planning for disaster response, damage assessment, loss estimation, and retrofitting decisions can all benefit from this method. Planning beforehand and spotting potential dangers early may greatly decrease injuries and property damage. An effective design goal is to evaluate performance under the anticipated seismic load. It is urgently necessary to speed up this process of quantifying vulnerability through a careful study using the technologies at hand, including accurate material and structural models that can forecast a structure dynamic reaction. Numerous approaches have been identified in the literature for addressing this issue, and researchers have separated the method onto two major groups for the purpose of the loss prediction: qualitative techniques and analytical methods. While analytical approaches relied on limitation stages and skeletal characteristics or features of the buildings, empirical exposure approaches used the level for damage as a method of inquiry to develop post-event data that came with data analysis examines as a basis of building damages (El-Maissi et al., 2020).

The common regulation under which these two methods for addressing seismic vulnerability are usually undertaken is the Federal Emergency Management Agency (FEMA). When the walls are improperly connected to the floor, the building is more vulnerable to earthquake damage. The damage is primarily concentrated on the upper levels of tall buildings because the movement is greater there, and in buildings with lighter wall and roof materials the damage is greater. The damage is not only dependent on the magnitude of the earthquake or the ground motion but also on the type of structural system, the number of floors, and the construction technique.

The seismic design gradually advances from a stage in which a linear elastic analysis was sufficient for the structure's elastic and ductile design to a stage in which a nonlinear analysis using a unique method was used. The nonlinear static analysis can predict the failure mechanism and also detect the mechanism and the location of any in advance, negating the need for sample methods to predict the nonlinear attitude of a structure under the seismic load. It additionally sheds light on how that dynamic analysis known as gradually clarifying how the failure in the structure happens and determines the final failure pattern, and it's easy to conduct a nonlinear analysis to estimate the capacity.

For this, incremental dynamic analysis (IDA) is a good alternative due to the uncertainty of upcoming ground vibrations, it is appropriate to utilize probabilistic strategies to forecast physical damage and loss during earthquakes. Fragility curves can be used to quantify the likelihood of structural damage caused by ground motions of various Intensity measures (IM) including Peak Ground Acceleration (PGA), Elastic Spectral Acceleration (Sa), Elastic Spectral Displacement (Sd), and so on. The Bracing System considerably lessens inter-story drift. Bracing provides better resistance to seismic and wind forces. In order to stabilize the building structure against lateral stresses, bracing is a construction technique. It improves a building's ability to endure lateral loads brought on by wind and earthquakes.

A shear wall has a major axis that is stiffer than its other axis. It is regarded as a basic structure that offers rather stiff resistance to forces acting in its plane from the vertical and horizontal directions. A shear wall experiences compatible axial, shear, torsional, and flexural strains under this combined loading scenario, leading to a complex internal stress distribution.

## **1.2 Goals of the research**

This study aims to evaluate and understand the failure mechanism by shedding light on the damage measure of the structure. The yield and collapse state can be observed from the graphs of the analysis. The use of bracing and shear wall allows the enhancement of the moment-resisting frame to resist the lateral loads. This provides engineers with a consistent framework to assess how a building might behave during an earthquake, especially when a building does not comply with a lot of standard prescriptive requirements and responds in a highly non-linear manner with a potential

mixed-ductility response. The use of historic ground motion data is really important since it can be seen how the structure might have been behaving and how future structures will be designed. By means of SAP2000 software, the IDA is performed for this study, and the ground motion data are downloaded on PEER.

### **1.3 Generic earthquake idea**

The seismic or earthquake is a common naturally occurring phenomenon that causes serious harm to people's lives and property. A subfield of seismology known as earthquake prediction focuses on setting boundaries for the timing, place, and magnitude of impending earthquakes. It establishes conditions for future powerful earthquakes to happen in a specific location. The technologies that specify an earthquake and give a real-time warning of seconds to nearby locations that may be affected are further distinguished from prediction. There are several methods for predicting whether or where earthquakes may occur. Despite substantial investigations by seismologists, objectively credible projections regarding a specific day or month have not yet been developed. Turkey, Japan, Italy, Indonesia, China, and Iran are a few examples of countries that are situated in seismically active areas (Rasol, 2014).

### **1.4 Seismic Performance Analysis**

Later study has reached the very accurate decision that exhibiting ambiguities may have an important part when assessing earthquake resilience, especially when it comes to the forecasting of earthquakes response parameters near structural collapse, which is extremely complex even when the uncertainties are ignored and break down is calculated using non-linear dynamic approach. To reduce the high costs associated with lost productivity and the repair of severely damaged structures, it is crucial to create and implement streamlined techniques that are not overly computationally demanding. A technique where design requirements are centred on accomplishing a performance objective is known as performance-based design, to put it simply (Celarec, & Dolšek, 2013). Performance-based engineering is the newest idea in seismic engineering. The seismic design is improved in large part because of the work of civil engineers and architects. When a structure is subject to a seismic hazard, performance-based design explains design in terms of meeting performance targets.

The aim of performance levels must not exceed a limit state, a displacement, or a target damage state. Limit strains' serviceability allowed for a constant level of assessment to be attained, minimizing the substantial costs associated with lost productivity and structural repair of severely damaged buildings. A technique where design requirements are centered on accomplishing a performance objective is known as performance-based design, to put it simply.

### **1.5 Seismic performance analysis relevance**

Because predicting the seismic reaction of a structure is very uncertain, a probabilistic approach is necessary not only for determining the seismic danger but also for estimating the seismic response parameters. Two of the principal categories through which challenges often fall are the aleatoric unpredictability, that usually confined to an earthquake's arbitrarily character and are, therefore, unalterable, and semantic unpredictability, which are based on knowledge and often associated to the structure's physical features and modeling factors. Therefore, seismic performance analysis is the main mean by which this lack of knowledge in the broad event such as earthquakes but also the passivity in the modeling and survey during construction are construed.

This analysis shed light on the behavior that might undergo the structure from the safety state to the collapse of the structure in order to decide on the integrity of the building. Planning for disaster response, estimating losses and damages, including forming an opinion regarding retrofitting can all benefit from this strategy. The primary goals of a performance-based design is performance evaluation under the influence of anticipated seismic load. Due to the widespread use of RC in seismic force-resisting systems, it is necessary to adopt design techniques and systematic procedures that require little to no iteration after the initial design in order to achieve the intended design objectives (Liao & Goel, 2012).

### **1.6 Seismic resistant structures**

Aseismic design is meant to protect facilities from disasters to some extent or totally. The goal for structural engineer is to look at the impact of a controlled, randomized study on the efficacy of a new anti-cancer medicine in people. Building codes require earthquake-resistant structures to be capable of withstanding the largest earthquake

with the highest probability that is projected to impact the region where they are located. This means that in the event of a rare earthquake, the death toll should be kept to a minimum by preventing building collapse, while in the event of a more regular earthquake, the functional loss should be minimized as much as possible.

Wang & Zhao (2018) have pointed out the importance of lasting and adaptive facilities. The sustainable and resilient city has thus received increasing attention in recent years. A "resilient city" is required to quickly recover from any shock or stress and continue its key activities. Adverse occurrences are incorporated into the design of an earthquake-resistant construction. Which discipline will handle the design process for these structures is the biggest unknown in this regard. The creation of structures that can withstand earthquakes is often thought to be connected to the engineering field. Examining building damage after significant earthquakes over the past 20 years have revealed that this is incorrect, and many structures have become uninhabitable as a result of mistakes made during the architectural design process. To create high-quality structures, architects must have a thorough understanding of the necessary structural system and earthquake-resistant design. During an earthquake, a building's weak points are typically damaged. A long-lasting and sustainable structure against earthquakes will be attained if the decisions made during the architectural design phase, which are vital for the building's behavior against earthquakes, are based on the proper knowledge and utilizing the right methodologies. At this time, it is possible to state that the architects' efforts will result in the most palatable earthquake-resistant structural design.

### **1.7 Organization and scope**

Six chapters made up the study that was presented in this thesis: Chapter I provided an overview of the study's purpose, need, general understanding of earthquakes, and aseismic structure performance analysis significance. The literature reviews for this work are presented in Chapter II and information related to the parameters that are added to the structure, the methodology is shown in Chapter III, and the discussions and findings of all the models are presented in Chapter IV. Chapter V sheds light on the Discussion and eventually Conclusions and suggestions are included in Chapter VI for this thesis. The Appendices present some thorough information related to the work.



## CHAPTER II

### Literature Review

This chapter contains research and related basic concepts, descriptions, and information about a previously treated issue in the literature.

#### 2.1 Overview

Aseismic-resistant structures are the primary means of reducing losses since earthquake has been one of the most destructive events that buildings are facing. Recent earthquakes show that older structures that were not built to withstand quakes sustained damage instead of those that were built in accordance with seismic rules. A magnitude of 9.5 was credited to the biggest earthquake ever recorded, which struck Southern Chile on May 22, 1960. As stated by Chaulagain et al., (2015), almost 11,000 people have died in four major earthquakes in Nepal just in the last century. A magnitude 8.4 earthquake that struck Nepal in 1934 left 8,519 people dead and more than 80,000 houses destroyed.

Turkey has been hit by many moderate to big earthquakes during the past 20 years. Occurrences such as the 1992 Erzincan Earthquake, the 1999 Düzce and Gölcük Earthquake, the 2002 AY Earthquake, the 2003 Bingöl and Pülümür Earthquake, and the 2011 Van Earthquake have persuaded engineers society to appreciate the importance of earthquake mitigation strategies for needy buildings that currently have them in place, (DİLMAÇ et al., 2018). The latest major earthquake that left the entire world speechless and mourning happened on February 2023 in 11 provinces of Turkey and Syria. Two earthquakes of 7.7 and 7.6 centered in Pazarcik and Elbistan occurred and according to the Turkish Ministry of Interior and Emergency Management Presidency ( AFAD), 45 thousand 968 people died in these disasters. 115,000 injured people have been accounted and approximately two million people have migrated from the earthquake area. At least 1.5 million people are homeless according to the information. It is obvious that seismic calamities have made a lot of casualties whenever a severe motion has taken place because some buildings have been used beyond their life service, others have been constructed under ancient standards that are

not emphasizing seismic preventions and regulations and some other collapses are due to mal proper construction and poor control.

As a result of the need to figure out the seismic risk inherent in current constructions, studies pertaining to the growth of shaking risk assessment has received increased attention. IDA or the static pushover analysis have both been utilized in the literature to determine the maximum top story displacement. The analysis does a dynamic study of the structure using the provided accelerogram and then estimates the influence of those parameters on the greatest top story motion. IDA analysis, as opposed to the pushover method, which is a static analysis that account for the influences of accelerogram energy density, duration, and frequency content.

In line with findings of the study carried out by Baikerikar and Kanagali (2014), with the goal of assessing and contrasting the behaviour of lateral stress resisting systems for an array of high places, the authors applied a standard model that had 4 spans in all directions and a length of 5 m for each span. For a sake of simplicity, the highest height considered is 75 m. After modelling, to assess the effect of lateral load resisting systems with varied elevations based on displacement, lateral drift, base shear and time period, they discovered that all the considered parameters increased with increasing building height. MRF causes greater drift than a shear wall and bracings. Furthermore, with the installation of lateral load resisting devices, the building's lateral displacement is significantly reduced. Based on the findings, length of building rises with its height because of the stiffness that decreases while the mass of building as a whole raised up. Time has greatly shortened after installing lateral load resisting devices since the building has become more rigid.

Hyderkhan & Murnal (2014) compared the best choice in between IDA and POA for structural behavior using three distinct ancient earthquake time history data to investigate the special moment resisting frames and ordinary moment resisting frames structures with a variation on the number of story. According to the results, when comparing IDA to pushover analysis, the structures' reaction is greater for the same base shear value, and the result produced by progressive dynamic evaluation are larger and more plausible when compared to non-linear static pushover analysis.

Seyedkazemi & Rofooei, (2019); the goal of the study was to apply the principles of the FEMA P-695 guideline while proposing a more straightforward framework for estimating and validating SPFs. The findings demonstrated that the R factors for steel diagrid systems acquired using the SPA process were conservative and that a more logical value for the R coefficient could be found using the IDA-based probabilistic method.

In the work of Maniyar et al., (2009) for performing a probabilistic analysis, the buildings are analyzed relying on 20 substantial and medium distance ground motions scaled to varied degrees of intensity indicated by peak ground speed and 5% damped elastic spectral. The hysteretic model takes pinching induced by gap opening and closure into consideration, as well as stiffness deterioration, ductility-based endurance breaks down, including energy-based strength loss. The maximum ISDR determined by IDA investigations are shown against base motion energies. When the PGA is 0.12g, they infer that there is a 5% risk that anything may collapse. The aforementioned value is similar to the ground vibrations observed in Ahmadabad during the Bhuj earthquake. The scaled PGA was 0.11g, and the detected impact caused by these non-seismic RC frame structures is thus in line with the projected 5% likelihood of collapse. The graphic results depict the probability of yielding and collapsing in response to various intensities. of ground motion.

Brunesi et al. (2015) concluded that the delicateness models developed in the study were best matched to discrete vulnerability estimates supplied by IDA paired with Monte Carlo simulation for the life safety and total collapse prevention states, which are crucial to progressive collapse evaluation. Distinct fragility levels are connected with distinguished damage phases depending on the building class and modeling technique used to perform the study. The fragility functions proposed here validate and quantify considerable advances in RC building resilience from seismic calculations. Based on the seismic evaluation findings, a structure may be modified to minimize seismic demand, boost capacity, or demolished.

Any danger of suffering an earthquake is based on the area seismic hazards and the strength of its built environment. While assessing seismic risk, a site vulnerability to earthquakes of a certain magnitude or intensity is taken into account. A

structure sensitivity to damage from ground shaking is known as its seismic vulnerability, and this includes the structure foundation, columns, beams, and floor slabs, (El-Betar, 2018). The soil or rocks around the foundation of a reinforced concrete structure serve as the primary support for the loads delivered to the structural components, which subsequently transfer those loads to the foundation and the surrounding soil or rocks.

Inel et al., (2018), "Nonlinear static and dynamic analyses of RC Buildings". Recent earthquakes that significantly damaged reinforced concrete (RC) structures highlight nonlinear behaviour during significant seismic events. It is well acknowledged that lateral displacements are the primary cause of both structural and non-structural damages incurred during earthquakes. The relevance of seismic displacement predictions in performance-based seismic planning and evaluation is thus able to be seen. So, it would seem that the most important aspect of considering, designing, and implementing a retrofit solution is totally reliant on engineering judgment. This fact is inconsistent with the intricate and inherently accurate analytical techniques employed to evaluate a building. Although linear analyses are commonly employed in the design of innovative constructions, nonlinear techniques based on the foundation performance have swiftly become apparent and are now widely utilized in the field of appraising structures (Baros, & Dritsos, 2008).

Ricci et al., (2019), an evaluation of the seismic activity of existing residential reinforced concrete buildings is presented, with visuals of selection and design criteria for the case-study structures, the method of modelling employed to simulate both structural and non-structural components typical of such structures, the investigated limit states, finally, the results of static pushover and time history both nonlinear in multi-stripe analyses. The life safety, immediate occupancy, and collapse prevention levels of performance in refurbishment requirements are frequently used as classifications. A rising number of structures, both new and old, are being subjected to nonlinear testing as a technique of monitoring their seismic performance. Structural engineers often choose nonlinear static analysis because it is so user-friendly, although the reality that non-linear time history analysis is a far more reliable technique for determining seismic demand and assessing the performance of structures.

The most suitable and practical strategies for strengthening seismic resistance are bracing and shear walls. These methods can withstand seismic movements and serve as an earthquake barrier. A combination of its increased stability, stiffness, and excellent performance, shear walls are at present an extremely frequently employed retrofitting method in low to high story types of structures. Previous investigations have verified that shear walls have the capacity to both resist the effects of seismic activity and absorb ground vibrations. On the other hand some studies have concluded the bracing provides a way better resistance.

Dharanya et al., (2017), a tall residential structure having significant seismic loads is developed. That structure is thought to be situated in Bhuj, one of India's seismically active areas (zone V). In order to strengthen the building's integrity against sideways stress, an additional structural component is added to the design and examined, such as shear barriers and bracings. Each additional part is individually installed in two comparable models to examine how well it responds to lateral stress. According to the research, building's base shear rises noticeably, enhancing its resilience to seismic stress. While installing shear walls and bracing, the lateral resisting system has also been executed successfully. Since shear wall has significantly shortened the structure's natural lifespan compared to the bracings, the structure will be more earthquake-resistant and stable. Compared to normal frame, the structure has least amount of lateral displacement with shear walls and bracings. The conclusion drawn from the foregoing explanation is shear walls increases the lateral stability of building more than bracings.

Atif et al., (2015, this study compared seismic analysis of G+15 structure that has been braced and has a shear wall. The building's performance is examined in Zones II, III, IV, and V. To attain a suitable behaviour under upcoming earthquakes, the study comprises identifying the primary factor leading the structure to perform unsafely during earthquakes. The structure under analysis is symmetric, G+15, and an ordinary RC moment-resisting frame. (OMRF). The result shown that shear wall components are highly effective in reducing lateral displacement of the frame because they cause significantly less drift and horizontal deflection than braced or planar frames do.

Thorat, & Salunke (2014), in the investigation, shear walls and bracing are used to compare how structural systems respond to earthquakes. They compared floor displacements with member axial forces and moments. Because they significantly lessen drift and horizontal deflection for braced frames than shear wall framing and planar structures, they concluded that braced members are particularly useful in minimizing frame lateral displacement. Even though a braced frame's column axial force is higher than a shear-wall frame's or a plane frame's, the braced frame's column and beam stresses and drift are significantly lower. Therefore, compared to shear-wall and plane frames, a braced structure is far more effective in resisting seismic force. It is also conclude that the X bracing worked better than other bracings.

Azad, & Hazani (2016, this research uses a numerical approach to demonstrate how the steel bracing system and the shear wall system differ from one another. This research's novel strategy involves using steel bracing to strengthen the lateral force resisting system. To demonstrate understandable contrasts between the systems, a steady procedure has been carried out step by step. It is discovered that, compared to the shear wall system, the X type of steel bracing system greatly increases stiffness and decreases the highest inter-story drift but also the lateral displacement, and demand capacity of buildings.

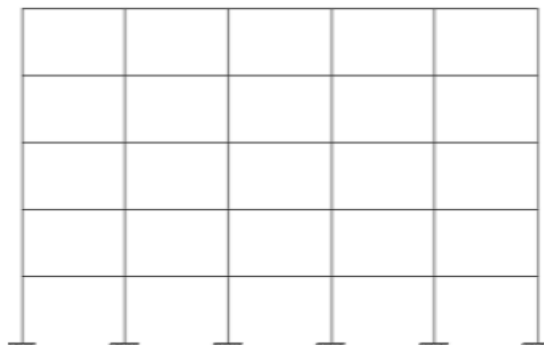
## **2.2 Moment resisting frames (MRF)**

A moment-resisting frame is made up of a rigidly connected rectilinear arrangement of beams and columns. Growing moments of bending and shear stress in the members of the frame and joints is known as rigid frame action, is what provides the majority of the resistance to lateral forces. It cannot move laterally due to the inflexible column to beam connections without bending the members, depending on the connexion shape. Therefore, the bending rigidity and strength of frame components serve as a main source of lateral stiffness and strength throughout overall structure. The joints or connections between columns and beams in moment-resisting frames are intended to be stiff. These structural parts are made to be strong in bending because doing so leads the columns and beams to bend during an earthquake.

Sadjadi et al., (2007) moment resisting frames are often divided into three categories known as formally ductile, ductile and gravity load designed. These structures' lateral load resistance, inter-story drift distribution, and member yielding order can all be used to assess their seismic performance. This work offers a pushover and nonlinear time history analysis method for seismic evaluation of RC frames. Models are tested against the experimental data that are available, and they are then employed to assess the seismic behaviour of all frames. The ductile and supposedly ductile frames both responded admirably to the earthquake under consideration, while the seismic performance of the gravity load designed structure was unsatisfactory. Figure 1 presents an illustration of MRF.

Figure 1

*Moment resisting frame*



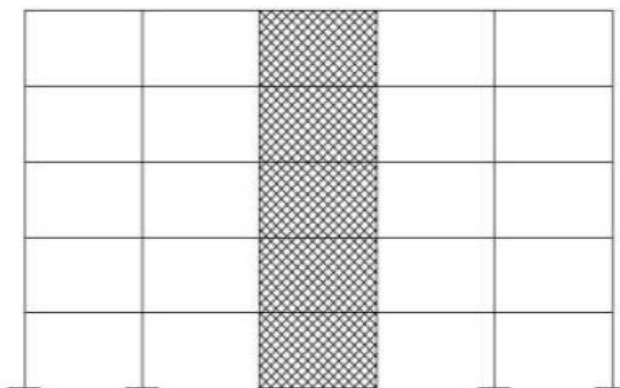
### **2.3 Moment resisting frame using shear wall (MRFSW)**

RC shear walls are structural components used to withstand lateral forces that are intended to be applied in-plane, usually due to wind and seismic loads. It withstands loads as a result of cantilever action. Since resilient walls withstand lateral stresses, they are vertical parts of the system. In addition to the weight of the building and its inhabitants, lateral pressures resulting from wind, earthquakes, and uneven settlement loads also result in strong twisting (torsional) forces. A building may be torn (sheared) apart by these pressures and a frame can be strengthened by adding a stiff wall inside of it or by attaching one to it. The above preserves the geometry of the frame and stops joint rotation. Shear walls are especially important in tall buildings that are susceptible to sideways wind and seismic pressures.

Seo et al., (2015), a 12 store RC structure situated in Seismic Zone 4, which is regarded as having an important seismic risk according to the U.S. Geological Survey have been assessed. The results showed that as height increased, the floor fragility generally reduced for all considered FEMA levels of performance, and the ratios from both techniques generally complied with the established restrictions. Utilization of shear walls clearly increased the structure's capacity and ability to resist lateral loads more, as indicated by findings of the time history study. Figure 2 is an example of moment resisting frame using shear wall.

Figure 2

*Moment resisting frame using shear wall*



#### **2.4 Moment resisting frame with bracing (MRFB)**

The resilient bracing framing system is widely used in structures that are susceptible to lateral stresses, including wind and quake pressure. A form of structural system called a braced frame is primarily designed to handle lateral stresses, including those brought on by wind and seismic activity. Members of a braced frame are designed to function in tension and compression, equivalent to a truss-style frame. In comparison to concrete frames, bracing systems are far more typical in steel frames. Concentric steel bracing and eccentric steel bracing are the two main forms of bracing frames. One type of bracing that resembles a truss member is concentrated steel bracing. Such bracing uses an axial compression and tension-based approach for resisting lateral stress. Contrarily, eccentric braced frames (EBFs) are a relatively recent lateral force resisting technique used to counteract the expected impacts of earthquakes. The bracings with shear links has been another prevalent style. It is utilized because it gives

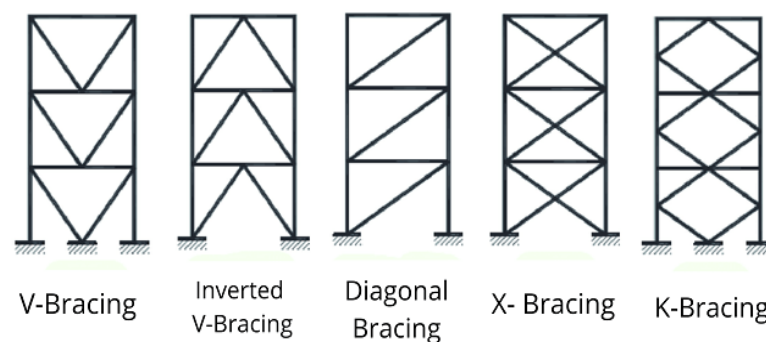


the frame extra rigidity. However, the placement of bracing can be challenging because they can obstruct opening placement and façade design. This has led to the bracing being expressed as an interior or external architectural component in high-tech or post-modernist architecturally inspired structures. Steel bracings are intended to resist any potential lateral forces applied to a particular construction. There are numerous varieties of steel bracing systems, including:

- X-bracing.
- Diagonal-bracing
- V-bracing
- K-bracing

*Figure 3*

*Type of bracing used in moment resisting frames*



*(Bisht, 2020)*

## 2.5 Seismic performance analysis and design code

Standards and design norms serve as a reference for safe construction design in order to safeguard human life. Structures must be built to handle loads from earthquakes in addition to frequent and permanent loads like snow and wind loads, dead loads, and living loads. The vast majority of codes usually concur that structures should be able to function after an earthquake and not ruin either during or following one. When performing seismic analysis for structures, there are certain guidelines, recommendations, and presumptions that must be taken into account. These details are provided in standards and design codes. By applying increasingly advanced techniques, the growing computing power may improve the accuracy of analytical results. In order to account for this, analyses are changed from linear (static to

dynamic), nonlinear (static to dynamic). In the purpose of better understand the seismic performance of structures, seismic performance analysis, frequently known as seismic analysis that is an intellectual process of earthquake engineering. Seismic analysis typically relies on structural dynamics techniques. Earthquake response spectrum method, which also helped shaping the current proposed building code, has been the most popular seismic analysis method for many years. However, structures having only a single degree of freedom perform best when using their response spectra. Multi degree of freedom structural systems appear to be better analyzed using numerical incrementally integration and seismic performance charts in the event of severe earthquake excitation. Structures are designed using approved engineering practices, tenets, and standards intended for new construction or retrofitting of buildings exposed to earthquakes. These requirements are entirely congruent with the current state of our understanding of building structures. Hence, a building's design that slavishly adheres to seismic code requirements cannot ensure safety from serious harm or collapse. Poor seismic analysis may come at a very high cost. Regardless of whether it was based on physical rules or empirical information, seismic analysis has always been an experimentation procedure.

Table 1

*Design code used in the USA*

Design Code	Purpose
ASCE 7-16: Guidelines for Basic Design Loads in buildings and besides structures	Earthquake and seismic chart load specifications
ANSI/AISC (341-16): Quake safety for steel framed buildings	Steel structure designed for seismic activity
FEMA 356: For the seismic renovation of buildings, pre-standard and interpretation	Damage evaluation on seismic performance is included within the standard for seismic refurbishment of existing buildings.
ATC 40: Seismic assessment and repairs of buildings made of concrete	Design criteria for concrete structures
ASCE 41-13: Building retrofitting and seismic examination	Guidelines for seismic inspection and upgrading existing structures
UBC 97: Modelling of buildings and other structures to withstand earthquakes.	Provide Earthquake Loads and Combination

### **2.5.1 Nonlinear static procedure**

This method is used in order to analyse load patterns proportional to the fundamental mode. Based on material characteristic and dimensioning of member, the study provides an estimation of the structural system's seismic capacity. Then, a variety of structural demands (including component pressures, story moves, plastic hinge rotations, etc.) are evaluated at this target displacement against an array regarding set acceptability criteria. Several variables influence whether or not a member satisfies the acceptability standards, including: construction material, member type and importance, as well as the performance level. A globally collapse is believed to have happened when the lateral displacement of the base shear curve acquires a substantial negative slope that came from  $P\Delta$ -effects and eventually reaches a point of zero or three inconsequential base shears. A position like this suggests the lateral resistance is unable to withstand gravity stresses. But some studies have found that this analysis has some limitations in terms of result accuracy as explained by Chopra & Goel, (2004). That could result in a glaring underestimating of tale drifts and a failure to accurately locate hinges and especially true for structures that experience a major loss in lateral capacity and flex substantially into their inelastic behaviour. Improved nonlinear static approaches have been suggested in response to these flaws.

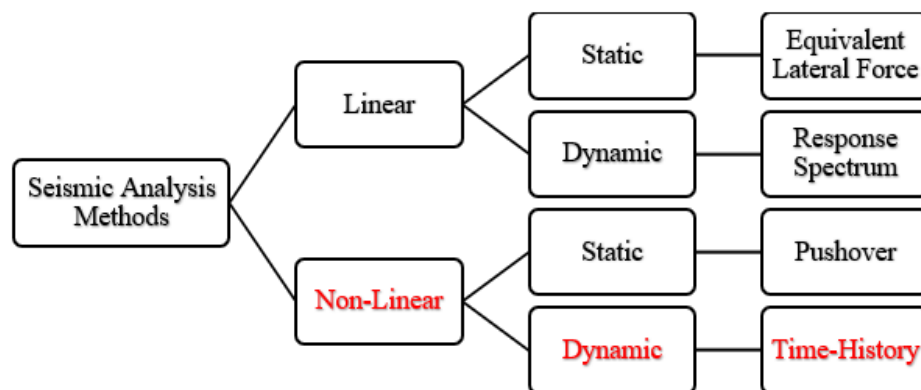
### **2.5.2 Generic of incremental dynamic analysis (IDA)**

This approach has recently developed into a successful method for investigating the behaviour of a structure overall, from elastic to yielding including nonlinear reaction to dynamic instability. It has been recognized as the most recent approach for estimating the worldwide collapse capacity according to FEMA criteria. The aim of IDA is to determine a structure's maximal global collapse capacity by performing a sequence of nonlinear dynamic evaluations that involve the strength of a selected ground motion is steadily raised. It can depict the link between an IM of the ground motion (such as  $S_a$  or PGA) and any engineering demand parameter (EDP) of the construction, such as peak inter-story drift ratio. Since different ground movements with varying frequency content and durations result in different intensity versus responsiveness graphs, the trial is repeated under a variety of ground motions to obtain comparative statistics that are significant.

Vamvatsikos and Cornell (2002) gave a thorough explanation of the procedure to be followed when determining the curves of a given intensity responses upon any number, investigated the features of these curves, proposed techniques for effectively carrying out an IDA, and assembled information pertaining to various curves that several ground motions generate. They have found that IDA is a useful technique to deal mitigating the global limits of structures and the resulting seismic stresses exerted on them. They also draw attention to several odd properties of the curves, such as asymmetrical behavior, gaps, various forms of collapse, and variations in the curves' behavior in response to ground motion. Since IDA is more competent and sophisticated than the nonlinear static technique, it is utilized to study the seismic performance of the conventional RC frame construction. This is no more a novel method since it has been used by a lot of researchers and engineers in order to provide more detailed information with great respect to accuracy.

Figure 4

*Seismic analysis methods*



## 2.6 Regulations base on the federal emergency management agency (FEMA)

Operating engineers are increasingly using the nonlinear static method to determine the seismic deformation needs for building structures and to evaluate both global and local capabilities for evaluating the resilience of currently operational buildings against expected future earthquakes. It first appeared in FEMA-273 (1997), enhanced in 2000 with FEMA-356, and most recently in FEMA-440 in 2005. This method is suggested for buildings whose larger frequency consequences are not evident. If higher mode effects are significant, this technique has to be supplemented by a method

known as linear dynamic analysis. The nonlinear deformation of the structure's parts is explicitly taken into account while building a model of the structure according to FEMA-356.

According to FEMA P695, there is a method for evaluating the seismic design requirements for a building type or LFRS by methodically analyzing how well archetypal building designs collapse under a variety of earthquake conditions. Nonlinear static studies are first required for the technique to assess ductility and over-strength. The collapse capability of a given archetype is evaluated using nonlinear dynamic studies with various ground movements and slowly rising excitation levels. The analytical technique that was utilized in IDA may be considered as a dynamic extension of pushover analysis. The far field movement of the ground record set in FEMA P695 is an example of an accumulation of quake excitation data that is linearly scaled and used to create a structural model until collapse is seen. The collapse margin ratio (CMR) essentially reflects the capacity of the archetype to collapse, is derived from the IDA data.

Two pairs of ground motion recordings are given for nonlinear dynamic analysis. 22 motion record pairs from places that are between and to 10 km from a fault rupture make up one set of records, referred to as the far field data set. The other collection, known as the near field record set, includes 28 pair of ground movements that were captured less than 10 km from a fault rupture. Although either near and far field record sets are provided, solely the far fault recording set is required for collapse evaluation. This is being done for pragmatic reasons and in recognition of the many open issues surrounding the classification of near fault risk and ground-moving consequences. All great magnitude event records from the Pacific Earthquake Engineering Research Center (PEER; Next Generation Attenuation, NGA) database are included in the record sets. Tracks were picked to meet a variety of oftentimes conflicting objectives. In order to prevent event bias, just two of the strongest recordings from each earthquake were gathered, however there are enough movements in the record sets to provide statistical evaluation of records-to-record (RTR) variance and breakdown frailty. Severe vibrations from the ground were not identifiable due to the site conditions or the underlying source.

## 2.7 Friction dampers

Researchers have suggested an additional strategy to lessen the seismic stress placed on structures. The technique entails adding passive energy dissipation components, such as dampers, to the structural system of both new and old structures. Dampers are used to minimize the effect of horizontal loads on a structure in order to maintain the other structural components in the elastic stage while avoiding inelastic changes. The damper acts as a "sacrificial" part in this way. With the inclusion of damping devices, a structure can achieve extra damping of 20–50% in contrast to the typical damping of 1-5% without a damping mechanism. The stresses operating on the frame, the deformations, and the vibration intensity are all significantly reduced by using these techniques. Dampers can be categorized into two groups: viscoelastic and hysteretic. The displacement of the parts inside the device that dissipate energy by friction between two surfaces or metallic yielding affects the hysteretic dampers. Velocity affects viscoelastic dampers. In comparison to the aforementioned dampers, friction dampers offer a number of benefits. Furthermore, since the frictional absorber is acceleration detached and its pulling power is constant for all earthquakes, it is possible to build connections and members more affordably. A friction damper, in contrast to viscous dampers, also makes the structure stiffer, which will help keep it from topple over. The friction that forms whenever surfaces slide in relation to one another upon dampers distributes the energy from stressors like seismic ones. When designing a structural system using friction dampers, a slip load is included into the damper. The sliding pressure can be adjusted to a number that allows the structure respond to lateral loads in the best possible way.

Sun & Dias, (2018), the importance of Rayleigh damping in the computational response of earthquake excited tunnels is discussed in this work. The study demonstrated that, under certain conditions, viscous damping significantly affects numerical predictions derived from an array of two-dimensional numerical evaluations. This damping in dynamic research resulted in a decrease in the time step and an increase in calculation time. Unconservative tunnel designs might be created if small quake internal force changes could be predicted. Given that the frequency interval has a substantial impact on the tunnel response, it should be carefully examined.

Dai et al., (2022), A six-story concrete-framed structure that features an isolation system is subjected to a range of seismic ground motions as part of the investigation. The impacts of hardness and in both directions, coupling is considered when analysing how the isolation layer and superstructure affect earthquake response. The results demonstrate that the peak responses of the superstructure to high-intensity earthquakes significantly increase when stiffness hardening and coupling effects are taken into consideration. According to the analytical results, it is crucial to consider the stiffness hardening and the impact of the HDRBs' bidirectional coupling while constructing HDRB isolation systems.

## CHAPTER III

### Methodology

This chapter summarizes the study approach, sample, data collection and analysis procedures, and it also describes how the results are analysed.

#### 3.1 Overview

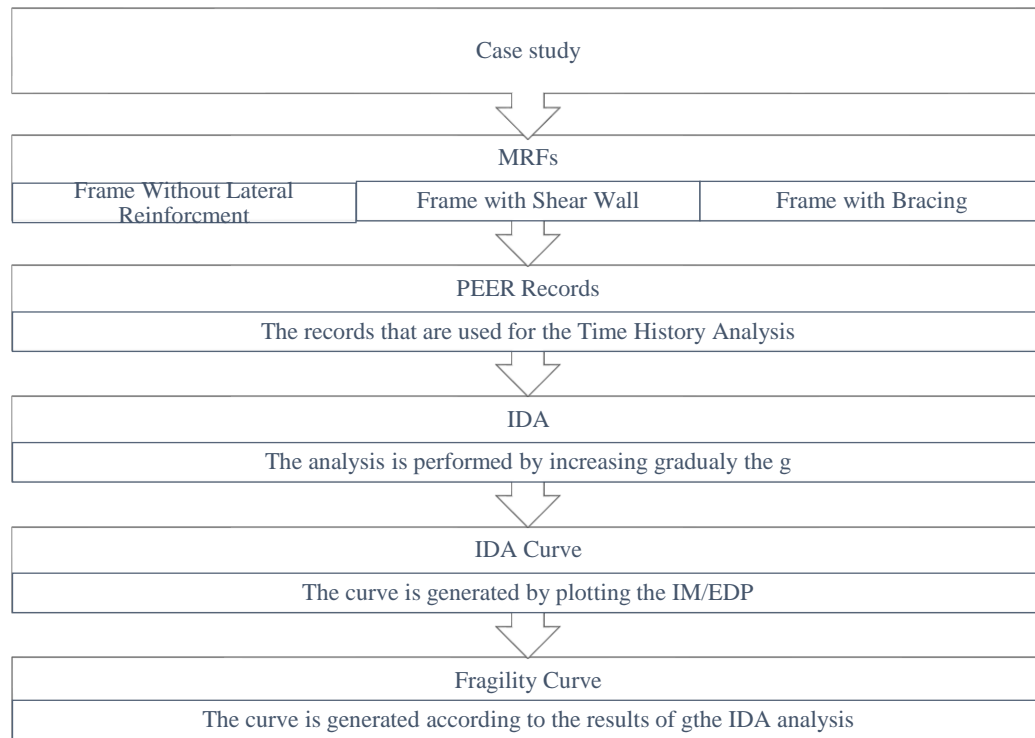
Here is covered the analysis, design, and evaluation processes for the models used throughout the study. It provides the assumptions approach that was used for the evaluation and development of the models according to the code regulation. Incremental Dynamic Analysis (IDA) was used afterwards to evaluate each model. Numerical modelling is needed for the analysis, design, and evaluation of the structures and their execution assessment. Therefore, in the current study, models are built using the computer program SAP 2000 V23.3.1, which also performs the corresponding IDA procedure.

#### 3.2 Analysis strategy

This investigation seeks to evaluate the structure's damage under various earthquake records, with an emphasis on the 3 RC frame system. Different moment resisting frames (MRFs) without lateral reinforcement but also MRFs with shear wall and Bracing. The IDA has been chosen owing to the fact that it provides more accurate results in terms of seismic assessment. It is now feasible to more precisely assess the structure's resilience against quake stresses because to recent improvements in a variety of different types of IDA, which is a parametric approach. A structural model must be exposed to a number of ground motion records, each scaled to a distinct degree of intensity, so as to obtain one or several curves of response scaled versus intensity degree. Figure 5 below is an illustrative example of the process that this research is based on.



Figure 5

*Study process***3.3 Location of the case study**

This project is located in Nicosia a city of the Northern Cyprus which is a medium seismic zone. The framing system that are used for this study have been explained earlier in the previous chapter that are:

- MRFs
- MRFs with Shear Wall
- MRFs with Bracing

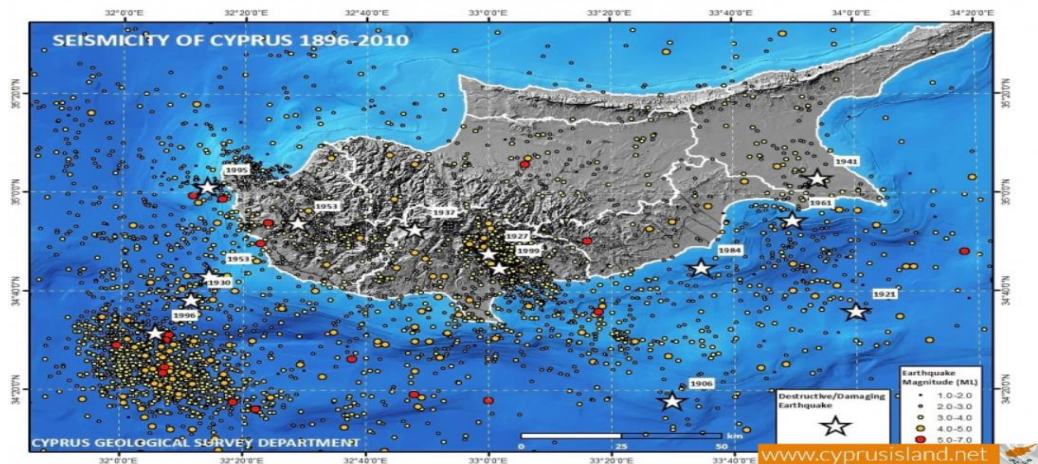
**3.3.1 Cyprus seismic activity**

Since Cyprus is situated in one of the seismically active regions of the eastern Mediterranean basin, numerous strong earthquakes have had an impact on the country over the course of its history. Figures 6 a) and b) show the island's history of many earthquakes that have occurred. On May 11, around 06:15 UTC, the 1222 Cyprus earthquake struck. Its estimated magnitude was between 7.0 and 7.5, and it caused a tsunami that was seen in Alexandria and Libya. Nicosia, Limassol, and Paphos

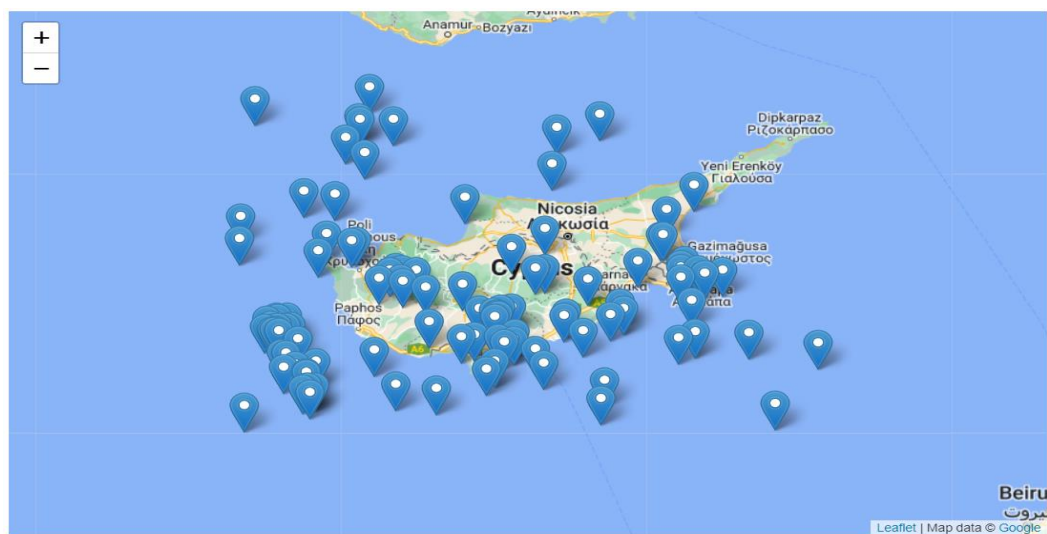
experienced the most intense shaking. Although there are no figures for the entire number of victims, numerous people died. (Wikimedia Foundation. 2023).

Figure 6

a) Seismicity of Cyprus, b) Earthquake map of Cyprus



a)



b)

(<https://www.cyprusisland.net/earthquakes-cyprus>)

Here below in table 2 is listed some major earthquakes by magnitude that occurred in Cyprus over the past 5 years.

Table 2

*The largest past 5 years earthquakes in Cyprus*

<b>Years</b>	<b>Location</b>	<b>Magnitude</b>
2022	West of Nicosia	6.6
2021	Near Larnaka	4.9
2020	Eastern Mediterranean	5.2
2019	Eastern Mediterranean	4.6
2018	Eastern Mediterranean	4.9

**3.4 Peer records**

Due to ambiguity regarding structural characteristics and ground motion, a probabilistic approach is necessary for an appropriate assessment of RC structural performance systems in seismic activities. Gathering and downloading ground motion data are available on the PEER website which has become a powerful tool for ground motion acquiring for engineers. These data are used due to the fact that they are realistic data gathered from past earthquakes that can help to better understand and forecast the seismic behaviour by assessing the damage of the model under study.

Applying IDA necessitates a number of non-linear dynamic time-history analyses, therefore having the right ground motion record series is crucial. Since different ground movements may affect the response of structures differently relying on their characteristics, adopting one initial motion for an analysis of time history is a particularly challenging task. This problem is further compounded by the fact that the amount of chosen ground motions has an impact on how accurate IDA conclusions are. The PEER website has been used to download the ground motions. This database proposed 2 different types of ground motion which are far and near field, but according to FEMA 365 for the IDA analysis, far-fault records should be used. 100 ground motions have been downloaded and the minimum set of ground motions that can be used is 3 regarding the code regulation, but for this study 7, records are used with

different magnitudes and from different periods of time. Table 3 sheds light on the used ground motion for the present research. The records are selected according to the following assumptions:

- Magnitude: In between 5-9
- Soil shear wave velocity ( $V_s$ ): 200-500 m/s
- Joyner-Boor distance to rupture plane ( $R_{jb}$ ): 10-100 km
- Fault type: All type has been selected

Table 3

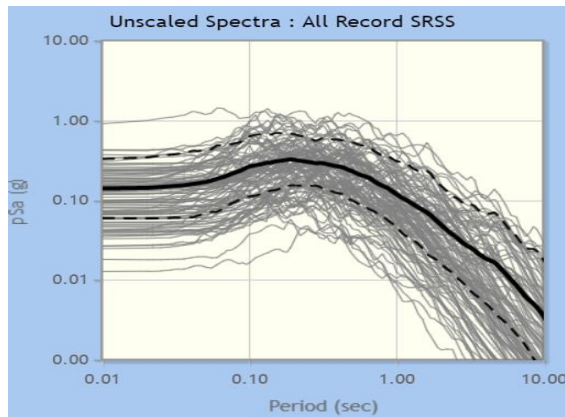
*Properties of the GM used for this investigation*

<b>GM</b>	<b>Name of the station</b>	<b>Year</b>	<b>Magnitude of the record</b>	<b><math>V_s</math> (m/s)</b>	<b>Slip mechanism</b>	<b><math>R_{jb}</math> (km)</b>	<b><math>R_{rup}</math> (km)</b>
1.Humbolt Bay	Ferndale City Hall	1937	5.8	219.31	Strike-slip	71.28	71.57
2.Northwest Calif-01	Ferndale City Hall	1938	5.5	219.31	Strike-slip	52.73	53.58
3.Northwest Calif-02	Ferndale City Hall	1941	6.6	219.31	Strike-slip	91.15	91.22
4.Tabas_ Iran	Ferdows	1978	7.35	302.64	Reverse	89.76	91.14
5.Borah Peak_ ID-01	CPP-601	1983	6.88	279.97	Normal	82.6	82.6
6.Taiwan SMART1(25)	SMART1 E01	1983	7.3	275.82	Reverse	56.18	56.18

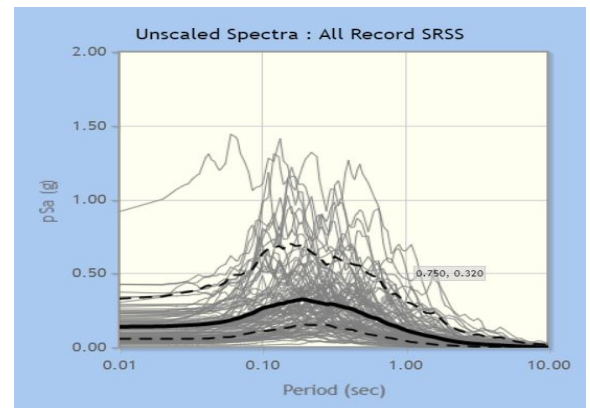
Applying scaled ground movements to the models in the SAP2000 program is the next step after choosing them from the PEER database online. When performing incremental dynamic analysis, this software features a scale factor module. Below Figure 7 from (a) to (c) are the illustration of the spectra of the 100 ground motions that have been downloaded among which the 7 GM have been chosen.

Figure 7

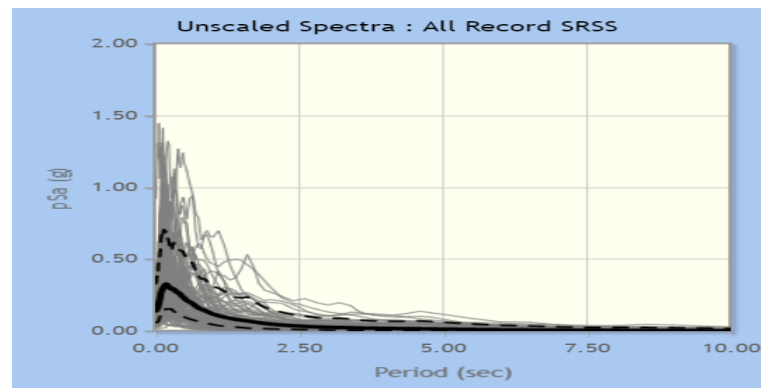
a): Spectra axe loglog, b): Spectra axe semilog X, c): Spectra axe linear



a)



b)

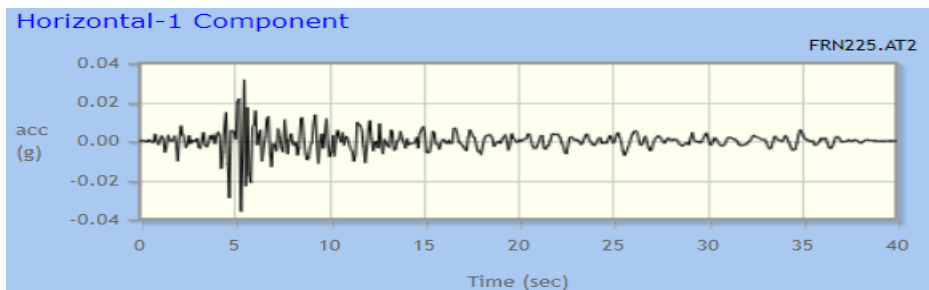


c)

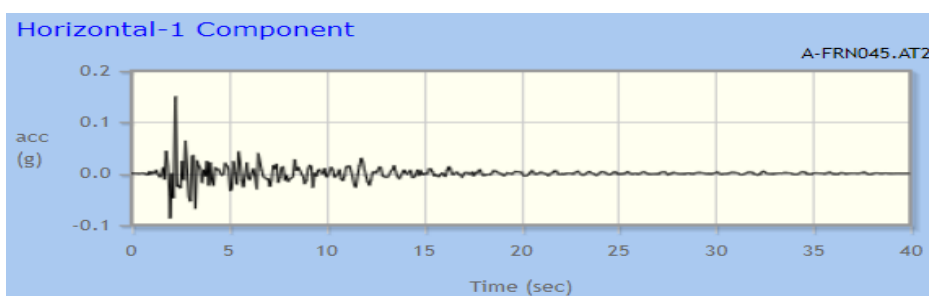
The data downloaded are given in 3 horizontal components, which are in both X and Y direction components, and the vertical component which is in the Z direction. The components are given in each direction according to: acceleration, velocity, and displacement. The acceleration component in X direction is the one considered in this work. The following Figure 8 are the acceleration spectra of the 7 selected GMs used for scaling the different models.

**Figure 8**

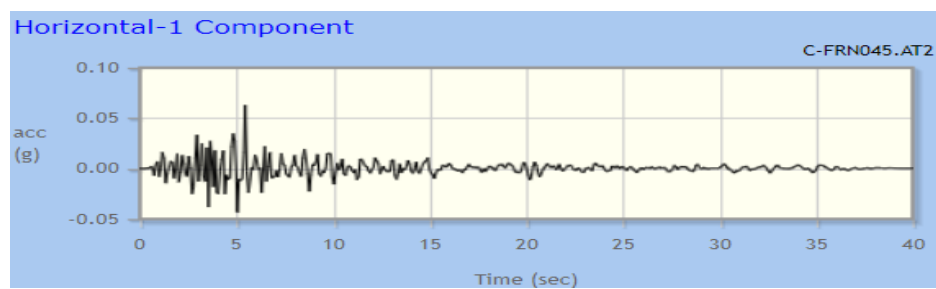
Selected earthquake ground acceleration: a): Humbolt Bay, b): Northwest Calif- 01, c): Northwest Calif-02, d): Tabas\_ Iran, e): Borah Peak\_ID-01, f): Taiwan SMART1 (45), g): San -Fernando



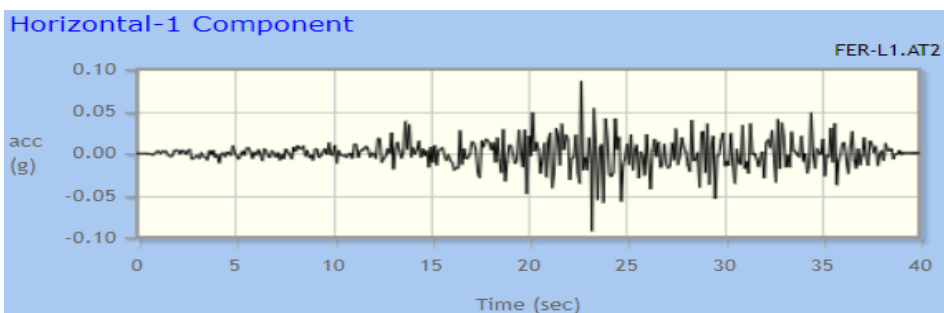
a)



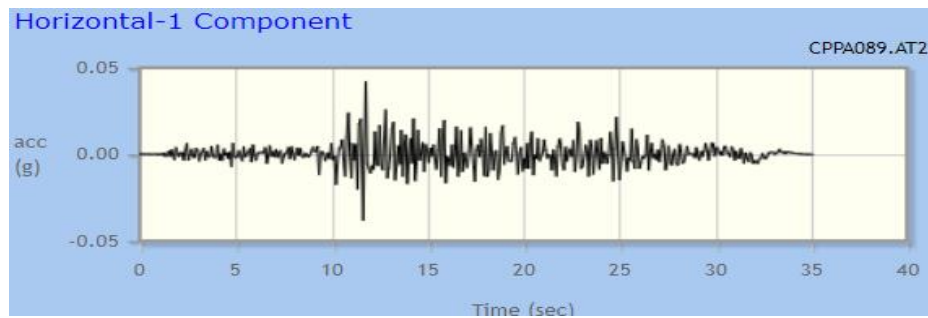
b)



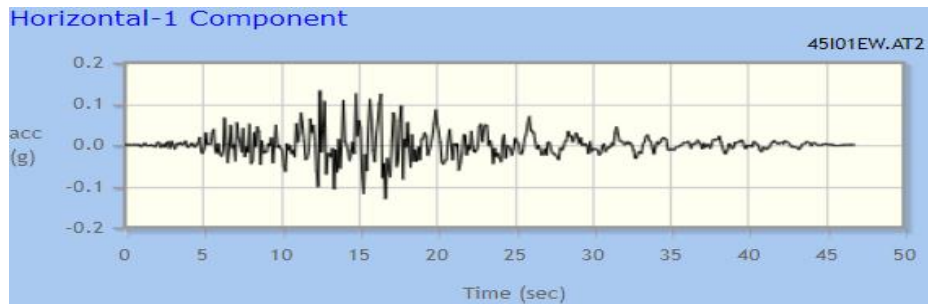
c)



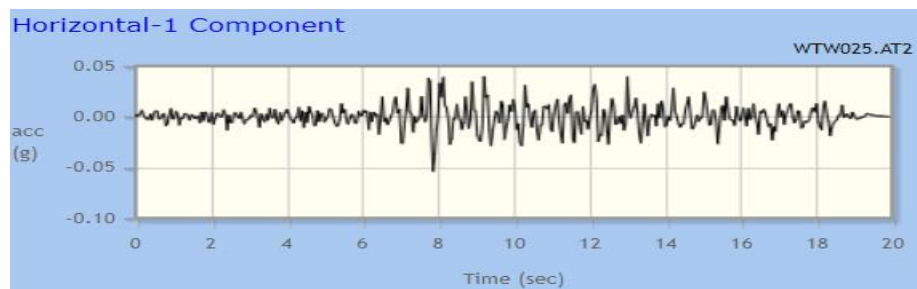
d)



e)



f)



g)

### 3.5 Scale factor

The scale factor or SF, is the positive scalar that when repeatedly applied on an unscaled acceleration time-history, produces a calibrated accelerogram. SF ranging from 0.1g to 0.8g are progressively added to the structure in the current investigation up until the point of collapse. The gravitational acceleration, or g, is calculated to be 9.81 m/s<sup>2</sup>.

### 3.6 Intensity measure (IM)

A positive scalar that is raised gradually with the SF is often referred to a monotonic scaled motion of the ground intensity measure of a calibrated accelerogram. It is a

function that depends on the un-scaled accelerogram. This IM are: PGA, PVA, PVD, or any combination of them, for instance and for this study, the IM chosen is the PGA.

### 3.7 Damage measure (DM)

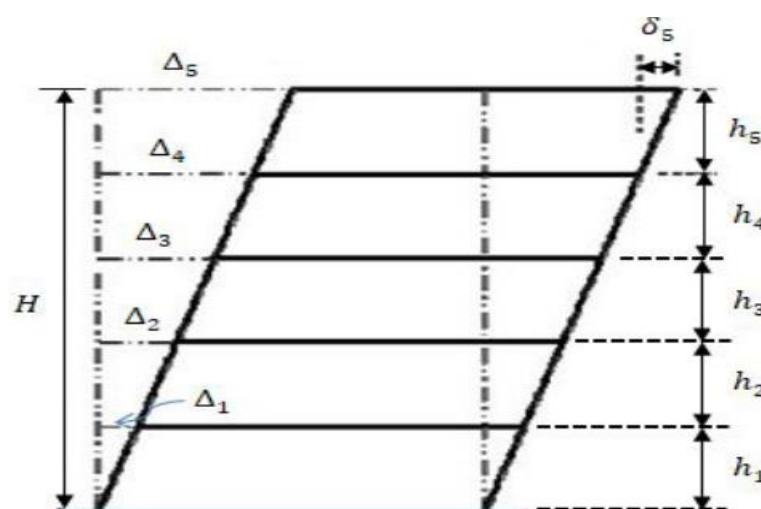
Engineering Demand Parameters (EDPs) are structural response metrics that can be used to anticipate damage to systems and components that are both structural and non-structural. Damage measure is a positive scalar with values  $[0, +\infty]$  that describes the structural model's additional response to a specified seismic stress. There are a number of potential EDPs that can be chosen, including ultimate base shear, node turns, peak levels ductility, various suggested damage indicators or the equilibrium index, highest roof drift and peak inter-story drift, but also the floor peak inter-story drift angles of n-story constructions. However, the ISDR is chosen for this study.

### 3.8 Inter-story drift ratio or ISDR

Inter-story drift, also known as the percentage translational motion between two succeeding floors, is an important engineering demand parameter and an indicator of structural performance. Accurate inter-story drift measurements would be very helpful to the structural engineering community, especially in areas where structures experience inelastic deformation.

Figure 9

*Drift measurement*



(Bhatt, 2020).

The equations defining ISDR in percentage is the following:



- Inter-story drift of  $i$  floor is  $\delta_i = \Delta_i - \Delta_{i-1}$
- Inter-story drift Index of  $i$  floor is  $ISDR = \delta_i/h_i$

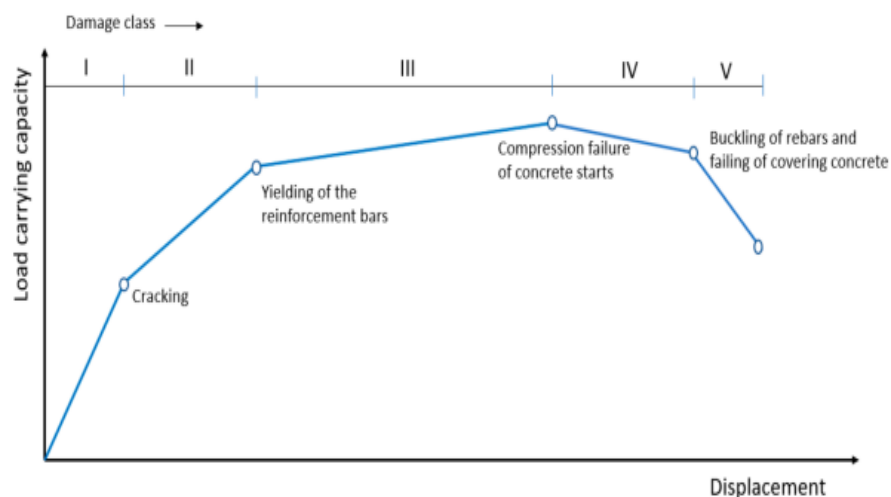
Where:  $\delta_i$  = Inter-story drift of  $i$  floor,  $h_i$  =storey height of  $i$  floor and  $\Delta_i$ = total drift of  $i$  floor

### 3.9 Damage state (DS)

Users can examine the post-earthquake status of structures using the damage states, which provide unambiguous definitions of the damage and failure processes. The damage states also enable categorization of the damage for further uses, such as determining seismic intensity. The structural and non-structural damage, as well as the cost of damage, are effectively linked by the damage states defined on the basis of cost-ratio or damage factor, which are helpful in evaluating economic losses.

Figure 10

*Different damage states*



(Kristiawan et al., 2021).

The relationship between damage features, EDP, and damage state needs to be stressed the most with regard to Figure 10. The relationship serves as the foundation for the damage limit state definition. The damage characteristics explain the physical damage that can be measured in terms of concrete crack width, reinforcing bar yield strain, and other physical damages that have been noticed. The degree of physical damages is correlated with the load-displacement (or moment-curvature) curve's shape. As a result, damage parameters can be chosen from deformation values connected to the curve, such as strain, displacement, rotation, etc. For the purpose of

this work, 3 damage states are considered to express the state of the structure based on the ISDR obtained from each GM as stated by FEMA:

- I. Immediate Occupancy known as IO
- II. Life Safety or LS means that repairs are required also
- III. Collapse Prevention (CP) collapsing

Table 4 sheds light on the drift percentages of each limit state quoted above.

Table 4

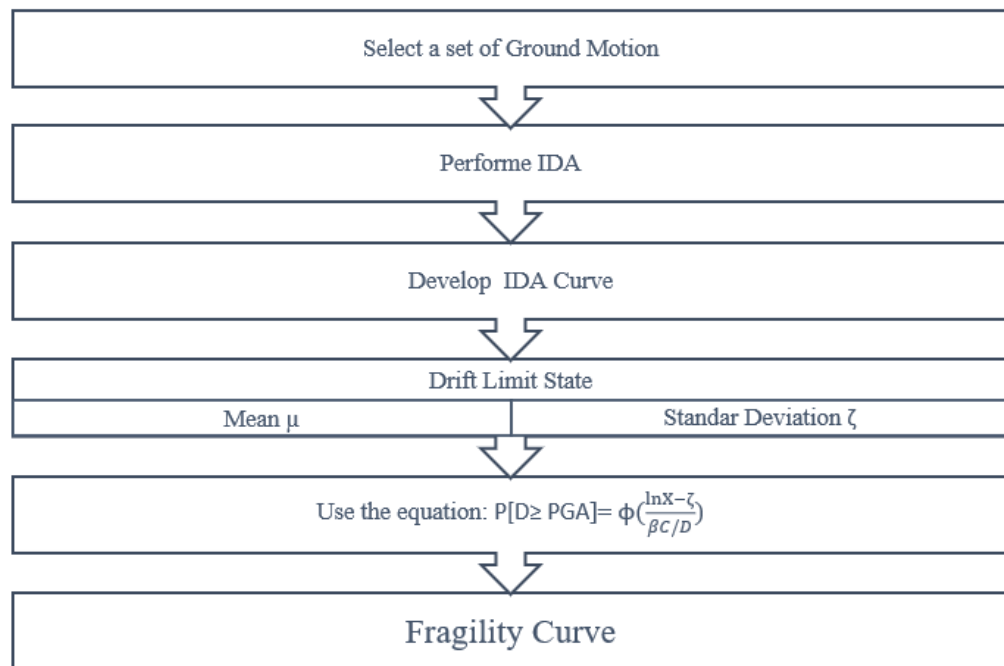
*Different Limit state*

Damage State	IO	LS	CP
ISDR%	1	2	4

### 3.10 Fragility curve

It's representing the likelihood of going above a given limit state, such as collapse, in relation to an indicator of the intensity of ground motion, such as spectral acceleration at the fundamental period. It is crucial to produce a more realistic evaluation of seismic fragility by taking more influencing factors into account with regard to the earthquake behaviour of buildings and their bearing medium because of their significance in the global management of earthquake disasters. It is well recognized that the soil's pliability beneath a building's foundation can have a significant impact on the structure's response to earthquakes. The significance of the aforementioned fact is increased in terms of the calculation of seismic fragility when taking into account the effects of large-scale decisions based on fragility curves. Figure 11 illustrates the process that is followed in order to develop the fragility curve.

Figure 11

*Fragility curve process*

The equation:  $P [D \geq \text{PGA}] = \Phi \left[ \frac{\ln X - \zeta}{\beta C/D} \right]$  with:

- $\Phi$  is the commonly used cumulative distribution function (CDF)
- $P [D \geq \text{PGA}]$  relates to the likelihood that a ground motion will push the structure into its limit condition.
- $\zeta$  is the deviation
- $X$  is the PGA (lognormally distributed PGA) required for the occurrence of the collapse damage condition.

The median of the natural log of  $X$  value  $\zeta$  is estimated by computing the geometric mean of the data:

$$\zeta = \exp(\overline{\ln X})$$

- $\overline{\ln X}$  is the basic logarithm of the  $X$  record's mean.
- This following formula is used to calculate the natural log of the  $X$  value standard deviation  $\beta C/D$

$$\beta C/D = \sigma \ln X = \sqrt{\sum_{i=1}^n \frac{(\ln X_i - \overline{\ln X})^2}{n-1}}$$

These equations are used for each PGA in order to develop the function going with each limit state so that the fragility curve is constructed with different states of damage.

### 3.11 Frames configuration

To fulfil the purpose of this study, three types of structural systems are chosen to be applied on the residential models: moment resisting frame system (MRF), shear walls system (SW) and bracing system. All the model are 3D are mid-rise building with 10 story with a variation on the span length that is consider with 5m, 6m and 7m and all frames have same span length in X and Y direction. The seismic zone medium has been chosen to conduct this investigation. All the modelling and analysis process have been undertaken on SAP 2000 and Microsoft Excel have been used to extract data and plot the different graphs. A total of 9 frames have been modelled and analysed to identify the seismic behaviour of RC structures under realistic earthquake records. The analysis is based on ACI 318-08, ASCE 7-10, UBC 97 and FEMA 365 regulations.

#### 3.11.1 Material properties

The materials used for this research are concrete and rebar for reinforcement but also steel for the bracing. To ensure accurate values for the various material attributes, materials are selected from the software's integrated American databases. This database also contains and automatically defines nonlinear material properties. C25/30 concrete and rebar reinforcing are the materials that are employed for the design in this study. The following table shed light on the material properties.

Table 5

#### *Material Properties*

Material	Type	Property
Concrete	Modulus of Elasticity. E	24855.58 MPa
	Shear Modulus. G	10356.49 MPa
	Unit Weight	23.5631 kN/m <sup>3</sup>
	Compressive strength. $f_c$	27.58 MPa
	Expected. $f_c$	27.58 MPa
Rebar	Modulus of Elasticity. E	199947.98 MPa

Unit Weight	76.9729 kN/m <sup>3</sup>
Yield stress. $f_y$	413.68 MPa
Expected. $f_{ye}$	455.05 MPa
Tensile Strength. $f_u$	620.53 MPa
Expected. $f_{ue}$	682.58 MPa

### 3.12 Applied loads

All potential loads and cases are assigned while designing and analyzing are performed. The applied loads are on the slabs and frame for the residential models and all the loads are given according to UBC 97 regulations.

### 3.13 Dead load

For the dead load, 11.5 kN/m has been added to the self-weight already calculated by the software SAP 2000 because it determines directly the DL as the self-weight of the structural members to be considered.

### 3.14 Live load

Those areas LL are assigned to the slabs and have been divided into 2 because the load carried by the current floor slabs and roof slabs are different. Therefore, with respect to table 16.A of UBC 97, a magnitude of 2 kN/m<sup>2</sup> and 3 kN/m<sup>2</sup> are distributed LL assigned to the current floor slabs and roof slab respectively.

### 3.15 Super dead load

SDL are essentially dead loads that are applied to a structure but are overlaid. For instance, the slab's own weight is a dead load, however, any finished loads such as partitions, cladding, and false ceilings are all super dead loads. But these SDL are not taking into account the self-weight of the structural members. They have been divided into 2 as well for the current and roof floor slab and a magnitude of 2.58 kN/m<sup>2</sup> and 3.11 kN/m<sup>2</sup> are respectively assigned to the current floor slabs and roof slab.

### 3.16 Seismic lateral load

The wind load and the earthquake load were applied as lateral loads to the models. Buildings and structures must be made to bear the minimal wind load, per section 1609 of the IBC-2012. A site's exposure category, needed type of opening protection, and final design wind speed may all be determined in accordance with this. In the table 6 below is listed all wind loads applied.

Table 6

*Wind loads assigned*

Models	Roof floor joints (kN)	Current floor joints (kN)
5m	43.75	87.5
6m	52.5	105
7m	61.25	122.5

### 3.17 Gravity loads

The self-weight of each permanent member, including each beam, column, slab, and wall, is considered one of the structure's gravity loads. Automatically, the software considered the weight of beams, columns, and slabs. The computed wall loads have been allocated to the beams as evenly distributed loads. All the model's hinges were designed only to follow the GL pattern.

#### 3.17.1 *Plastic hinges*

The term "plastic hinge" describes the situation where the yielding stress is exceeded by the bending moment within an element. As a result, the structural member loses its capacity to withstand large bending moments and begins to function somewhat like a hinge. The three main categories of plastic hinges are listed below:

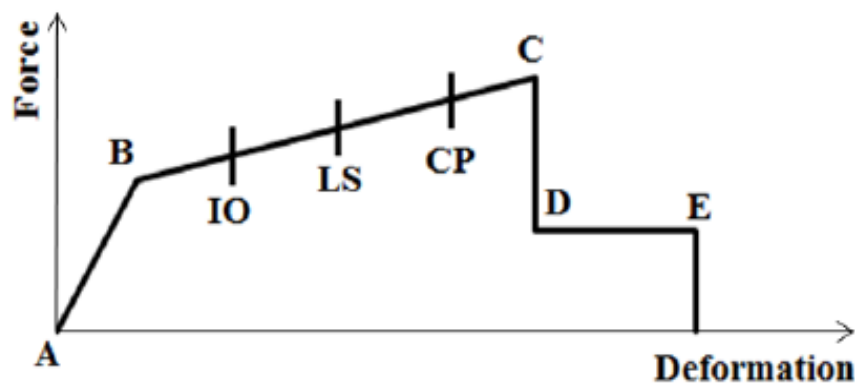
- Immediate occupancy: the structural element is undamaged.
- Life safety: the structural elements are partially damaged.

- Collapse prevention: the structural element is extremely damaged or even collapsed.

Figure 12 chart of plastic hinge phases can be used to establish the performance level of each plastic hinge.

Figure 12

*Plastic hinge chart according to FEMA*



(<https://www.researchgate.net/publication/261171164>)

### 3.18 Shear wall

Layered/nonlinear shell sections are used to define the shear walls. With this kind of shell section, it is possible to specify the different wall layers as well as the linear and nonlinear layers and orientations. In SAP2000, a shell section integrates membrane and plate behavior; therefore, all displacements and plate-bending rotations result in layer strains, and all forces and plate-bending moments are influenced by stresses. In most apps, you should use the shell section. The quick start tool is used to specify the layers. Some characteristics must be defined in order for the layers to be defined automatically. Two layers of rebars are used in the shear walls. Each layer of rebar has the same size and spacing, and C25/30 concrete and rebar materials are utilized for the shear wall as presented in Figure 13. The component is specified with linear or nonlinear material in each direction for each layer. A simpler model should be utilized even though it is more realistic to define all components as nonlinear as this is time costly and can include multiple failing mechanisms. S11 identifies the rebars as

nonlinear. The defined rebars align with the S22 direction since they are vertical, which is consistent with the S22 shell stress behavior the concrete fractures, rebars may transmit shear pressures if the rebar stress component S12 is set to nonlinear. Despite the model's lack of dowels, this may depict dowel action. In each situation, it is necessary to determine if this should be computed, although the most cautious course of action is to designate the rebar stress component S12 as inactive. The S12 behavior in this instance is set to linear

Figure 13

*Shear wall layer definition in SAP2000*

Shell Section Layer Definition

Layer Definition Data

Layer Name	Distance	Thickness	Type	Num Int. Points	Material	Material Angle	Type	Material Component S11	Material Component Behavior S22	Material Component Behavior S12
ConcM	0.	0.3	Membrane	1	concrete	0.	Directional	Linear	Nonlinear	Linear
ConcM	0.	0.3	Membrane	1	concrete	0.	Directional	Linear	Nonlinear	Linear
TopBar2M	0.110475	0.000946	Membrane	1	Rebar	90.	Directional	Nonlinear	Inactive	Linear
BotBar2M	-0.110475	0.000946	Membrane	1	Rebar	90.	Directional	Nonlinear	Inactive	Linear
ConcP	0.	0.3	Plate	2	concrete	0.	Directional	Linear	Linear	Linear

Quick Start   Add   Insert   Modify   Delete

Section Name

Highlight Selected Layer

### 3.19 Bracing

The bracing has been chosen from the steel channel data base provided by the program according to the AISC code.

### 3.20 Slab design

The ACI 318-14 was utilized as the primary standard for the design of the slabs, and the equations were derived from it. One of two slab types two-way or one-way had to be chosen before the design could begin. The ratio of (long span/short span) must be more than 2, according to the regulation, for a slab to be considered one-way. However, if (long span/short span) equals 2, it is a two-way slab. Following the



determination of the type, the slab thickness was choosing from code minimum thickness requirement.

### 3.21 Geometry of frames

The following table shed light on the cross section of the elements that have been defined for the purpose of this study. A total number of 9 3D concrete frames have been modelled and analysed with same cross section and identical number of span but different span length and number of story. Models with 10 story has same cross and identical beams and columns size. The bellow Table 7 illustrate the details of the building configuration.

Table 7

#### *Details of the frame's configuration*

No. of Models	Storey Height (m)	No. of Storey	Number of Span	Span Length (m)	Thickness of Shear Wall (mm)	Bracing System	Slab Thickness (mm)
1	3.5	10	5	5m	-	-	200
2	3.5	10	5	5m	300	-	200
3	3.5	10	5	5m	-	C150×26	200
4	3.5	10	5	6m	-	-	200
5	3.5	10	5	6m	300	-	200
6	3.5	10	5	6m	-	C150×26	200
7	3.5	10	5	7m	-	-	200
8	3.5	10	5	7m	300	-	200
9	3.5	10	5	7m	-	C150×26	200

#### **3.21.1 Reinforcement Details**

The columns and beams were set up in accordance with method-to-capability design, and the buildings were erected in accordance with code ACI318-14. In Tables 8 and 9 below in this section, the reinforcement details for beams and columns for mid-rise buildings are displayed.

Table 8

*Reinforcement details of beams for 10-story models*

No Model.	Storey	Cross Section (mm)	Longitudinal Reinforcement		Shear Reinforcement (mm)
			Top	Bottom	
1	1 <sup>st</sup> to 7 <sup>th</sup>	300×500	8 Ø20	4 Ø20	Ø12 @100
	8 <sup>th</sup> to 10 <sup>th</sup>	300×400	6 Ø22	4 Ø20	
2	1 <sup>st</sup> to 7 <sup>th</sup>	300×500	8 Ø20	4 Ø20	Ø12 @100
	8 <sup>th</sup> to 10 <sup>th</sup>	300×400	6 Ø22	4 Ø20	
3	1 <sup>st</sup> to 7 <sup>th</sup>	300×500	8 Ø20	4 Ø20	Ø12 @100
	8 <sup>th</sup> to 10 <sup>th</sup>	300×400	6 Ø22	4 Ø20	
4	1 <sup>st</sup> to 7 <sup>th</sup>	300×500	8 Ø20	4 Ø20	Ø12 @100
	8 <sup>th</sup> to 10 <sup>th</sup>	300×400	6 Ø22	4 Ø20	
5	1 <sup>st</sup> to 7 <sup>th</sup>	300×500	8 Ø20	4 Ø20	Ø12 @100
	8 <sup>th</sup> to 10 <sup>th</sup>	300×400	6 Ø22	4 Ø20	
6	1 <sup>st</sup> to 7 <sup>th</sup>	300×500	8 Ø20	4 Ø20	Ø12 @100
	8 <sup>th</sup> to 10 <sup>th</sup>	300×400	6 Ø22	4 Ø20	
7	1 <sup>st</sup> to 7 <sup>th</sup>	300×500	8 Ø20	4 Ø20	Ø12 @100
	8 <sup>th</sup> to 10 <sup>th</sup>	300×400	6 Ø22	4 Ø20	
8	1 <sup>st</sup> to 7 <sup>th</sup>	300×500	8 Ø20	4 Ø20	Ø12 @100
	8 <sup>th</sup> to 10 <sup>th</sup>	300×400	6 Ø22	4 Ø20	
9	1 <sup>st</sup> to 7 <sup>th</sup>	300×500	8 Ø20	4 Ø20	Ø12 @100
	8 <sup>th</sup> to 10 <sup>th</sup>	300×400	6 Ø22	4 Ø20	
	8 <sup>th</sup> to 10 <sup>th</sup>	300×400	6 Ø22	4 Ø20	

Table 9

*Reinforcement details of columns for 10-story models*

No Model.	Storey	Cross Section (mm)	Longitudinal Reinforcement	Shear Reinforcement (mm)
1	1 <sup>st</sup> to 7 <sup>th</sup>	600×600	14 Ø22	Ø12 @150
	8 <sup>th</sup> to 10 <sup>th</sup>	500×500	12 Ø22	
2	1 <sup>st</sup> to 7 <sup>th</sup>	600×600	14 Ø22	Ø12 @150
	8 <sup>th</sup> to 10 <sup>th</sup>	500×500	12 Ø22	

3	1 <sup>st</sup> to 7 <sup>th</sup>	600×600	14 Ø22	Ø12 @150
	8 <sup>th</sup> to 10 <sup>th</sup>	500×500	12 Ø22	
4	1 <sup>st</sup> to 7 <sup>th</sup>	600×600	14 Ø22	Ø12 @150
	8 <sup>th</sup> to 10 <sup>th</sup>	500×500	12 Ø22	
5	1 <sup>st</sup> to 7 <sup>th</sup>	600×600	14 Ø22	Ø12 @150
	8 <sup>th</sup> to 10 <sup>th</sup>	500×500	12 Ø22	
6	1 <sup>st</sup> to 7 <sup>th</sup>	600×600	14 Ø22	Ø12 @150
	8 <sup>th</sup> to 10 <sup>th</sup>	500×500	12 Ø22	
7	1 <sup>st</sup> to 7 <sup>th</sup>	600×600	14 Ø22	Ø12 @150
	8 <sup>th</sup> to 10 <sup>th</sup>	500×500	12 Ø22	
8	1 <sup>st</sup> to 7 <sup>th</sup>	600×600	14 Ø22	Ø12 @150
	8 <sup>th</sup> to 10 <sup>th</sup>	500×500	12 Ø22	
9	1 <sup>st</sup> to 7 <sup>th</sup>	600×600	14 Ø22	Ø12 @150
	8 <sup>th</sup> to 10 <sup>th</sup>	500×500	12 Ø22	
	8 <sup>th</sup> to 10 <sup>th</sup>	500×500	12 Ø22	

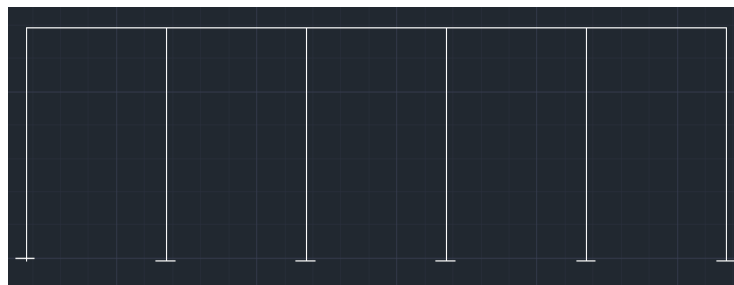
### 3.21.2 Models description

Three frames system: a moment-resistant frame (MRF), a moment-resistant frame with a shear wall (MRFSW), and a moment-resistant frame with bracing (MRFB) are under analysis in this study. For all of the modeling, the bonding condition for the support has been taken to be fixed, and the accompanying various parameters are provided throughout this thesis:

- Number of spans(N): 5 spans

Figure 14

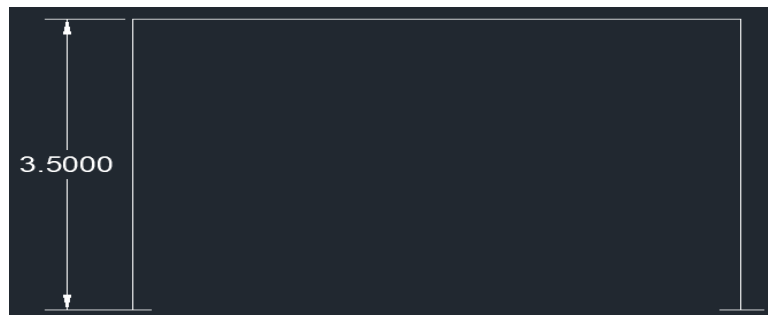
*Number of spans*



- Height of stories (H): Typical story height

Figure 15

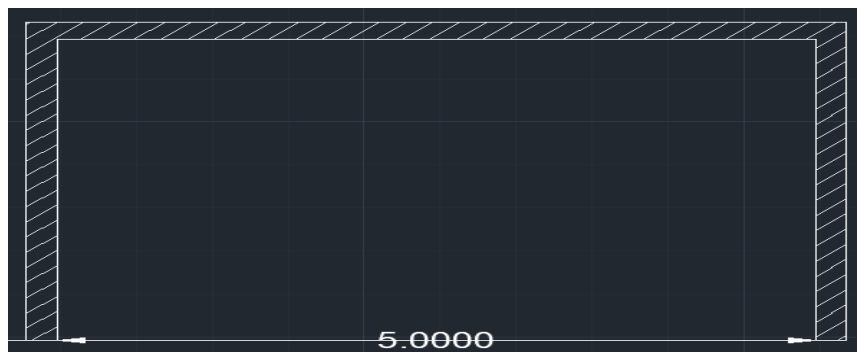
Typical story height



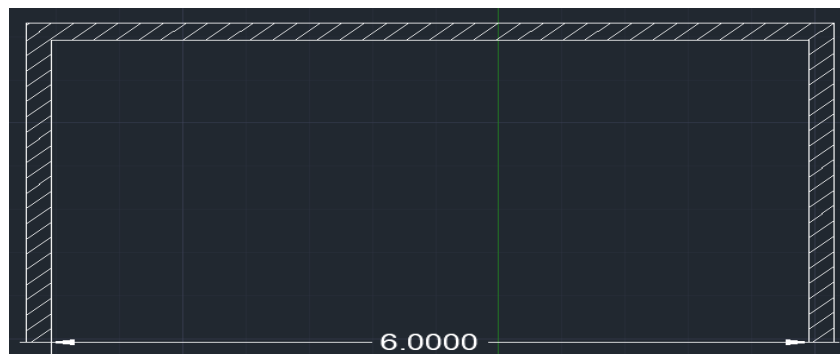
Span length(L): 5m, 6m, and 7m

Figure 16

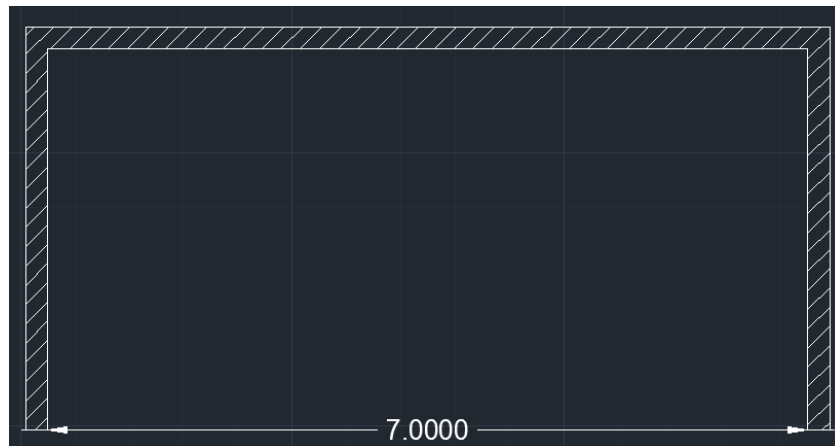
Span length of the frames; a) 5m, b) 6m, c) 7m.



a)



b)



c)

- Different 3D models

The following figures depicted the different models that have been modeled on SAP 2000 with respect to the code specification.

Figure 17

*MRF model with 10-story different views; a) Elevation; b) 3D*

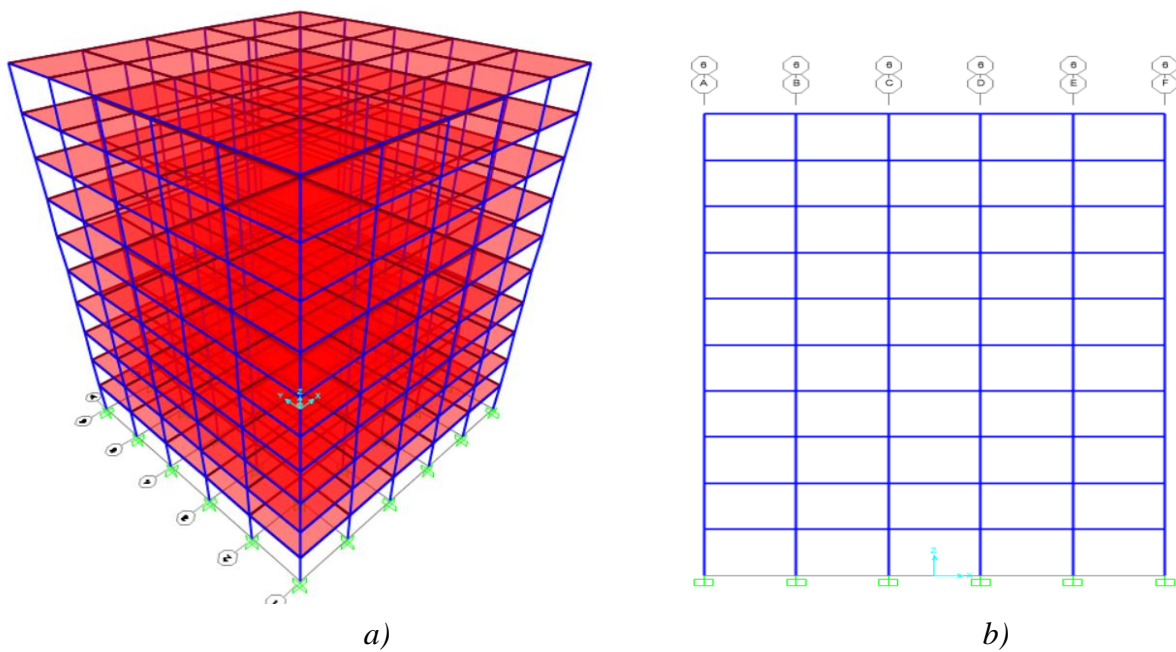


Figure 18

MRFSW model with 10-story different views; a) Elevation; b) 3D

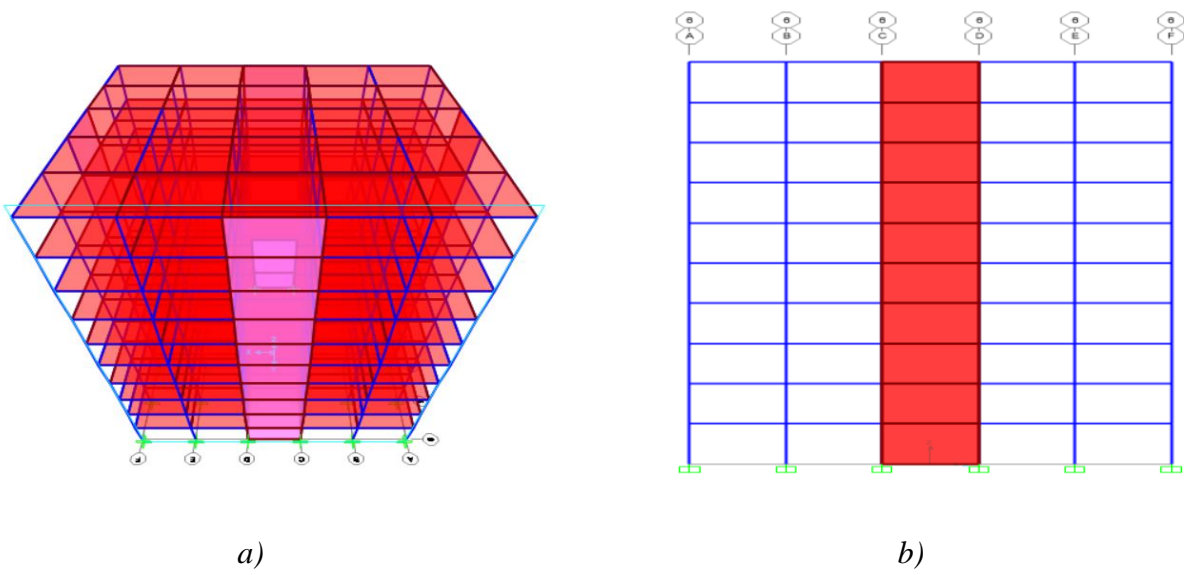


Figure 19

MRFB model with 10-story views ; a) Elevation; b) 3D

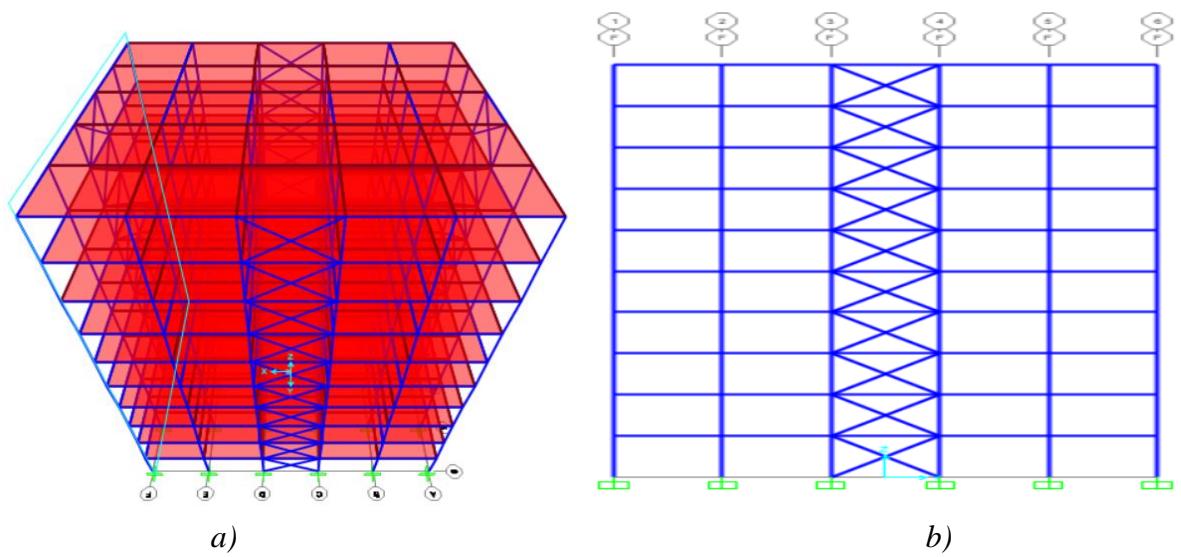
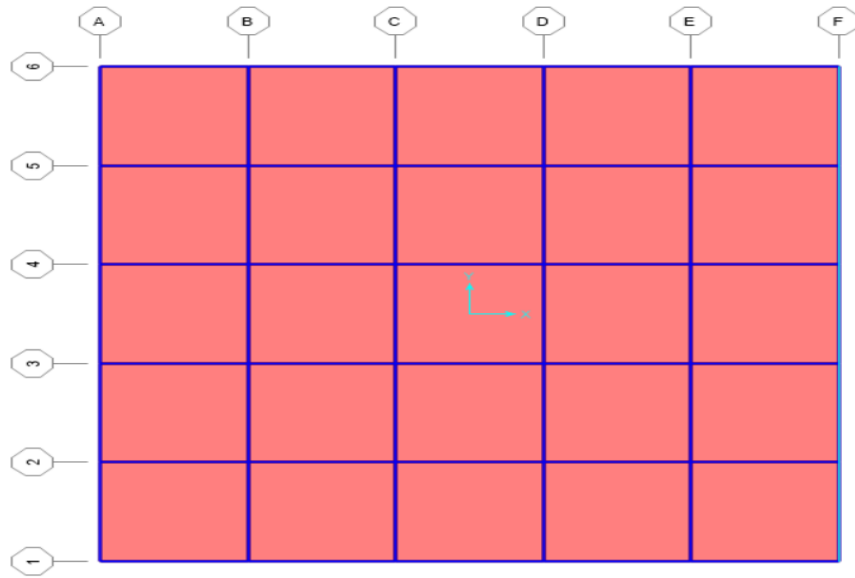


Figure 20

*Plan view*

## CHAPTER IV

### Results and discussions

This chapter not only gives the results that were drawn from the analysis and data gathered, but also discusses the outcomes.

#### 4.1 Introduction

Under seismic load, the structure will bend substantially more if it loses elasticity. Additionally, any structure's ability to withstand any lateral load without collapsing is referred to as ductility. Because it employed actual ground motion to forecast the damage measure, IDA is an effective technique for analyzing a building's response during seismic activity. Here discussed all results of the analyses methods that are obtained from SAP 2000 software, the inter-story drift ratio is obtained for all the 3D moment resisting frames and a comparison is made based on the IDA curve that shed light on the capability of the structure to go from minimum cracks to the global instability in order to provide the fragility curve that will assess the probability of damage. Besides this, the fundamental time period and drift will also be used for this comparison since they give also an overall understanding of the structural capacity.

The discussion of the results is divided into four sections: a) the first part discusses the effects of span length on the ductility under different ground motions through the IDA curve; b) the second part discusses the effects of span length on the likelihood of exceeding the limit level according to the fragility curve; c) the third point of this discussion is based on the story drift; and d) emphasis on the fundamental time period that will complete the analysis by comparing the different framing system in seismic activities. A global comparison will be raised among all the different systems eventually.

#### 4.2 Moment resisting frame

The 3 tables below from 10 a) to c), show the information related to the different framing systems that have been adopted for this study are: MRFs with 5m, 6m, and 7m.



Table 10

*a) Inter-story drift ratio of the MRFs with 5m span length*

	GM1	GM2	GM3	GM4	GM5	GM6	GM7
	ISDR	ISDR	ISDR	ISDR	ISDR	ISDR	ISDR
IM(g)	(%)	(%)	(%)	(%)	(%)	(%)	(%)
0	0	0	0	0	0	0	0
0.1	0.68	0.84	0.96	1.34	1.47	0.43	0.11
0.2	0.76	1.56	2.27	2.18	2.35	0.67	0.22
0.3	1.14	2.23	3.5	3.8	1.85	0.95	0.33
0.4	1.58	2.79	7.94	10	3.05	1.21	0.45

*b) Inter-story drift ratio of the MRFs with 6m span length*

	GM1	GM2	GM3	GM4	GM5	GM6	GM7
	ISDR	ISDR	ISDR	ISDR	ISDR	ISDR	ISDR
IM(g)	(%)	(%)	(%)	(%)	(%)	(%)	(%)
0	0	0	0	0	0	0	0
0.1	0.41	0.87	1.21	1.12	0.9	0.4	0.17
0.2	0.82	1.5	2.52	2.53	1.82	0.76	0.34

*c) Inter-story drift ratio of the MRFs with 7m span length*

	GM1	GM2	GM3	GM4	GM5	GM6	GM7
	ISDR	ISDR	ISDR	ISDR	ISDR	ISDR	ISDR
IM(g)	(%)	(%)	(%)	(%)	(%)	(%)	(%)
0	0	0	0	0	0	0	0
0.1	0.47	0.86	2.73	20.89	1.73	0.59	0.2
0.2	1.1	3.73	13.8	12.31	15.38	1.26	0.4

### *4.2.1 Discussion of the results*

#### *a) IDA Curve for all MRFs*

The scaled accelerogram that is employed in the study for one several IM is determined by the behaviour of an EDP variable, which is represented by the IDA curve. Depending on the number of IMs, the IDA curve can be drawn in one or more dimensions, one of which must clearly be scalability. The figures below from 21 a) to c) shed light on the behaviour of the structure that is given in 3 assets: the appearance of the first cracks, the yielding, and eventually the collapse. From figures 21 (a-b) of the MRFs with a 5m and 6m span length that all the segments of the graph exhibit a linear elastic region that ends at  $PGA = 0.1g$  apart from the GM7 that exhibits a progressive degradation toward the appearance of the first crack which corresponds to the IO limit state till the CP limit state that is the collapse region. The IDA curve for MRFs with 7m in Figure 21 c), is quite similar to other system but the segment of the graphs tend to reach a quick collapse stage due to the span length that has increased. It can be observed that the target PGA was fixed to 0.8g but for all the MRFs the dynamic instability that appeared earlier in the analysis, could not allow it to reach the target. This is due to the fact that when a structure is designed to allow a lower collapse mechanism, the use of PGA as EDP takes it into account and the final straightening zone occurs when EDP is deposited in the structure at a higher rate, signalling the onset of dynamic instability.

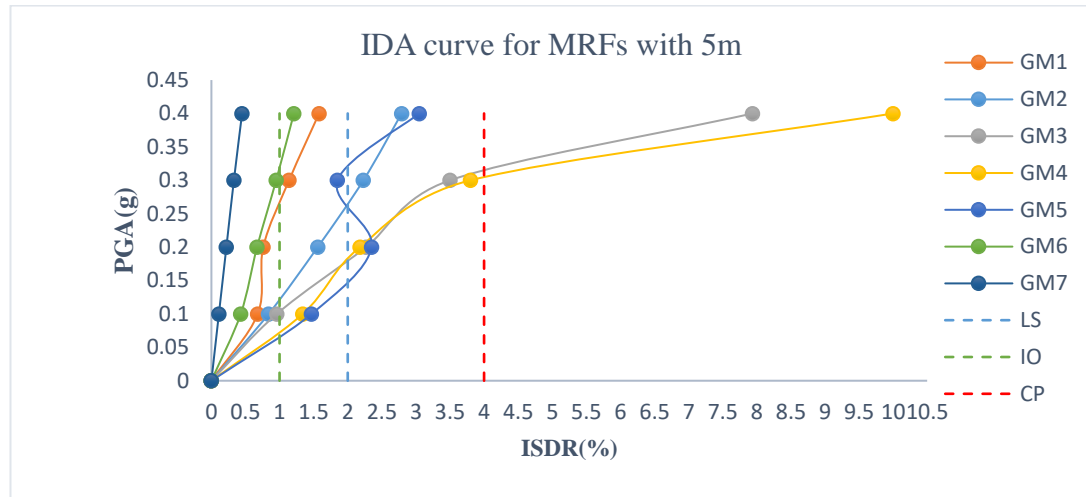
Similarly, to that, this phenomenon is described by static instability, where the deformations alter to infinity with only a few increments in IM. At the point where IM reaches its greatest value and both IM and EDP reach infinity, the curve then becomes straight. Therefore, any PGA up to 0.4g can be considered as the total collapse PGA for MRFs with 5m and up to 0.3g the collapse points for both MRFs with 6m and 7m. It can be observed that for the first MRFs in Figure 21 a) considering the GM3 and GM4 since they both have higher magnitudes, the first cracks appeared at 0.08g for GM4 and 0.1g for GM3, and both yield at 0.18g. Finally, the collapse point can be observed at 0.32g and 0.3g respectively.

For the MRFs with 6m in Figure 21 b), the first cracks are observed at 0.08g for GM3 and 0.07 for GM4; the yielding is at 0.15g and 0.18g respectively. The point of collapse can be seen at 0.22g for GM4 and 0.24g for GM3.

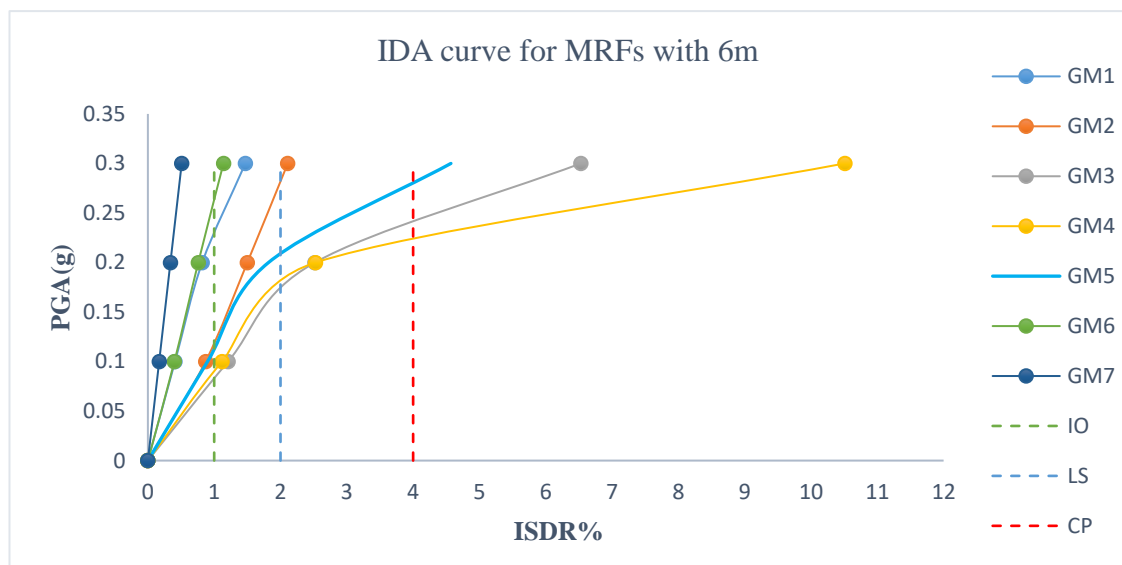
The MRFs with 7m in Figure 21 c), showed much susceptibility to ground motion because of the importance of the span length. The structure shown earlier points of reaching the undesired behavior compares to the other system. For GM4 and GM3, the cracking point starts at 0.01g and 0.05g respectively, and yields at 0.02g for GM4 and 0.08g for GM3. The collapse can be seen at 0.03g and 0.13g respectively.

Figure 21

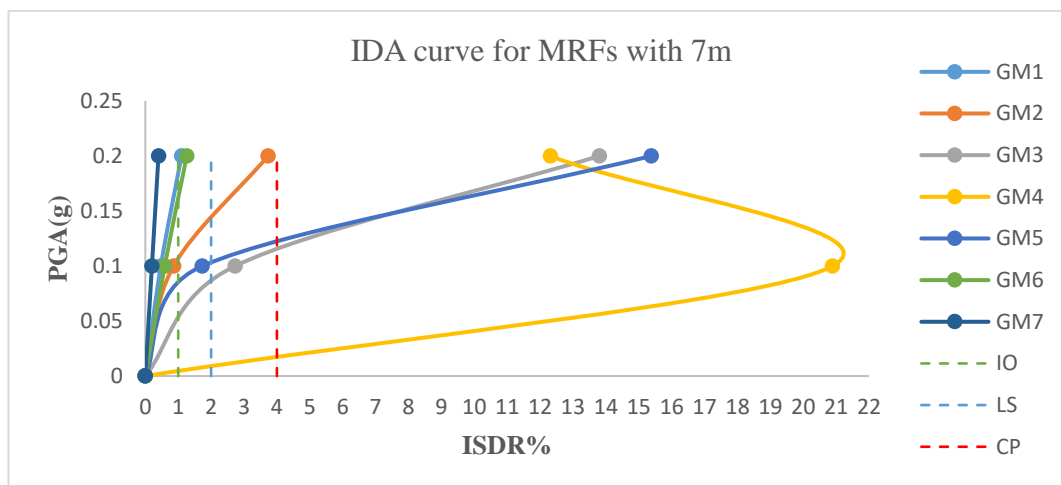
a) IDA Curve for moment resisting frame with 5m span length



b) IDA Curve for moment resisting frame with 6m span length



c) IDA Curve for moment resisting frame with 7m span length

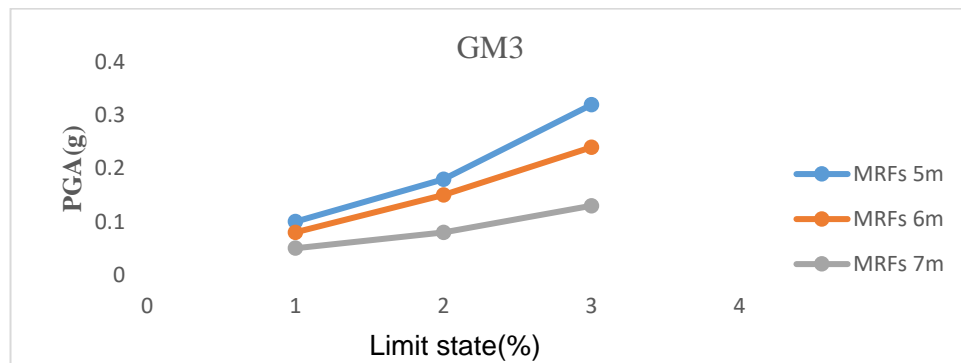


➤ *Comparison among the MRFs models with respect to IDA curve results*

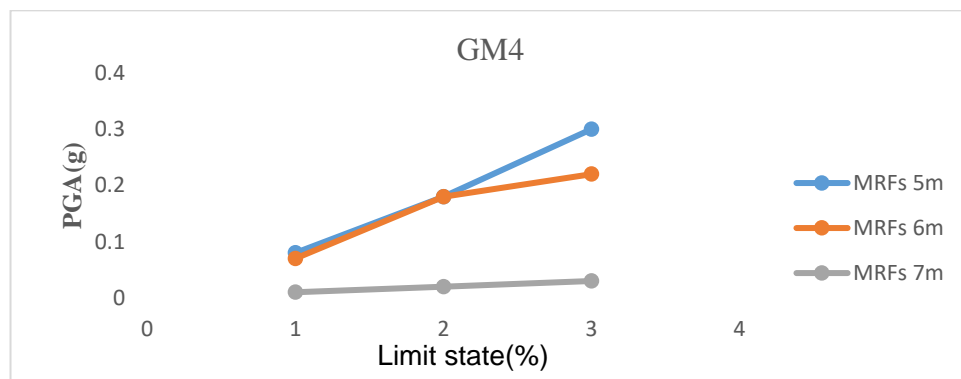
According to the figures below 22 a) and 22 b), it can be concluded that the increase in the length of the span affects the stiffness of the structure because as the span is becoming greater, the value of the limit states is decreasing. The moment-resisting frame is a framing system that is really weak in seismic environments and from the graphs below it is obvious that the MRFs with 5m from the GM3 and GM4, have a higher stiffness that allowed the structure to resist more. Based on the 2 graphs that depicted the rate of the decrease in the performance of the structure, it can be seen that the MRFs with 6m and 7m based on the GM3 have 20% and 50% for IO, 17% and 55.5% for LS, 25% and 59.4% for CP respectively less than the MRFs with 5m. According to the GM4, compared to the rate of the MRFs with 5m PGA, there is a decrease in the value of the MRFs with 6m and 7m respectively which is about 12.5% and 85.7% for IO, 88.9% for LS, 26.67% and 86.4% for CP.

Figure 22

Different limit state values according to: a) GM3 with MRFs, b) GM4 with MRFs



a)



b)

### b) Fragility curve for all MRFs

In the following Tables from 11 a) to c) is the tabled information related to the fragility function data for the 3-limit state that have been calculated for the 3 MRFs that are used to generate the fragility curve of each system the chance of going above each limit state. The input tables that give those fragility data will be presented in the Appendixes B.

Table 11

a) Fragility function data for the MRFs with 5m span length

Acceleration	Fragility for the Limit States of Drift at		
	1 (%)	2 (%)	4 (%)
<b>0.0100</b>	0.0143	0.0045	0.0012
<b>0.1667</b>	0.5373	0.3710	0.2260

<b>0.3333</b>	0.7441	0.5921	0.4247
<b>0.5000</b>	0.8376	0.7129	0.5552
<b>0.6667</b>	0.8884	0.7868	0.6452
<b>0.8333</b>	0.9191	0.8355	0.7100
<b>1.0000</b>	0.9391	0.8695	0.7584
<b>1.1667</b>	0.9527	0.8942	0.7956
<b>1.3333</b>	0.9625	0.9127	0.8250
<b>1.5000</b>	0.9697	0.9269	0.8485
<b>1.6667</b>	0.9751	0.9380	0.8677
<b>1.8333</b>	0.9793	0.9469	0.8835
<b>2.0000</b>	0.9825	0.9541	0.8968
<b>2.1667</b>	0.9852	0.9600	0.9080
<b>2.3333</b>	0.9873	0.9650	0.9175
<b>2.5000</b>	0.9890	0.9691	0.9257
<b>2.6667</b>	0.9904	0.9725	0.9328
<b>2.8333</b>	0.9916	0.9755	0.9389
<b>3.0000</b>	0.9926	0.9781	0.9443
<b>3.1667</b>	0.9935	0.9803	0.9491
<b>3.3333</b>	0.9942	0.9822	0.9533
<b>3.5000</b>	0.9948	0.9838	0.9570
<b>3.6667</b>	0.9954	0.9853	0.9604
<b>3.8333</b>	0.9958	0.9866	0.9634
<b>4.0000</b>	0.9962	0.9877	0.9660
<b>4.1667</b>	0.9966	0.9887	0.9685
<b>4.3333</b>	0.9969	0.9897	0.9707
<b>4.5000</b>	0.9972	0.9905	0.9726
<b>4.6667</b>	0.9974	0.9912	0.9744
<b>4.8333</b>	0.9976	0.9918	0.9761
<b>5.0000</b>	0.9978	0.9924	0.9776

*b) Fragility function data for the MRFs with 6m span length*

Acceleration	Fragility for the Limit States of Drift at		
	1 (%)	2 (%)	4 (%)
<b>0.0100</b>	0.0018	0.0004	0.0001
<b>0.1667</b>	0.5585	0.3855	0.2330
<b>0.3333</b>	0.8160	0.6780	0.5095
<b>0.5000</b>	0.9100	0.8166	0.6788
<b>0.6667</b>	0.9508	0.8878	0.7814

<b>0.8333</b>	0.9710	0.9275	0.8460
<b>1.0000</b>	0.9819	0.9511	0.8883
<b>1.1667</b>	0.9881	0.9658	0.9169
<b>1.3333</b>	0.9919	0.9755	0.9370
<b>1.5000</b>	0.9944	0.9820	0.9513
<b>1.6667</b>	0.9960	0.9865	0.9618
<b>1.8333</b>	0.9970	0.9897	0.9697
<b>2.0000</b>	0.9978	0.9920	0.9756
<b>2.1667</b>	0.9983	0.9937	0.9802
<b>2.3333</b>	0.9987	0.9950	0.9837
<b>2.5000</b>	0.9990	0.9960	0.9865
<b>2.6667</b>	0.9992	0.9967	0.9888
<b>2.8333</b>	0.9994	0.9973	0.9906
<b>3.0000</b>	0.9995	0.9978	0.9920
<b>3.1667</b>	0.9996	0.9982	0.9932
<b>3.3333</b>	0.9997	0.9985	0.9942
<b>3.5000</b>	0.9997	0.9987	0.9950
<b>3.6667</b>	0.9998	0.9989	0.9957
<b>3.8333</b>	0.9998	0.9991	0.9963
<b>4.0000</b>	0.9998	0.9992	0.9968
<b>4.1667</b>	0.9999	0.9993	0.9972
<b>4.3333</b>	0.9999	0.9994	0.9975
<b>4.5000</b>	0.9999	0.9995	0.9978
<b>4.6667</b>	0.9999	0.9996	0.9981
<b>4.8333</b>	0.9999	0.9996	0.9983
<b>5.0000</b>	0.9999	0.9997	0.9985

*c) Fragility function data for the MRFs with 7m span length*

Acceleration	Fragility for the Limit States of Drift at		
	1 (%)	2 (%)	4 (%)
<b>0.0100</b>	0.0163	0.0045	0.0010
<b>0.1500</b>	0.7102	0.5319	0.3469
<b>0.3000</b>	0.8930	0.7790	0.6160
<b>0.4500</b>	0.9501	0.8793	0.7573
<b>0.6000</b>	0.9733	0.9275	0.8373
<b>0.7500</b>	0.9843	0.9534	0.8859
<b>0.9000</b>	0.9902	0.9686	0.9172
<b>1.0500</b>	0.9936	0.9780	0.9382

<b>1.2000</b>	0.9956	0.9841	0.9528
<b>1.3500</b>	0.9969	0.9882	0.9632
<b>1.5000</b>	0.9978	0.9910	0.9709
<b>1.6500</b>	0.9983	0.9931	0.9766
<b>1.8000</b>	0.9987	0.9946	0.9810
<b>1.9500</b>	0.9990	0.9957	0.9844
<b>2.1000</b>	0.9993	0.9966	0.9871
<b>2.2500</b>	0.9994	0.9972	0.9892
<b>2.4000</b>	0.9995	0.9977	0.9909
<b>2.5500</b>	0.9996	0.9981	0.9923
<b>2.7000</b>	0.9997	0.9984	0.9934
<b>2.8500</b>	0.9997	0.9987	0.9943
<b>3.0000</b>	0.9998	0.9989	0.9951
<b>3.1500</b>	0.9998	0.9990	0.9957
<b>3.3000</b>	0.9999	0.9992	0.9963
<b>3.4500</b>	0.9999	0.9993	0.9967
<b>3.6000</b>	0.9999	0.9994	0.9971
<b>3.7500</b>	0.9999	0.9995	0.9975
<b>3.9000</b>	0.9999	0.9995	0.9978
<b>4.0500</b>	0.9999	0.9996	0.9980
<b>4.2000</b>	0.9999	0.9997	0.9982
<b>4.3500</b>	1.0000	0.9997	0.9984
<b>4.5000</b>	1.0000	0.9997	0.9986

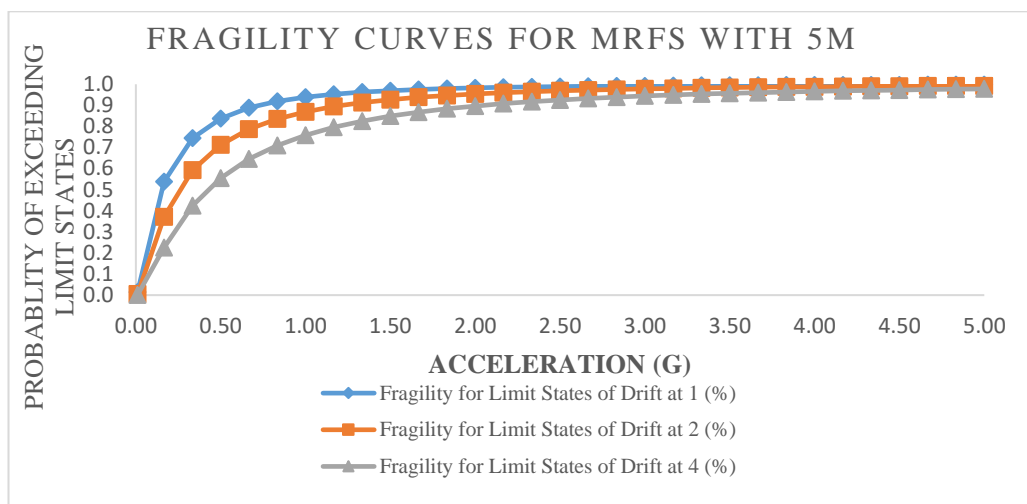
Disaster models frequently employ fragility curves to define the likelihood of going above a specific damage condition as a relation to environmental change. Fragility curves of the MRFs are presented in the Figures below from 22 a) to c) which gives the percentage of each PGA to overpass the given limit state. It is obvious from the figure below that the MRFs with 5m have better performance under seismic loads. As previously stated, based on the IDA curve, the fragility curve confirms the highest stiffness of the MRFs with 5m. For instance, in Figure 23 a) at PGA 0.5g, there is a 59% probability of exceeding the CP limit state, and compared to the MRFs with 6m and 7m presented in Figure 23 b) and c), there is a 70% and 80% probability of exceeding the CP limit state respectively. Even though the MRFs with 5m offered the lowest probability compared to the other models, the rate of 59% is a really high value because half of the structure is luckily to collapse under 0.5g which means that there



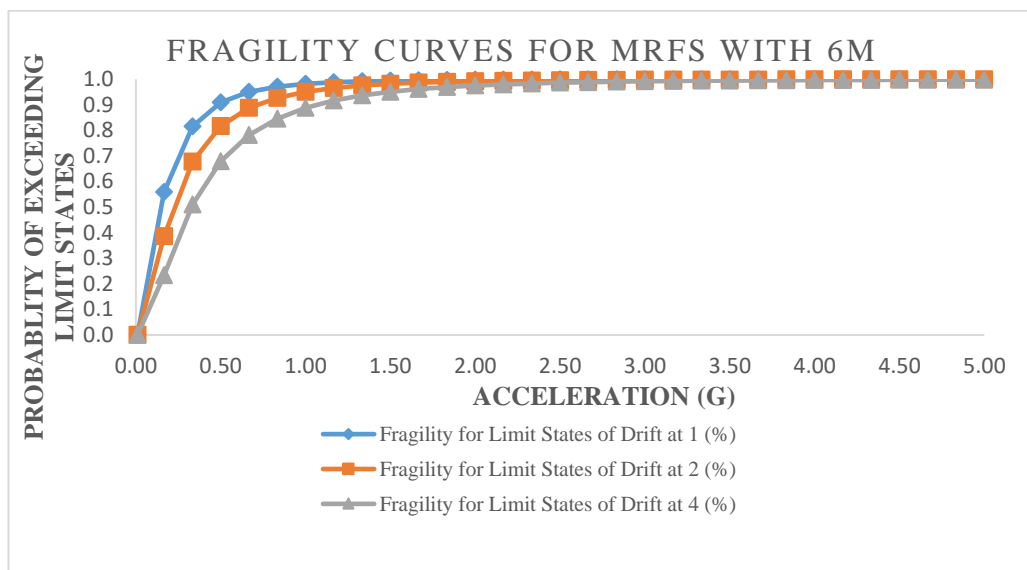
is no possibility of refurbishment. This susceptibility of the framing system is due to the lack of stiffness that the structures owing to the height of the structure but also the lack of lateral reinforcing parameters that can enhance the serviceability of the structure.

Figure 23

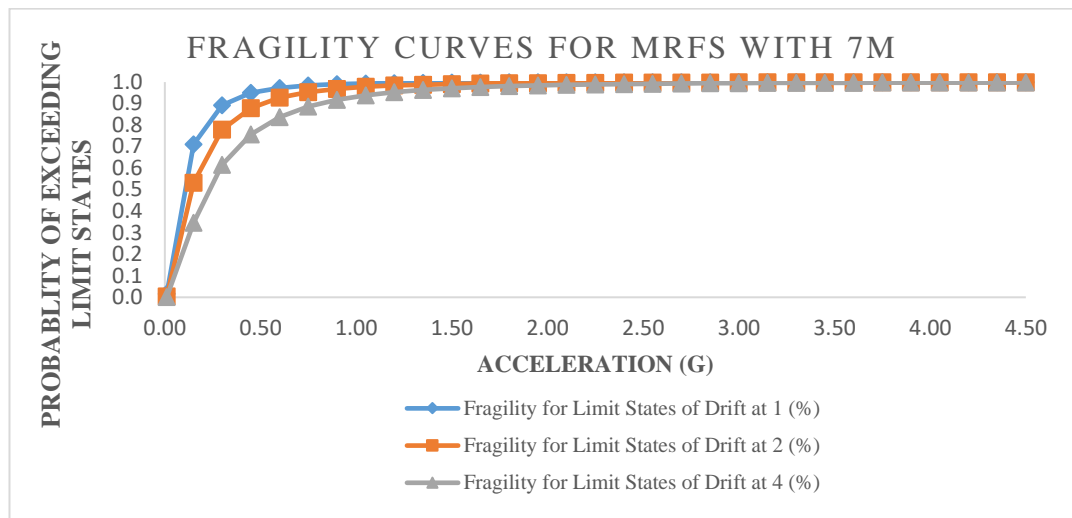
a) Fragility curve for MRFs with 5m span length



b) Fragility curve for MRFs with 6m span length



c) Fragility curve for MRFs with 7m span length

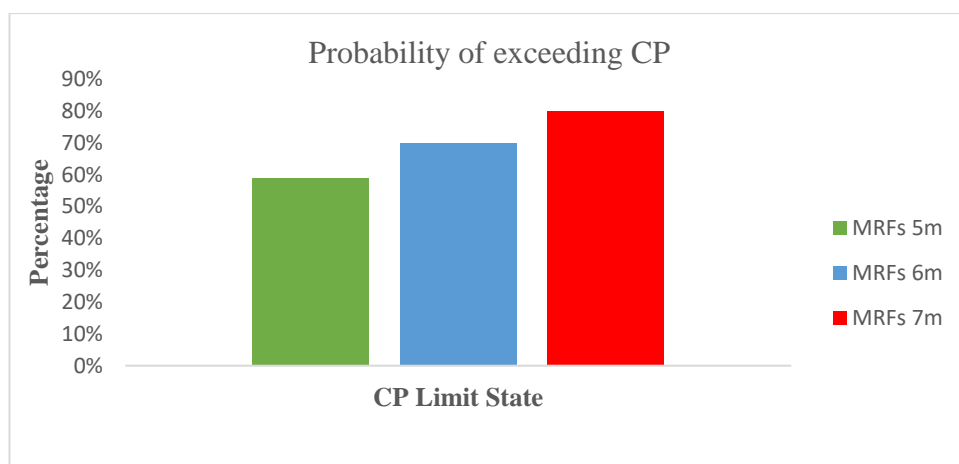


➤ *Comparison Among the MRFs models with respect to fragility curve results*

Figure 24 is depicted the values of the CP value that can be exceeded when the PGA is at 0.5 and it can be seen that the MRFs with a 5m span length have the lowest rate compared to the other models. The functioning of a building is directly impacted by the span length rise, which results in a reduction through system's stiffness. Compared to the susceptibility of MRFs with 5m, there is a 19% of increase with the MRFs with 6m and a 35, 6% of increase with the MRFs with 7m.

Figure 24

*Probability of exceeding the CP limit state graph for all the MRFs models*

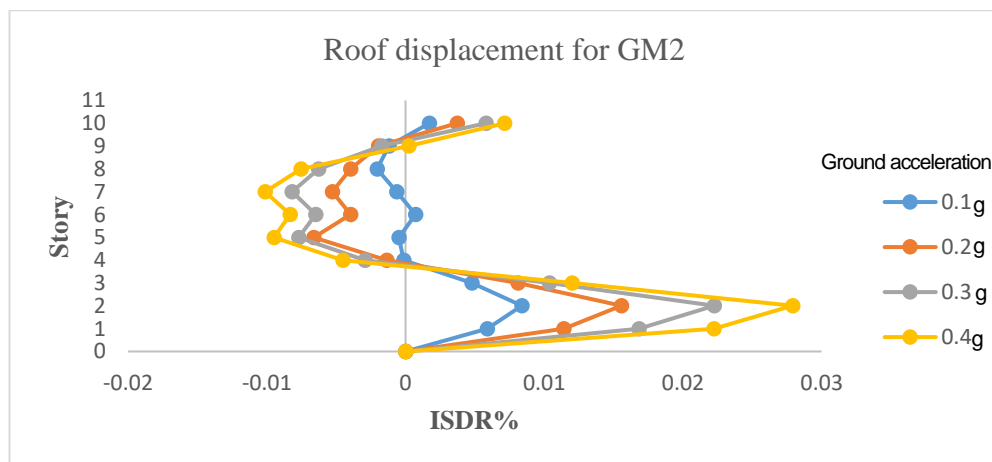


### C) Inter-Story Drift Ratio of all the MRFs models

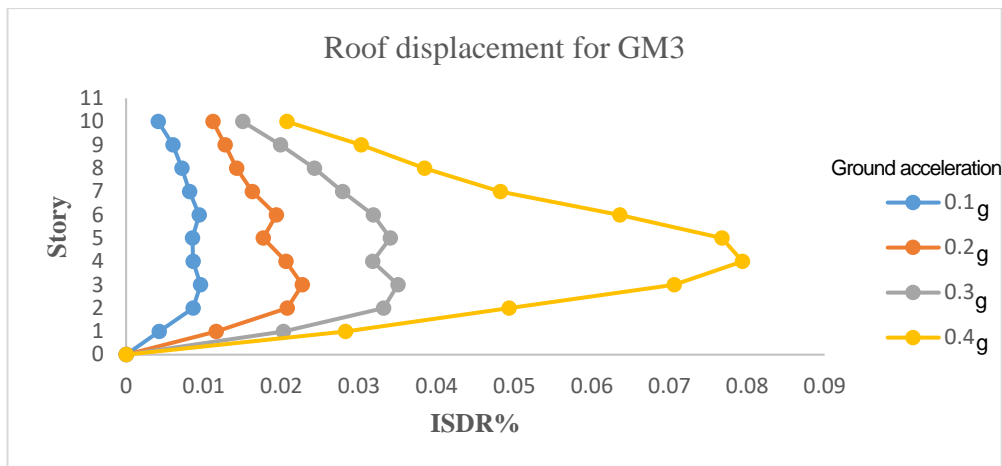
The analysed models from Figure 25 to 27, show the story drift ratio is inconsistent, especially with the GM2 which shows a negative multi-curvature plot but also the MRFs with 7m in general. The negative value of the ISDR is due to the effect of the higher mode that a structure might follow the second mode because each GM affects the structure differently owing to the amplitude, frequency, and duration of the shaking. This can be related to the design process where column and beam cross-section varies along the elevation of the building. In addition, the story drift ratio is the least at the top story. This can be related to the fact that the lateral story forces are higher towards the base of the structure and lower towards the roof, and the reason behind the low story drift at the base is the support fixities. Almost, all the models exhibit a similar higher value of displacement that is located at the first 4 story depending on the GM and model.

Figure 25

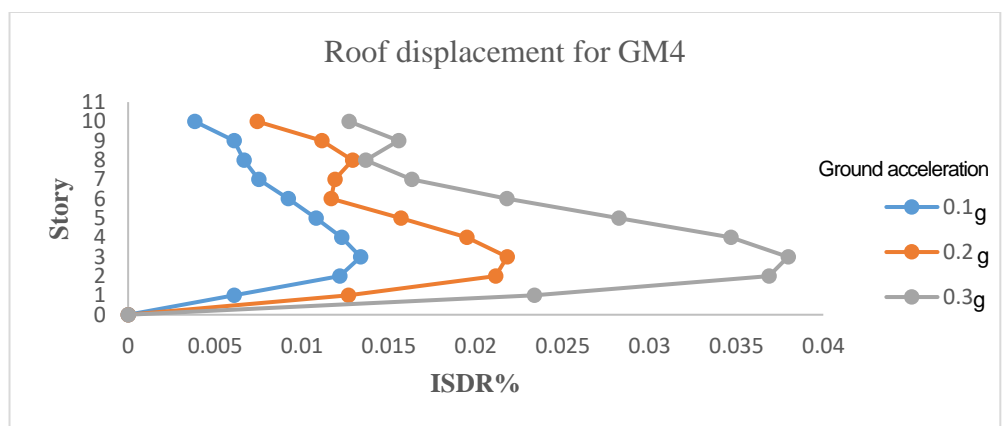
*Roof displacement for MRFs with 5m span length: a) GM2, b) GM3, c) GM4*



a)



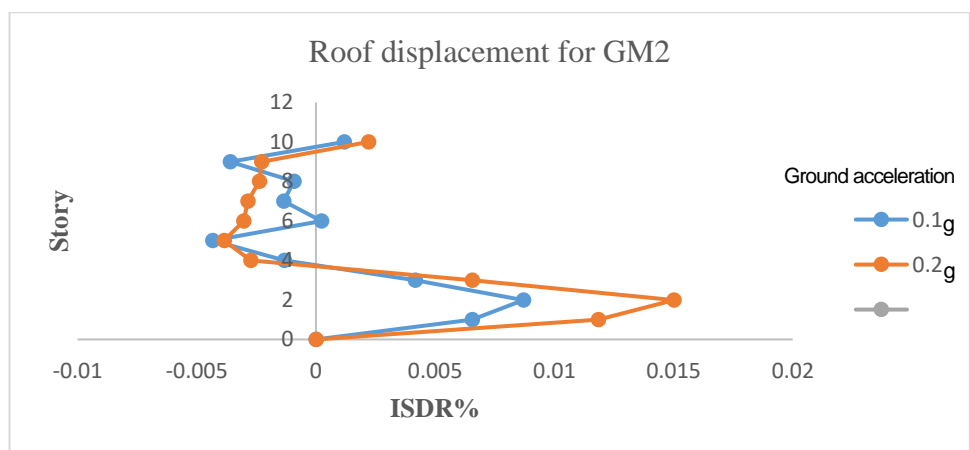
b)



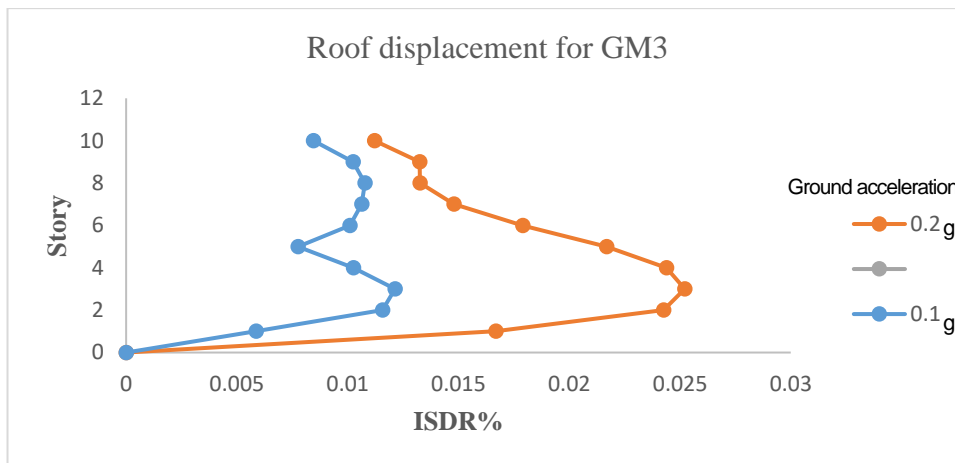
c)

Figure 26

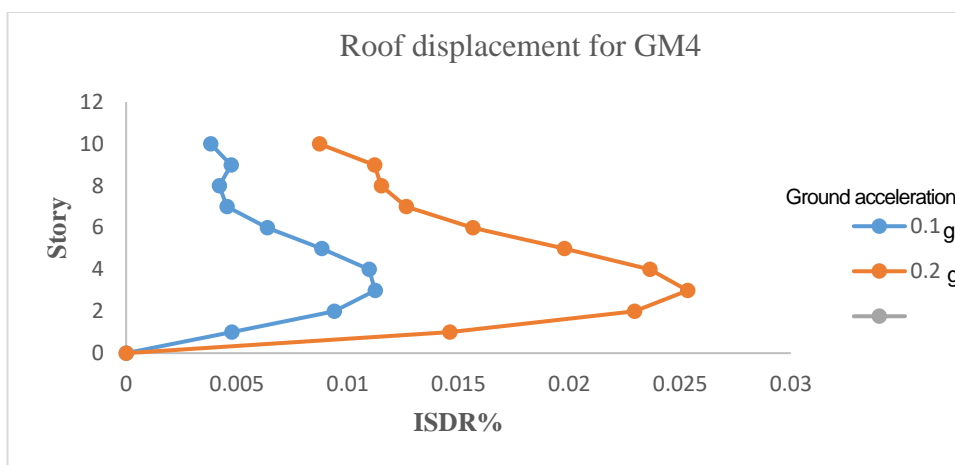
Roof displacement for MRFs with 6m span length: a) GM2, b) GM3, c) GM4



a)



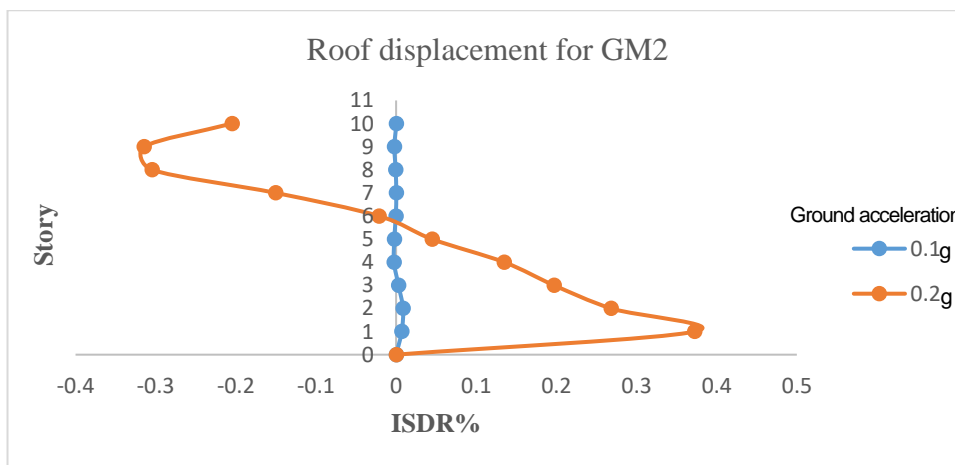
b)



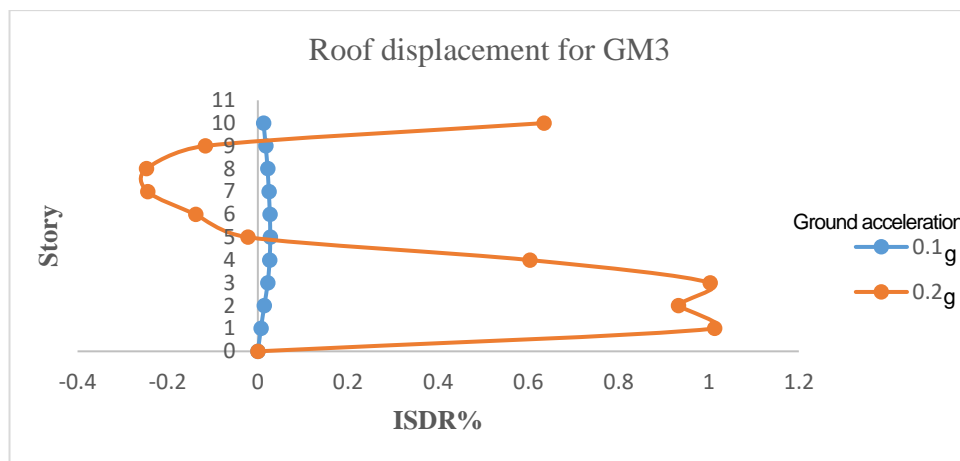
c)

Figure 27

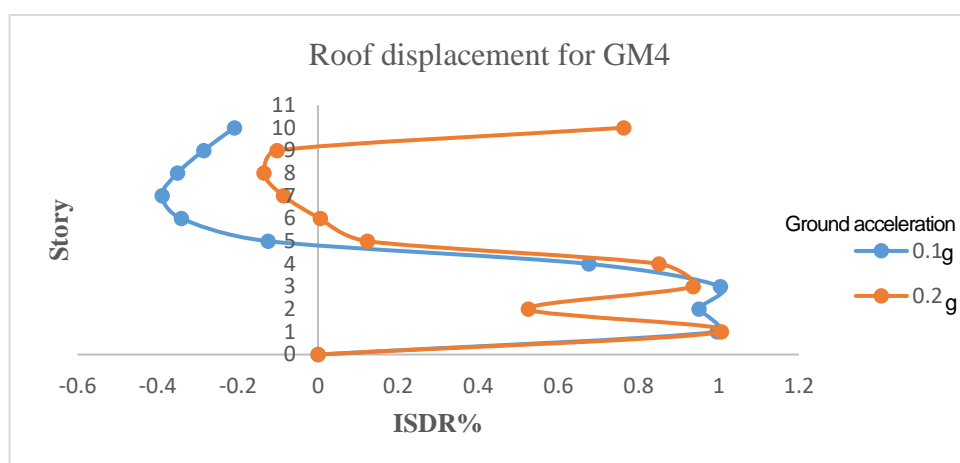
Roof displacement for MRFs with 7m span length: a) GM2, b) GM3, c) GM4



a)



b)



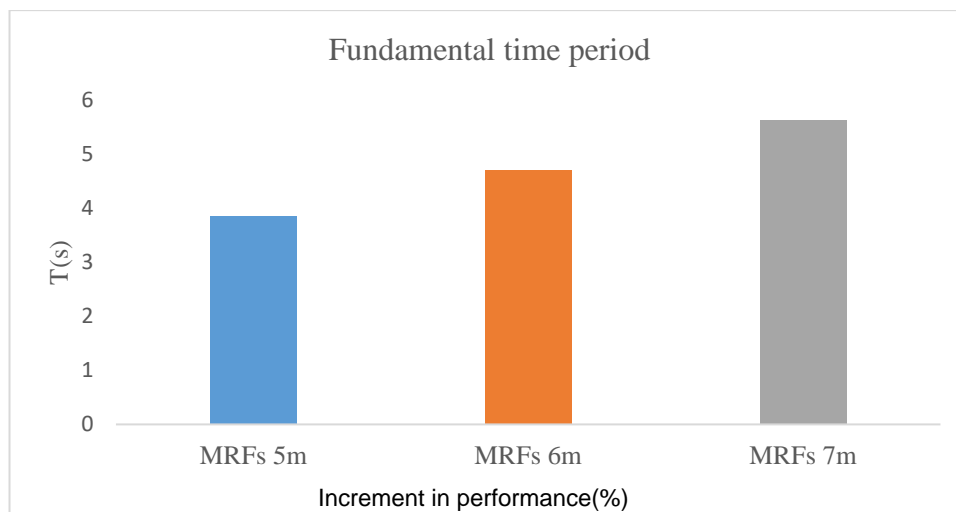
c)

#### d) Fundamental time period effect of all the MRFs models

Figure 28 sheds light on the first mode period of the 3 MRFs which is increasing with the increment of the span length. It can be seen that the MRFs with 5m have a lower mode compared to the other frames. From the graph, it is obvious that there are 21, 70%, and 45.48% of increases in the mode of the MRFs with 5m compared to the MRFs with 6m and 7m. The effect of the span length is due to the fact that longer spans are more flexible, which results in a longer period of vibration.

Figure 28

*The fundamental time period of all the MRFs models*



### 4.3 Moment resisting frame with bracing (MRFB)

The 3 tables below from 12 a) to c), show the information related to the ISDR to the different framing systems of bracing that have been adopted for this study which are: MRFB with 5m, 6m, and 7m.

Table 12

a) *Inter-story drift ratio of the MRFB with 5m span length*

	GM1	GM2	GM3	GM4	GM5	GM6	GM7
	ISDR	ISDR	ISDR	ISDR	ISDR	ISDR	ISDR
IM(g)	(%)	(%)	(%)	(%)	(%)	(%)	(%)
0	0	0	0	0	0	0	0
0.1	0.11	0.77	0.82	0.98	0.95	0.32	0.14
0.2	0.19	1.47	1.53	1.66	1.95	0.51	0.29
0.3	1.15	2.17	2.22	2.43	2.76	0.64	0.44
0.4	1.35	2.87	3.03	3.08	4.16	0.78	0.57
0.5	1.73	3.56	3.89	3.91	4.65	0.94	0.69
0.6	2.13	4.24	4.8	4.95	6.52	1.16	0.8
0.7	2.22	4.43	5.64	6.38	7.62	1.37	0.9
0.8	2.58	5.59	6.54	8.03	7.9	1.61	1.01

*b) Inter-story drift ratio of the MRFB with 6m span length*

	GM1	GM2	GM3	GM4	GM5	GM6	GM7
	ISDR	ISDR	ISDR	ISDR	ISDR	ISDR	ISDR
IM(g)	(%)	(%)	(%)	(%)	(%)	(%)	(%)
0	0	0	0	0	0	0	0
0.1	0.46	0.87	1.36	1.18	0.93	0.41	0.11
0.2	0.8	1.57	2.5	1.91	1.78	0.73	0.23
0.3	1.06	2.36	3.8	2.83	2.71	1.07	0.34
0.4	1.5	3.14	6.02	3.1	3.75	1.28	0.46
0.5	1.8	3.89	6.85	4.23	4.95	2.08	0.58
0.6	2.21	4.61	7.21	7.61	6.15	2.21	0.7

*c) Inter-story drift ratio of the MRFB with 7m span length*

	GM1	GM2	GM3	GM4	GM5	GM6	GM7
	ISDR	ISDR	ISDR	ISDR	ISDR	ISDR	ISDR
IM(g)	(%)	(%)	(%)	(%)	(%)	(%)	(%)
0	0	0	0	0	0	0	0
0.1	0.61	0.91	1.02	1.25	1.34	0.47	0.12
0.2	0.83	1.62	2.03	2.48	2.36	0.89	0.24
0.3	1.22	2.43	3.55	3.55	4.48	1.07	0.36
0.4	1.66	3.15	4.63	4.43	4.82	1.35	0.47
0.5	2.16	4.06	5.91	6.67	6.47	1.85	0.59
0.6	2.74	4.97	7.24	9.26	4.02	2.15	0.68

**4.3.1 Discussion of the results**

*a) IDA curve for all MRFB*

Here below presented from Figures 29 a) to 29 c), the IDA curves of the MRFB and all the segments exhibit a different linear elastic region that ends when the first



nonlinearity appears and this is due to the fact that each GM affects the structure differently. Only the GM7 follows a linear degradation toward the IO limit state which will continue to deteriorate till collapse with the increase of the PGA. Owing to the use of bracing that provides good performance under seismic loads, it can be seen that the analysis reaches higher PGA values that is 0.8g for MRFB with 5m and 0.6g for MRFB with 6m and 7m.

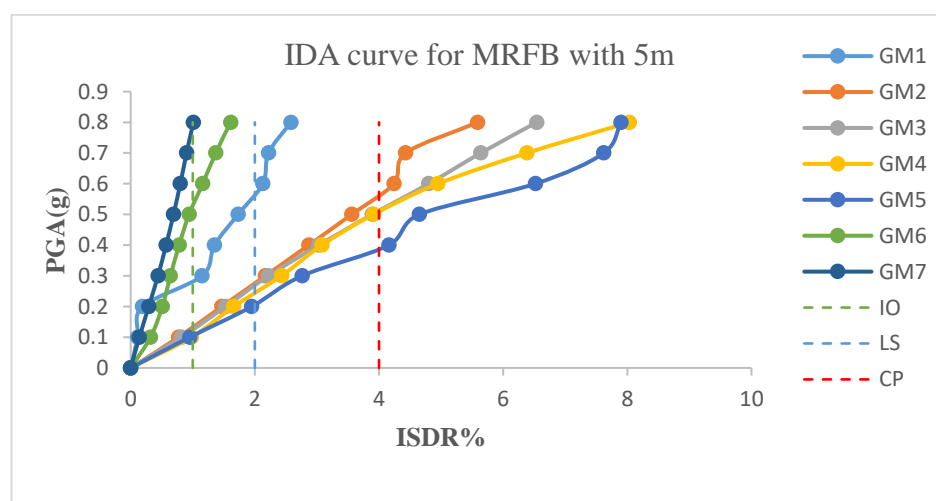
From Figure 29 a), GM3 and GM4 that has the highest magnitude, the first cracking appears at PGA 0.12g and 0.1g respectively. The yielding point is located at 0.24g and 0.26g respectively, and finally, the collapse appears to be around 0.51g and 0.52g for both ground motions.

For the MRFB with 6m in Figure 29 b), the cracks appear at 0.06g and 0.08g for GM4 and GM3 respectively. The yielding points are 0.21g and 0.14g, eventually, the collapse point is 0.48g and 0.31 for GM4 and GM3 respectively.

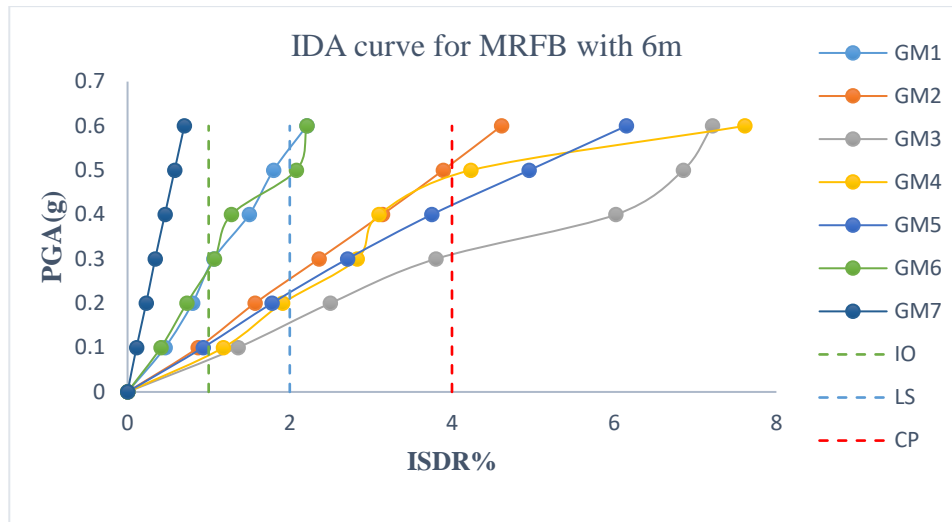
From the MRFB with a 7m graph presented in Figure 29 c), the GM4 shows the first cracks at 0.06g and 0.1g for GM3, and the yielding is located at 0.14g and 0.2 g respectively. The point of collapse can be seen at PGA 0.38g and 0.34g for GM4 and GM3 correspondingly. It is obvious that with the increase of the span length, the stiffness of the structure has decreased. This is owing to the fact that longer spans result in more deflection and deformation under load which reduces the overall stiffness of the structure.

Figure 29

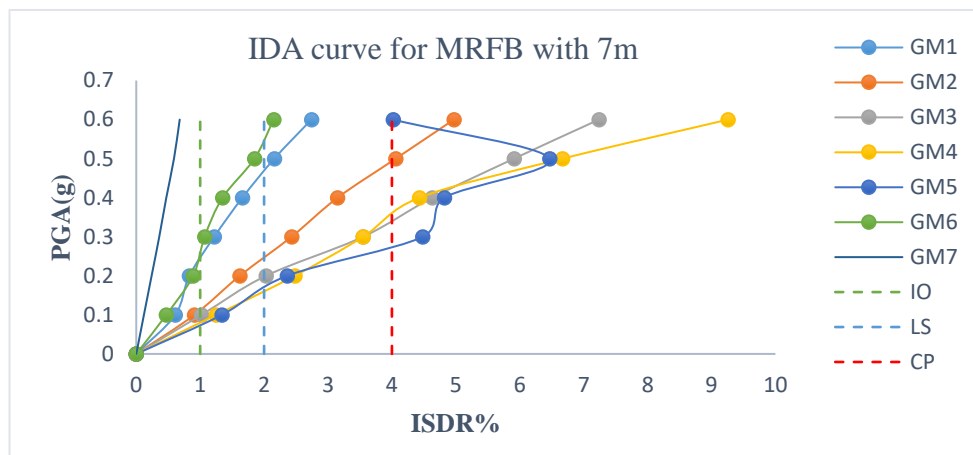
a) IDA curve for moment resisting frame with bracing with 5m span length



b) IDA curve for moment resisting frame with bracing with 6m span length



c) IDA curve for moment resisting frame with bracing with 7m span length

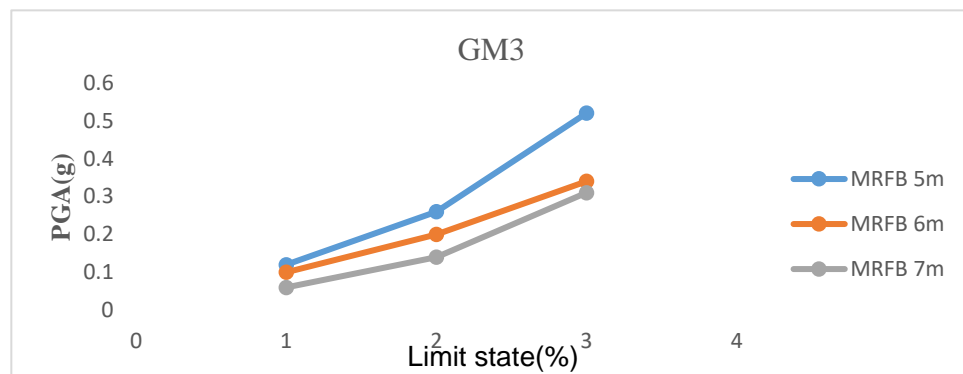
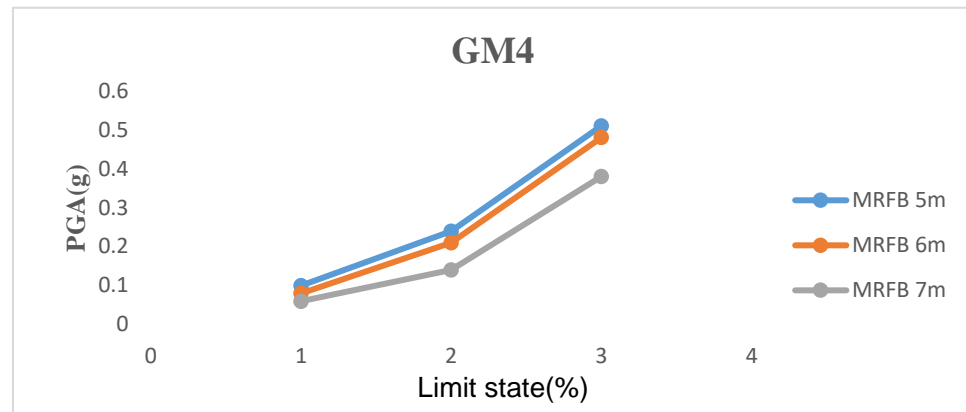


➤ **Comparison among the MRFB models with respect to IDA curve results**

The conclusion drawn from the figures below 30 a) and b) is that the length of the span influences the stiffness of the structure since the value of the limit states decreases as the span lengthens. It is clear from the graphs below that the MRFB with 5m from the GM3 and GM4, has a higher rigidity, which enabled the structure to withstand more. Based on the GM3, the MRFB with 6m and 7m have, respectively, 17% and 50% for IO, 23.1% and 46.1% for LS, and 34.6% and 40.38% for CP less than the MRFB with 5m, as shown by the graphs that showed the pace of the drop in the performance of the structure. The value of the MRFB with 6m and 7m, which is roughly 20% and 40% for IO, 12.5% and 42% for LS, as well as 6% and 25.5% for CP, respectively, is lower than the rate of the MRFB with 5m PGA, per the GM4.

Figure 30

Different limit state values according to: a) GM3 with MRFB, b) GM5 with MRFB



b)

### b) Fragility curve for all MRFB

The information associated with the fragility function data for each of the limit states that have been generated for the three MRFB that are utilized to construct the fragility curve of each system and provide us with the likelihood of surpassing the various limit states is tabled in the following Tables from 13 a) to c). The appendices contain the input tables that provide those fragility data.

Table 13

a) Fragility function data for the MRFB with a 5m span length

Acceleration	Fragility for Limit States of Drift at		
	1 (%)	2 (%)	4 (%)
<b>0.0100</b>	0.0008	0.0001	0.0000
<b>0.1667</b>	0.3745	0.1610	0.0484
<b>0.3333</b>	0.6486	0.3864	0.1687
<b>0.5000</b>	0.7859	0.5484	0.2915
<b>0.6667</b>	0.8607	0.6601	0.3983
<b>0.8333</b>	0.9048	0.7385	0.4873
<b>1.0000</b>	0.9324	0.7948	0.5607
<b>1.1667</b>	0.9505	0.8363	0.6213
<b>1.3333</b>	0.9629	0.8675	0.6715
<b>1.5000</b>	0.9716	0.8914	0.7134
<b>1.6667</b>	0.9778	0.9099	0.7485
<b>1.8333</b>	0.9825	0.9246	0.7783
<b>2.0000</b>	0.9859	0.9364	0.8036
<b>2.1667</b>	0.9886	0.9459	0.8252
<b>2.3333</b>	0.9907	0.9536	0.8439
<b>2.5000</b>	0.9923	0.9600	0.8600
<b>2.6667</b>	0.9936	0.9653	0.8740
<b>2.8333</b>	0.9946	0.9698	0.8863
<b>3.0000</b>	0.9954	0.9735	0.8971
<b>3.1667</b>	0.9961	0.9767	0.9065
<b>3.3333</b>	0.9967	0.9794	0.9149
<b>3.5000</b>	0.9971	0.9818	0.9223
<b>3.6667</b>	0.9975	0.9838	0.9290
<b>3.8333</b>	0.9978	0.9855	0.9349
<b>4.0000</b>	0.9981	0.9870	0.9402
<b>4.1667</b>	0.9984	0.9883	0.9449
<b>4.3333</b>	0.9986	0.9895	0.9492
<b>4.5000</b>	0.9987	0.9905	0.9531
<b>4.6667</b>	0.9989	0.9914	0.9566
<b>4.8333</b>	0.9990	0.9922	0.9597
<b>5.0000</b>	0.9991	0.9929	0.9626

*b) Fragility function data for the MRFB with a 6m span length*

Acceleration	Fragility for Limit States of Drift at		
	1 (%)	2 (%)	4 (%)
0.0100	0.0022	0.0001	0.0000
0.1500	0.4877	0.2030	0.0514
0.3000	0.7546	0.4558	0.1811
0.4500	0.8665	0.6217	0.3120
0.6000	0.9206	0.7287	0.4242
0.7500	0.9496	0.7997	0.5161
0.9000	0.9664	0.8485	0.5909
1.0500	0.9767	0.8830	0.6517
1.2000	0.9834	0.9080	0.7015
1.3500	0.9878	0.9266	0.7425
1.5000	0.9909	0.9407	0.7765
1.6500	0.9930	0.9515	0.8049
1.8000	0.9946	0.9599	0.8289
1.9500	0.9958	0.9666	0.8492
2.1000	0.9966	0.9719	0.8665
2.2500	0.9973	0.9762	0.8813
2.4000	0.9978	0.9797	0.8941
2.5500	0.9982	0.9826	0.9051
2.7000	0.9985	0.9850	0.9148
2.8500	0.9988	0.9870	0.9232
3.0000	0.9990	0.9887	0.9306
3.1500	0.9991	0.9901	0.9371
3.3000	0.9993	0.9913	0.9429
3.4500	0.9994	0.9924	0.9480
3.6000	0.9995	0.9932	0.9525
3.7500	0.9995	0.9940	0.9565
3.9000	0.9996	0.9947	0.9602
4.0500	0.9997	0.9952	0.9634
4.2000	0.9997	0.9957	0.9664
4.3500	0.9997	0.9962	0.9690
4.5000	0.9998	0.9965	0.9714

*c) Fragility function data for the MRFB with a 7m span length*

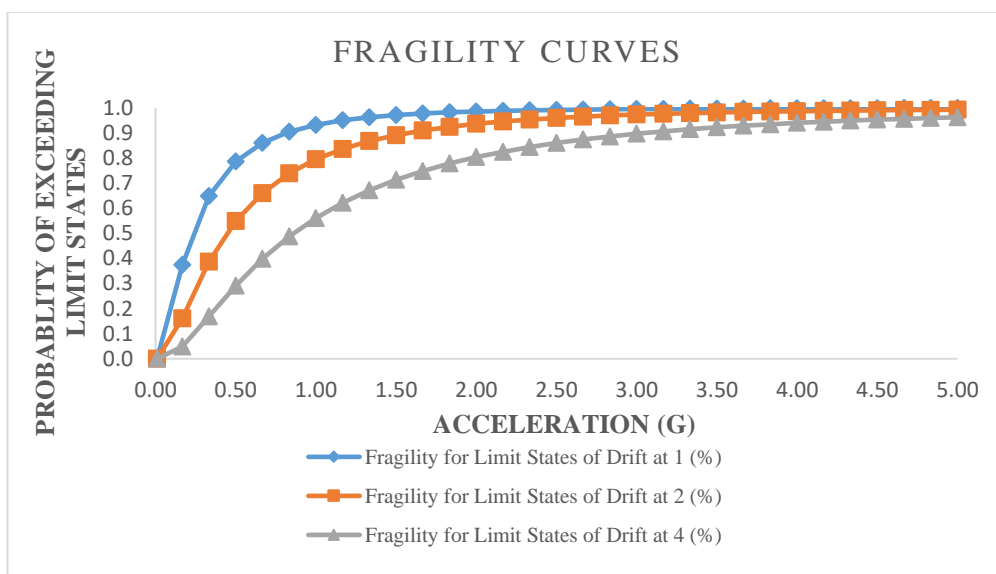
Acceleration	Fragility for Limit States of Drift at		
	1 (%)	2 (%)	4 (%)
<b>0.0100</b>	0.0163	0.0045	0.0010
<b>0.1500</b>	0.7102	0.5319	0.3469
<b>0.3000</b>	0.8930	0.7790	0.6160
<b>0.4500</b>	0.9501	0.8793	0.7573
<b>0.6000</b>	0.9733	0.9275	0.8373
<b>0.7500</b>	0.9843	0.9534	0.8859
<b>0.9000</b>	0.9902	0.9686	0.9172
<b>1.0500</b>	0.9936	0.9780	0.9382
<b>1.2000</b>	0.9956	0.9841	0.9528
<b>1.3500</b>	0.9969	0.9882	0.9632
<b>1.5000</b>	0.9978	0.9910	0.9709
<b>1.6500</b>	0.9983	0.9931	0.9766
<b>1.8000</b>	0.9987	0.9946	0.9810
<b>1.9500</b>	0.9990	0.9957	0.9844
<b>2.1000</b>	0.9993	0.9966	0.9871
<b>2.2500</b>	0.9994	0.9972	0.9892
<b>2.4000</b>	0.9995	0.9977	0.9909
<b>2.5500</b>	0.9996	0.9981	0.9923
<b>2.7000</b>	0.9997	0.9984	0.9934
<b>2.8500</b>	0.9997	0.9987	0.9943
<b>3.0000</b>	0.9998	0.9989	0.9951
<b>3.1500</b>	0.9998	0.9990	0.9957
<b>3.3000</b>	0.9999	0.9992	0.9963
<b>3.4500</b>	0.9999	0.9993	0.9967
<b>3.6000</b>	0.9999	0.9994	0.9971
<b>3.7500</b>	0.9999	0.9995	0.9975
<b>3.9000</b>	0.9999	0.9995	0.9978
<b>4.0500</b>	0.9999	0.9996	0.9980
<b>4.2000</b>	0.9999	0.9997	0.9982
<b>4.3500</b>	1.0000	0.9997	0.9984
<b>4.5000</b>	1.0000	0.9997	0.9986

Fragility curves are commonly used in disaster modeling to express the probability of surpassing a given damage condition as a function of environmental change. The MRFB fragility curves, which show the proportion of each PGA that exceeds the

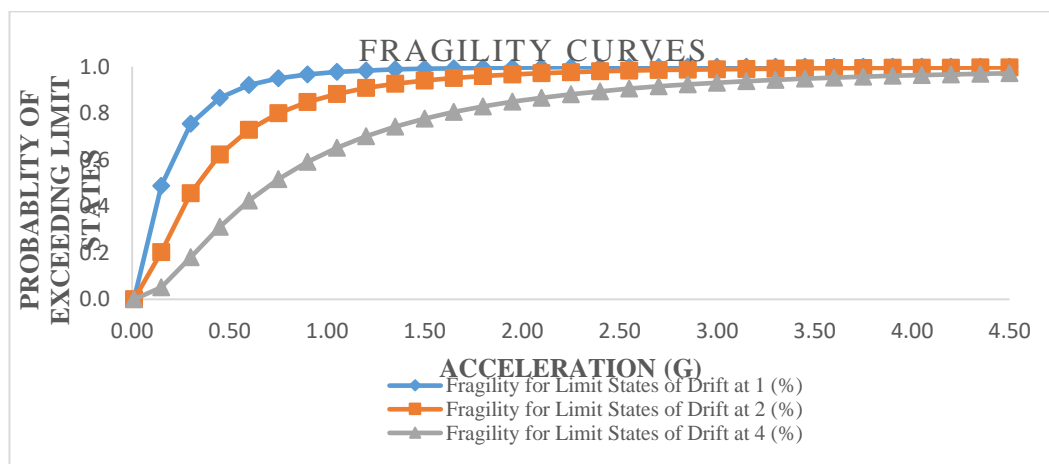
specified limit state, are shown in the Figures below from 31 a) to c). The MRFB with 5m has higher performance under seismic loads, as shown by the figure below. The fragility curve confirms the highest stiffness of the MRFB with 5m, as was previously reported based on the IDA curve. From Figure 31 a) with the minimum PGA of 0.5g, there is a 29% probability of exceeding the CP limit state which is relatively acceptable. In contrast with Figures b) and c) to Figure a), there is an increase in the value of the CP because it is around 32% and 39% for MRFB with 6m and 7m respectively. It is obvious that the use of bracing has considerably increased the stiffness of the frame because it can be seen that the susceptibility has decreased.

Figure 31

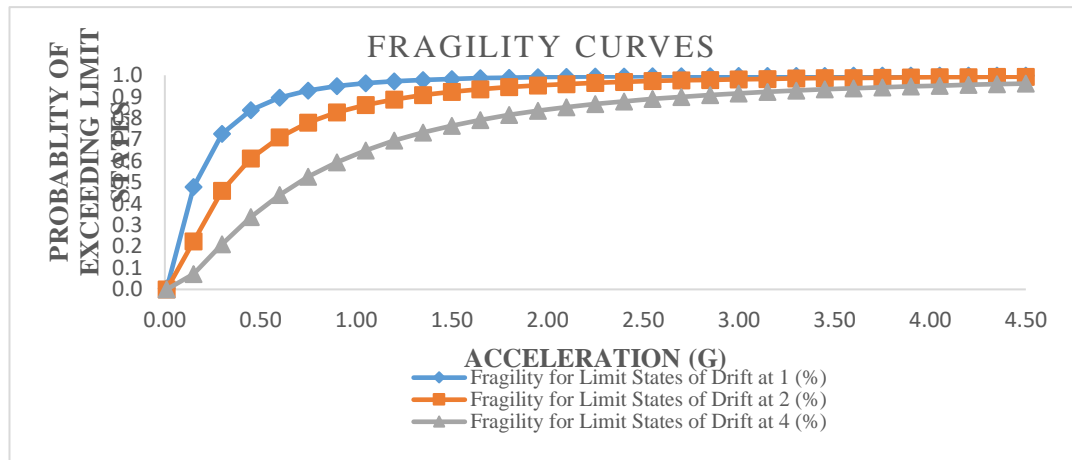
a) Fragility curve for MRFB with 5m span length



b) Fragility curve for MRFB with 6m span length



c) Fragility curve for MRFB with 7m span length

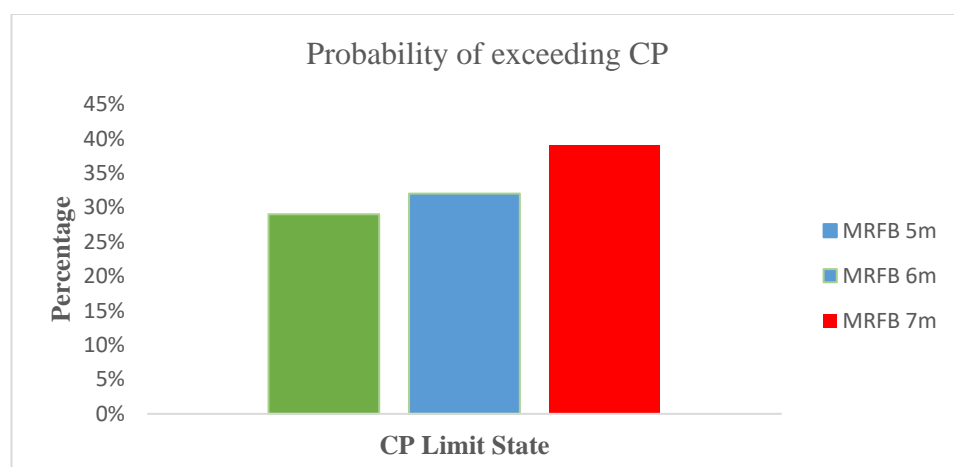


➤ *Comparison among the MRFB models with respect to fragility curve results*

The CP values that can be exceeded while the PGA is at 0.5 are shown in Figure 32, and it is clear that the MRFB with a 5m span length has the lowest rate when compared to the other models. The performance of the structure is directly impacted by the span length increase, which results in a reduction in the structure's stiffness. The susceptibility of MRFB with 6m and 7m increases by 10% and 34% percent, respectively, as compared to the susceptibility of MRFB having 5m. The bracing system has helped to distribute the seismic forces throughout the structure, which results in lowering the overall load.

Figure 32

*Probability of exceeding the CP limit state graph for all the MRFB models*



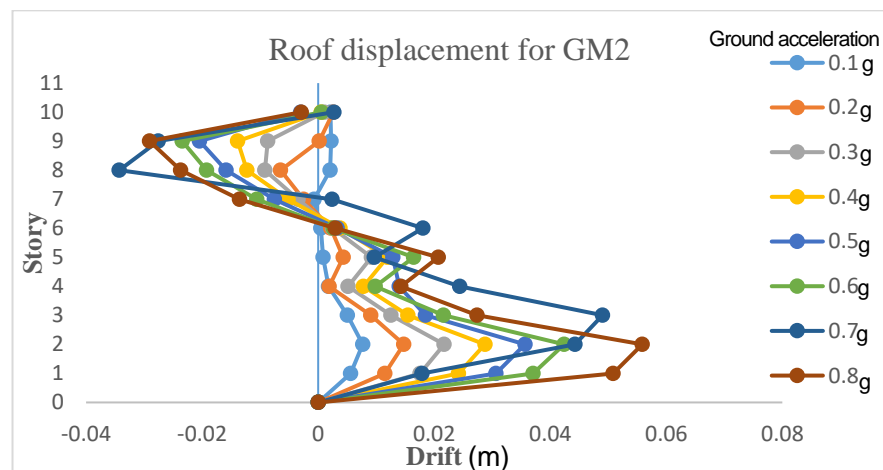


### C) Inter-story drift ratio of all the MRFs models

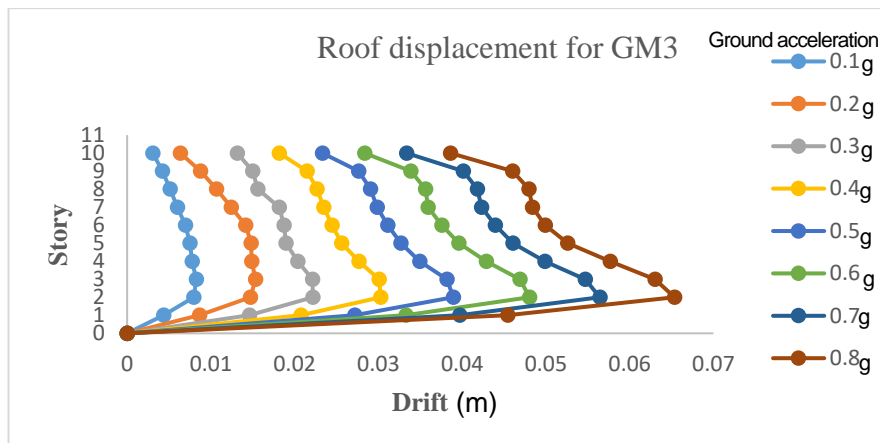
The analysed models from Figures 33 to 35, show that the story drift ratios are erratic, especially in the GM2 when a negative multi-curvature plot is displayed. This may be connected to how columns' cross sections varied depending on the building's elevation throughout the design but also the higher mode effect that refers to the fact that the structure can vibrate in multiple modes and when it follows the second mode, it can result in larger sway. Additionally, the top story drift ratio is the lowest. This is related to the fact that the lateral story forces are larger at the structure's base and lower at the roof and that the support fixities are what give rise to the low-story drift at the base. The increase of the span length results also in the increment of the ISDR.

Figure 33

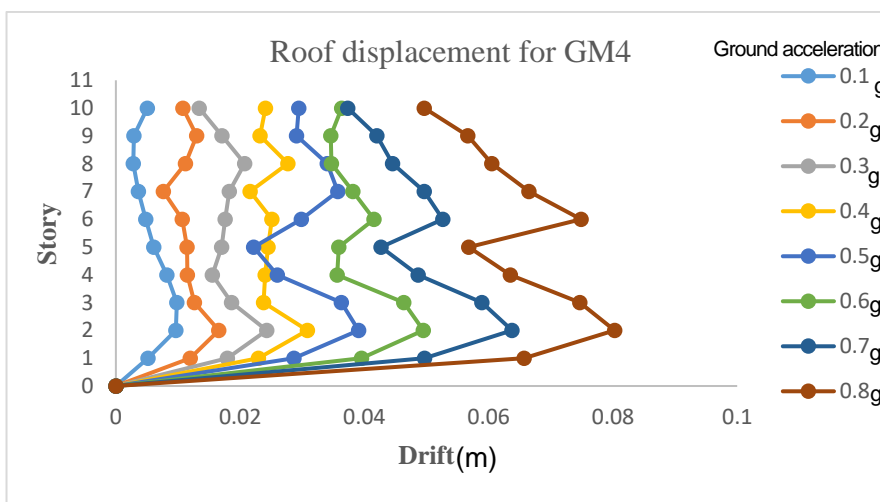
Roof displacement for MRFB with 5m span Length: a) GM2, b) GM3, c) GM4



a)



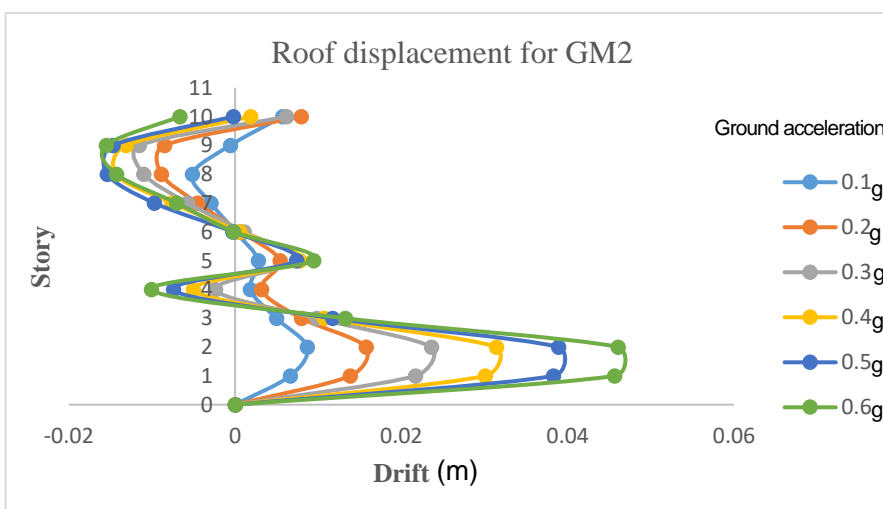
b)



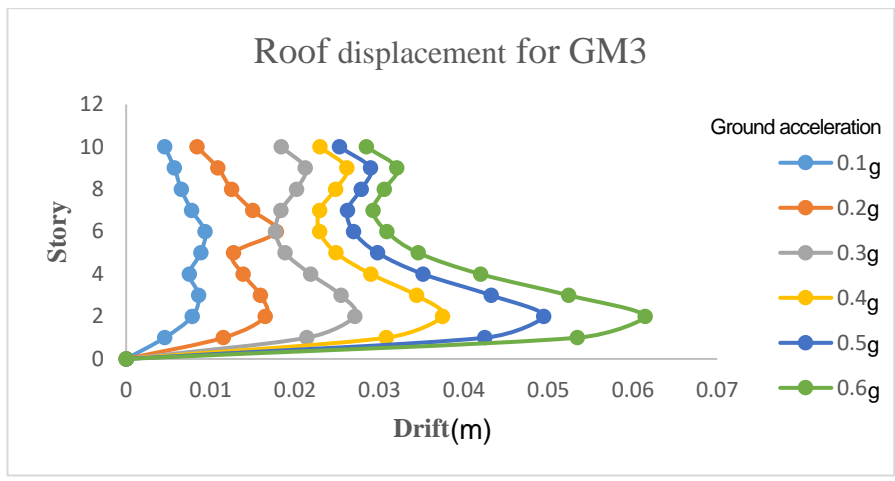
c)

Figure 34

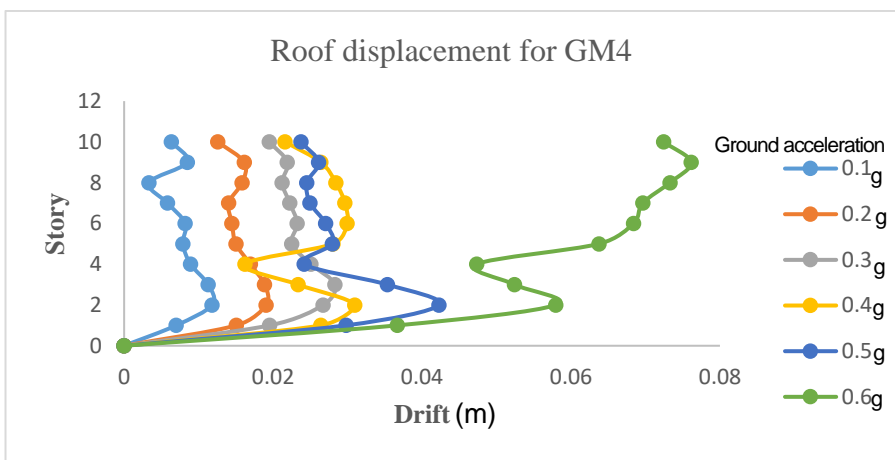
Roof displacement for MRFB with 6m span length: a) GM2, b) GM3, c) GM4



a)



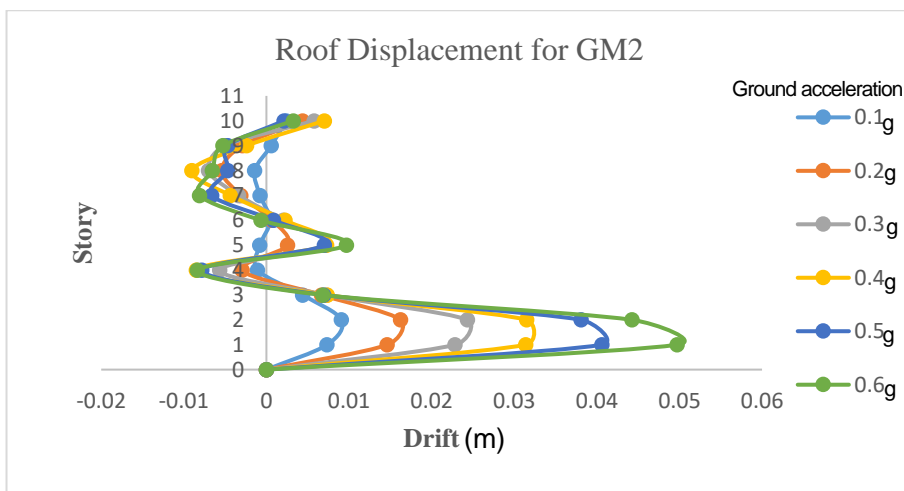
b)



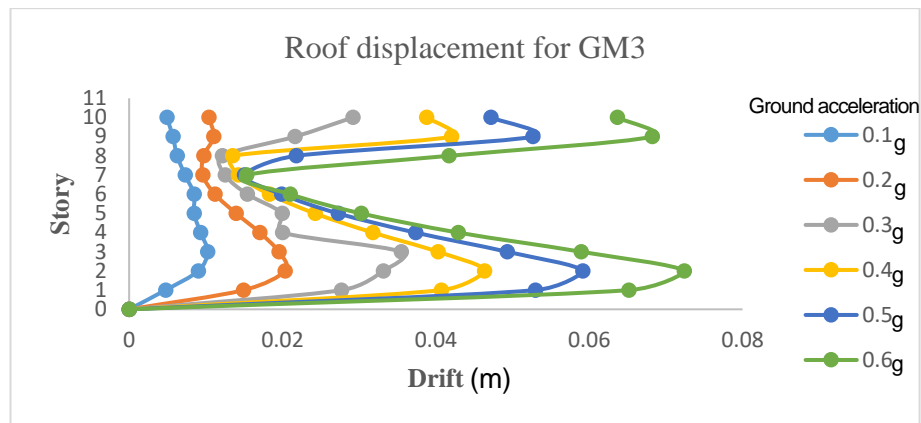
c)

Figure 35

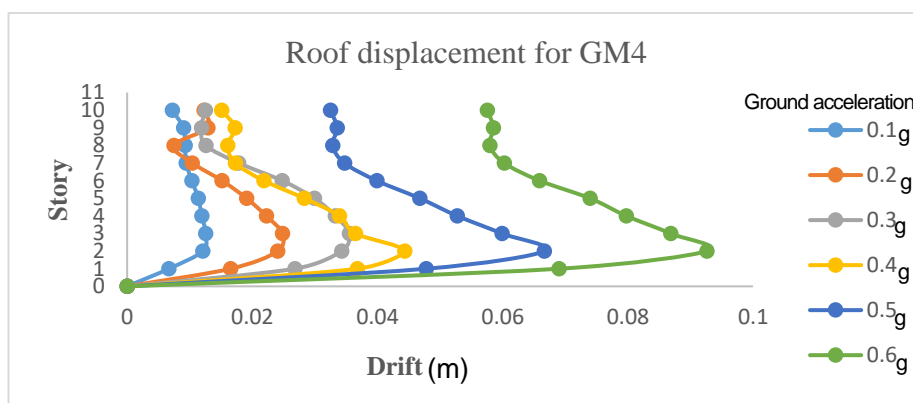
Roof displacement for MRFB with 7m span length: a) GM2, b) GM3, c) GM4



a)



b)



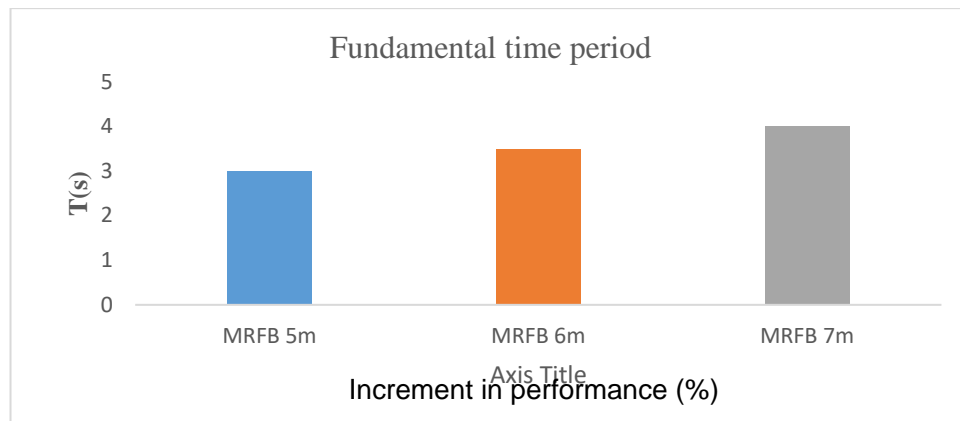
c)

**d) Fundamental time period effect of all the MRFB models**

Figure 36 provides information on the 3 MRFB's initial mode period, which rises as the span length does. It is evident that, in comparison to the other frames, the MRFB with 5m has a lower mode. It is clear from the graph that the MRFB with 5m mode has increased by 16%, and 34% when compared to the MRFB with 6m and 7m. The longer spans are more flexible, which causes a longer duration of vibration, which has an impact on the span length. The use of bracing has in general increase the performance of the structure by making it stiffer.

Figure 36

*The fundamental time period of all the MRFB models*



#### 4.4 Moment resisting frame with shear wall (MRFSW)

The information attributed to the ISDR to the various framing systems of shear walls that have been used for this study is shown in the three tables below, from 14 a) to c). 7m, 6m, and 5m MRFSW are displayed.

Table 14

##### a) Inter-story drift ratio of the MRFSW with 5m span length

	GM1	GM2	GM3	GM4	GM5	GM6	GM7
	ISDR	ISDR	ISDR	ISDR	ISDR	ISDR	ISDR
IM	(%)	(%)	(%)	(%)	(%)	(%)	(%)
0	0	0	0	0	0	0	0
0.1	0.29	0.69	0.85	0.66	0.5	0.59	0.19
0.2	0.57	1.26	1.72	1.4	0.96	1.01	0.39
0.3	0.9	1.55	2.56	2.01	1.49	1.44	0.58
0.4	1.23	1.93	3.49	2.88	1.99	1.94	0.77
0.5	1.58	3.06	4.38	3.34	2.47	2.42	0.95
0.6	1.96	3.42	5.29	4.47	3.01	2.92	1.12
0.7	2.25	3.87	6.17	4.14	3.56	3.39	1.28
0.8	2.69	3.78	6.91	6.44	4.25	4	1.44

##### b) Inter-story drift ratio of the MRFSW with 6m span length

	GM1	GM2	GM3	GM4	GM5	GM6	GM7
	ISDR	ISDR	ISDR	ISDR	ISDR	ISDR	ISDR
IM(g)	(%)	(%)	(%)	(%)	(%)	(%)	(%)
0	0	0	0	0	0	0	0
0.1	0.3	0.66	0.7	0.81	0.49	0.61	0.11
0.2	0.6	1	1.31	1.65	1.1	1.13	0.23

0.3	1.06	1.82	2.44	2.48	1.63	1.48	0.34
0.4	1.24	2.45	3	3.22	2.25	1.95	0.46
0.5	1.66	3.49	3.61	3.8	3	2.4	0.58
0.6	2.03	3.42	4.17	4.9	3.59	2.74	0.7

*c) Inter-story drift ratio of the MRFSW with 7m span length*

	GM1	GM2	GM3	GM4	GM5	GM6	GM7
	ISDR	ISDR	ISDR	ISDR	ISDR	ISDR	ISDR
IM(g)	(%)	(%)	(%)	(%)	(%)	(%)	(%)
0	0	0	0	0	0	0	0
0.1	0.35	0.64	0.7	0.79	0.49	0.59	0.2
0.2	0.65	1.2	1.16	1.55	1.08	1.21	0.37
0.3	1.13	2.16	1.72	2.41	1.66	1.42	0.6
0.4	1.2	2	2.91	4.05	2.13	1.83	0.81
0.5	1.93	3.58	3.38	5	2.84	2.31	1.02
0.6	1.93	3.76	3.88	6.14	3.58	3.08	1.06

#### **4.4.1 Discussion of the results**

##### **a) IDA curve for all MRFSW**

The accelerogram and structural models used in the IDA study are unique; when subjected to various ground motions, a model frequently produces highly distinct reactions that are challenging to predict beforehand. Take a look at Figure 37(a-c), where the frames display reactions that range from a slow back-twisting behavior to a quick, non-monotonic decline towards collapse. Each graph shows the demands that each ground motion record places on the structure at various intensities, and they are rather intriguing in both their parallels and differences. From Figures a) and c), it can be seen that the GM4 and GM2 respectively are exhibiting a twisting behavior that is due to the softening and hardening pattern or portions where the local slope or "stiffness" reduces with higher IM and others where it increases. In engineering terms, this means that occasionally the structure experiences an acceleration of the rate of DM accumulation, and occasionally it experiences a deceleration that can be strong enough to temporarily halt or even reverse the ISDR accumulation. This locally pulls

the IDA curve to a relatively lower ISDR and transforms it into a non-monotonic function of the PGA.

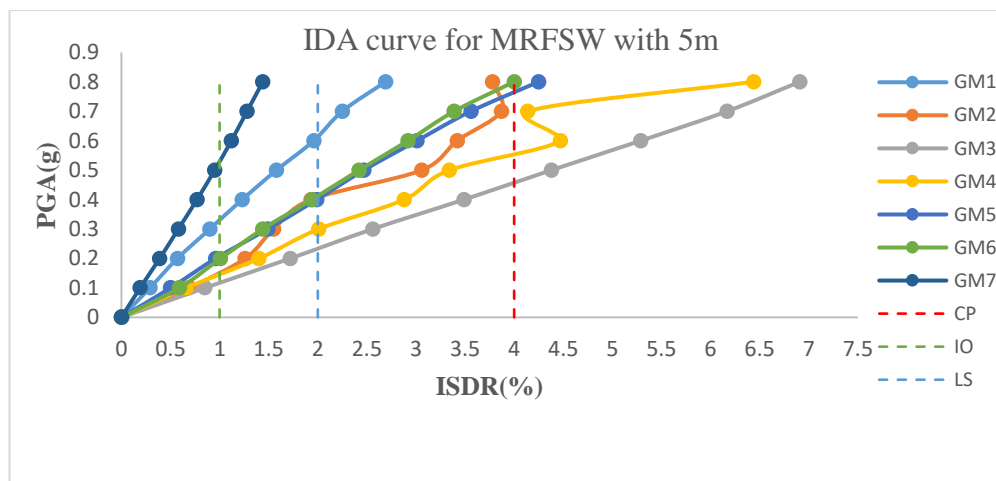
The initial breaking may be seen at PGA 0.16g and 0.14g in Figure 37 a), where GM3 and GM4 have the largest magnitude. Finally, the collapse seems to occur around 0.6g and 0.56g for both ground motions, with the yielding point around 0.32g and 0.3g, respectively.

The cracks start to show up for GM4 and GM3 at 0.14g and 0.13g, respectively, for the MRFSW with 6m in Figure 37 b). The yielding points for GM4 and GM3 are 0.25g and 0.26g, respectively, and the collapse points are 0.57g and 0.52g.

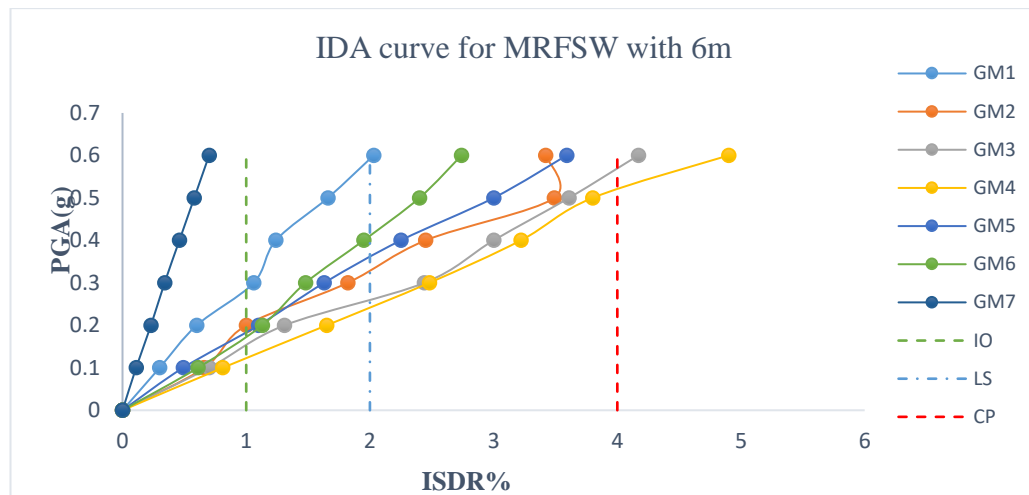
The GM4 displays the initial fractures at 0.12g and 0.11g for GM3, and the yielding is situated at 0.23g and 0.24g, and the collapse is at 0.4g and 0.47g respectively, according to the MRSW with a 7m graph shown in Figure 37 c). The used of shear wall has considerably enhance the performance of the structure compared to the other systems.

Figure 37

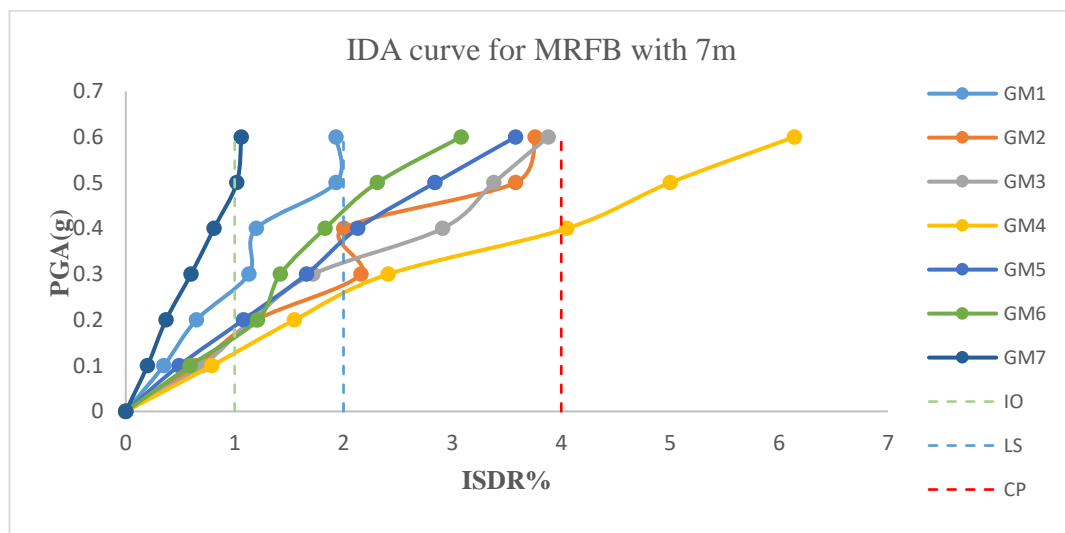
a) IDA curve for moment resisting frame with shear wall with 5m span length



b) IDA Curve for moment resisting frame with shear wall with 6m span length



c) IDA curve for moment resisting frame with shear wall with 7m span length



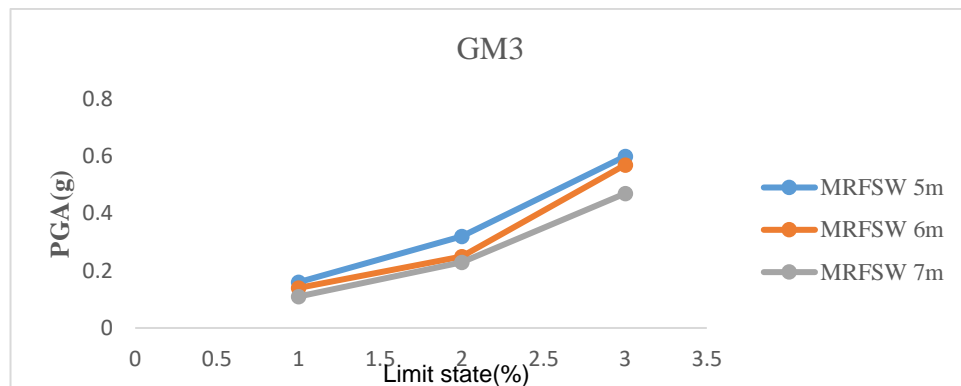
➤ **Comparison among the MRFSW models with respect to IDA curve results**

The conclusion from the figures below 38 a) and b) is that the length of the span influences the stiffness of the structure since the value of the limit states decreases as the span lengthens. It is vivid from the graphs below that the MRFSW with 5m based on the GM3 and GM4, has a higher rigidity, which enabled the structure to perform better. The MRFSW with 6m and 7m have, according to the GM3, respectively, 12.5% and 31.25% for IO, 22% and 28% for LS, and 5% and 22% for CP less than the MRFSW with 5m, as shown by the graphs that depicted the pace of the drop in the performance of the structure. The value of the MRFSW with 6m and 7m, which is roughly 7% and 14% for IO, 13.3% and 23.3% for LS, as well as 7% and 28.6% for CP, respectively, is lower than the rate of the MRFSW with 5m as per the GM4.

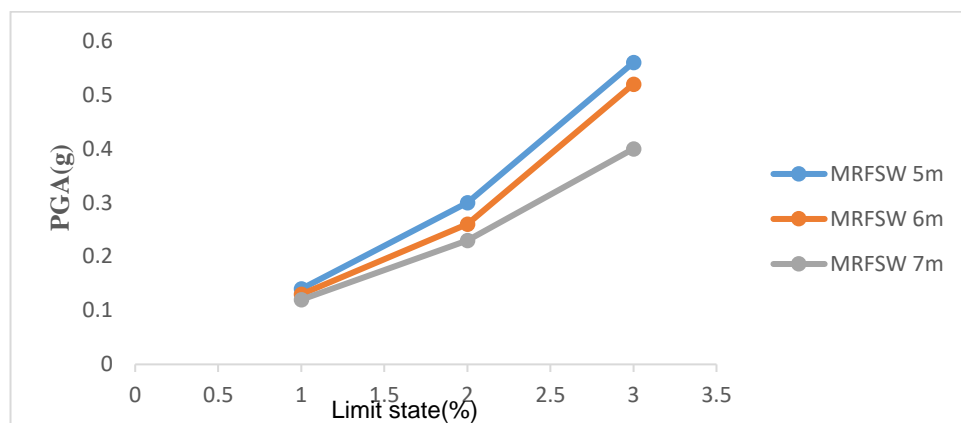


Figure 38

Different limit state values according to: a) GM3 with MRFSW b) GM5 with MRFSW



a)



b)

### b) Fragility curve for all MRFSW

The information related to the fragility function data for each of the limit states that have been generated for the three MRFSW is tabled in the following Tables from 15 a) to c). These data are used to construct the fragility curve of each system and give us the likelihood of exceeding the various limit states. The input tables for those fragility data can be found in the appendices.

Table 15

a) Fragility function data for the MRFSW with a 5m span length

Acceleration	Fragility for Limit States of Drift at		
	1 (%)	2 (%)	4 (%)
<b>0.0100</b>	0.0001	0.0000	0.0000
<b>0.1667</b>	0.3846	0.1245	0.0221

<b>0.3333</b>	0.7104	0.3803	0.1222
<b>0.5000</b>	0.8533	0.5759	0.2521
<b>0.6667</b>	0.9197	0.7066	0.3761
<b>0.8333</b>	0.9531	0.7929	0.4829
<b>1.0000</b>	0.9712	0.8507	0.5715
<b>1.1667</b>	0.9816	0.8903	0.6439
<b>1.3333</b>	0.9878	0.9180	0.7027
<b>1.5000</b>	0.9917	0.9377	0.7506
<b>1.6667</b>	0.9942	0.9520	0.7897
<b>1.8333</b>	0.9959	0.9626	0.8217
<b>2.0000</b>	0.9970	0.9705	0.8481
<b>2.1667</b>	0.9978	0.9765	0.8700
<b>2.3333</b>	0.9983	0.9811	0.8882
<b>2.5000</b>	0.9987	0.9846	0.9034
<b>2.6667</b>	0.9990	0.9874	0.9163
<b>2.8333</b>	0.9992	0.9897	0.9271
<b>3.0000</b>	0.9994	0.9914	0.9363
<b>3.1667</b>	0.9995	0.9929	0.9442
<b>3.3333</b>	0.9996	0.9940	0.9509
<b>3.5000</b>	0.9997	0.9950	0.9567
<b>3.6667</b>	0.9998	0.9957	0.9616
<b>3.8333</b>	0.9998	0.9964	0.9660
<b>4.0000</b>	0.9998	0.9969	0.9697
<b>4.1667</b>	0.9999	0.9973	0.9730
<b>4.3333</b>	0.9999	0.9977	0.9758
<b>4.5000</b>	0.9999	0.9980	0.9783
<b>4.6667</b>	0.9999	0.9983	0.9805
<b>4.8333</b>	0.9999	0.9985	0.9825
<b>5.0000</b>	0.9999	0.9987	0.9842

*b) Fragility function data for the MRFSW with a 6m span length*

Acceleration	Fragility for Limit States of Drift at		
	1 (%)	2 (%)	4 (%)
<b>0.0100</b>	0.0002	0.0000	0.0000
<b>0.1500</b>	0.3233	0.1053	0.0204
<b>0.3000</b>	0.6336	0.3256	0.1065
<b>0.4500</b>	0.7908	0.5063	0.2184
<b>0.6000</b>	0.8731	0.6360	0.3279
<b>0.7500</b>	0.9191	0.7275	0.4254
<b>0.9000</b>	0.9462	0.7927	0.5089

<b>1.0500</b>	0.9630	0.8398	0.5793
<b>1.2000</b>	0.9739	0.8745	0.6384
<b>1.3500</b>	0.9811	0.9004	0.6880
<b>1.5000</b>	0.9861	0.9200	0.7296
<b>1.6500</b>	0.9895	0.9351	0.7648
<b>1.8000</b>	0.9920	0.9469	0.7945
<b>1.9500</b>	0.9938	0.9562	0.8198
<b>2.1000</b>	0.9952	0.9636	0.8414
<b>2.2500</b>	0.9962	0.9695	0.8599
<b>2.4000</b>	0.9969	0.9743	0.8758
<b>2.5500</b>	0.9975	0.9782	0.8895
<b>2.7000</b>	0.9980	0.9814	0.9015
<b>2.8500</b>	0.9984	0.9841	0.9119
<b>3.0000</b>	0.9986	0.9863	0.9210
<b>3.1500</b>	0.9989	0.9881	0.9289
<b>3.3000</b>	0.9991	0.9897	0.9360
<b>3.4500</b>	0.9992	0.9910	0.9421
<b>3.6000</b>	0.9993	0.9921	0.9476
<b>3.7500</b>	0.9994	0.9931	0.9525
<b>3.9000</b>	0.9995	0.9939	0.9568
<b>4.0500</b>	0.9996	0.9946	0.9606
<b>4.2000</b>	0.9996	0.9952	0.9641
<b>4.3500</b>	0.9997	0.9958	0.9672
<b>4.5000</b>	0.9997	0.9962	0.9699

*c) Fragility function data for the MRFSW with a 7m span length*

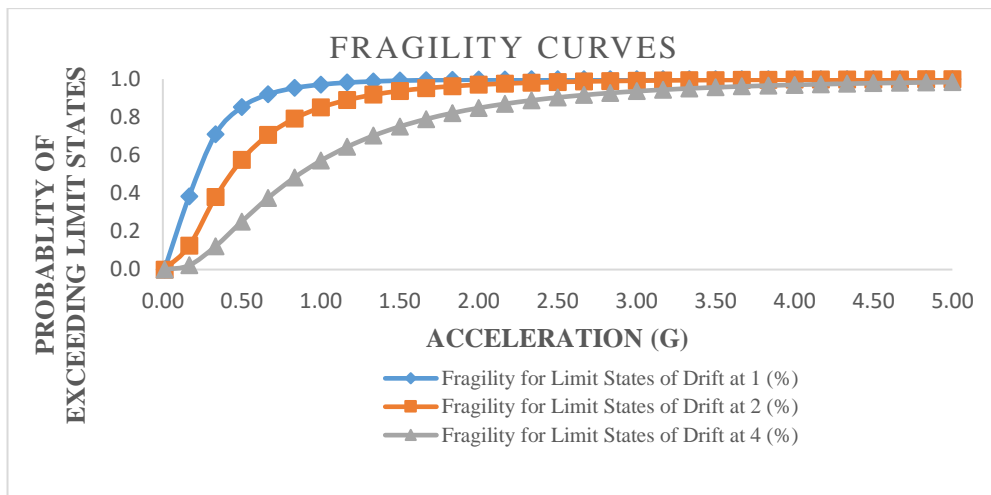
<b>Acceleration</b>	<b>Fragility for the Limit States of Drift at</b>		
	<b>1 (%)</b>	<b>2 (%)</b>	<b>4 (%)</b>
<b>0.0100</b>	0.0001	0.0000	0.0000
<b>0.1500</b>	0.3460	0.1049	0.0174
<b>0.3000</b>	0.6852	0.3537	0.1088
<b>0.4500</b>	0.8404	0.5551	0.2360
<b>0.6000</b>	0.9132	0.6925	0.3614
<b>0.7500</b>	0.9499	0.7840	0.4714
<b>0.9000</b>	0.9696	0.8454	0.5633
<b>1.0500</b>	0.9808	0.8873	0.6386
<b>1.2000</b>	0.9874	0.9164	0.6998
<b>1.3500</b>	0.9915	0.9371	0.7496
<b>1.5000</b>	0.9942	0.9520	0.7901

<b>1.6500</b>	0.9959	0.9629	0.8232
<b>1.8000</b>	0.9970	0.9710	0.8503
<b>1.9500</b>	0.9978	0.9771	0.8727
<b>2.1000</b>	0.9984	0.9817	0.8912
<b>2.2500</b>	0.9988	0.9853	0.9067
<b>2.4000</b>	0.9991	0.9881	0.9196
<b>2.5500</b>	0.9993	0.9903	0.9304
<b>2.7000</b>	0.9995	0.9920	0.9396
<b>2.8500</b>	0.9996	0.9934	0.9474
<b>3.0000</b>	0.9997	0.9945	0.9540
<b>3.1500</b>	0.9997	0.9954	0.9597
<b>3.3000</b>	0.9998	0.9961	0.9645
<b>3.4500</b>	0.9998	0.9967	0.9687
<b>3.6000</b>	0.9999	0.9972	0.9723
<b>3.7500</b>	0.9999	0.9976	0.9755
<b>3.9000</b>	0.9999	0.9980	0.9782
<b>4.0500</b>	0.9999	0.9983	0.9806
<b>4.2000</b>	0.9999	0.9985	0.9826
<b>4.3500</b>	0.9999	0.9987	0.9845
<b>4.5000</b>	1.0000	0.9989	0.9861

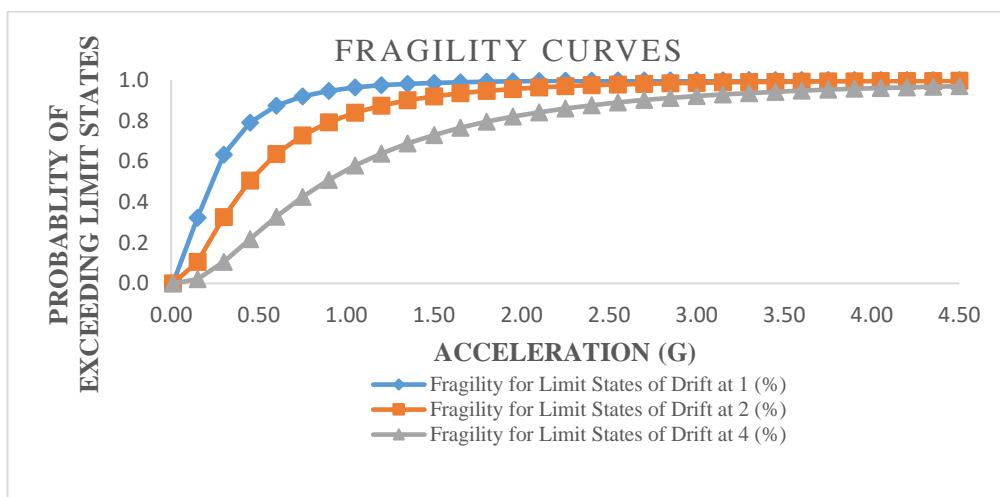
With a minimum PGA of 0.5g, as shown in Figure 38 a), there is a 22% probability of going over the CP limit state, which is a respectable amount. There is an increase in the value of the CP compared to Figures b) and c) to Figure a), as it is around 24% and 28% for MRFB with 6m and 7m, respectively. In disaster modeling, fragility curves are frequently used to depict the likelihood of exceeding a certain damage condition as a function of changing conditions. Figures below from 38 a) to c) display the MRFSW fragility curves, which display the proportion of each PGA that exceeds the designated limit state. According to the figure below, the MRFSW with 5m has better performance when challenged by seismic loads. The fragility curve supports previous reports based on the IDA curve that the MRFSW has the highest stiffness at 5m. It is clear from the lowered sensitivity that the addition of a shear wall has substantially raised the frame's rigidity.

Figure 38

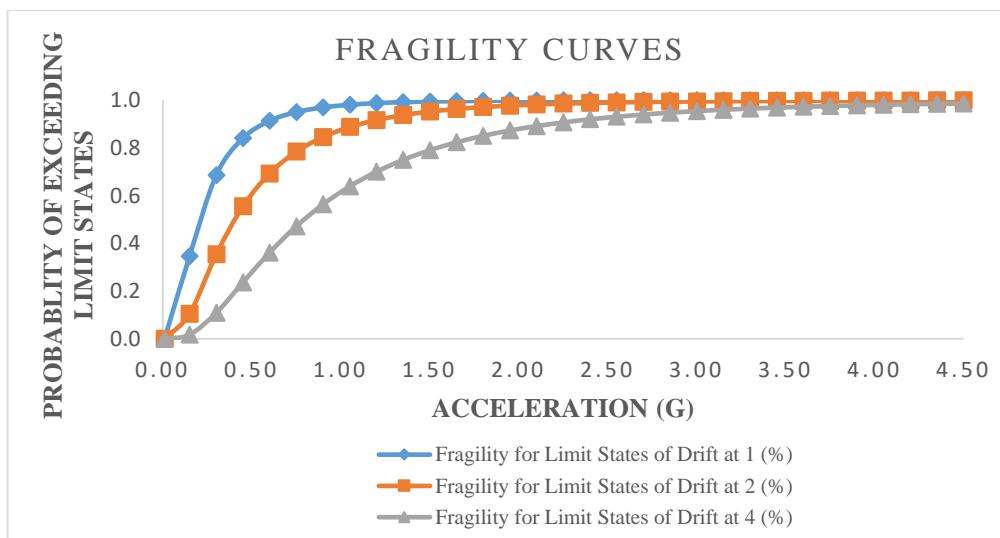
a) *Fragility curve for MRFSW with 5m span length*



b) Fragility curve for MRFSW with 6m span length



c) Fragility curve for MRFSW with 7m span length

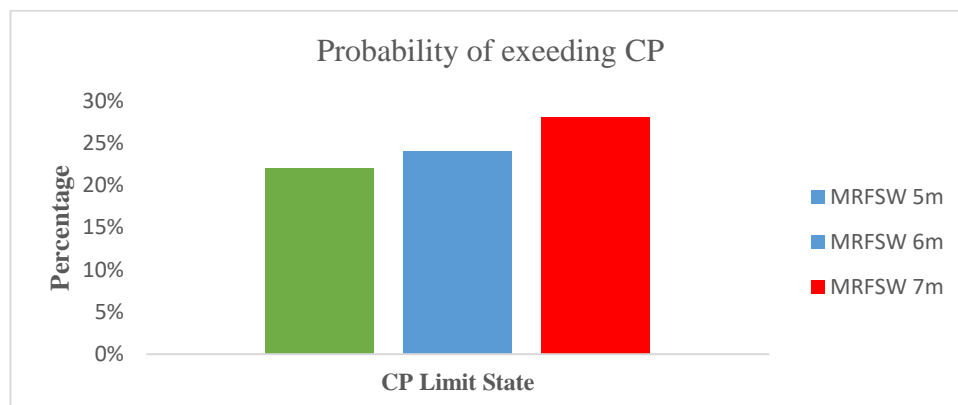


➤ ***Comparison among the MRFSW models with respect to fragility curve results***

The CP values that can be exceeded while the PGA is at 0.5 are depicted in Figure 39, and it is obvious that the MRFSW with a 5m span length has the lowest rate when compared to the other models. The span length increase has a direct effect on the structure's performance since it causes the structure's stiffness to decrease. Contrasting the vulnerability of MRFSW with 6m and 7m to that of MRFSW with 5m, the corresponding rises are 9% and 27%, correspondingly. The shear wall system has assisted in dispersing the seismic forces over the structure, thereby reducing the overall load.

Figure 39

*Probability of exceeding the CP limit state graph for all the MRFSW models*



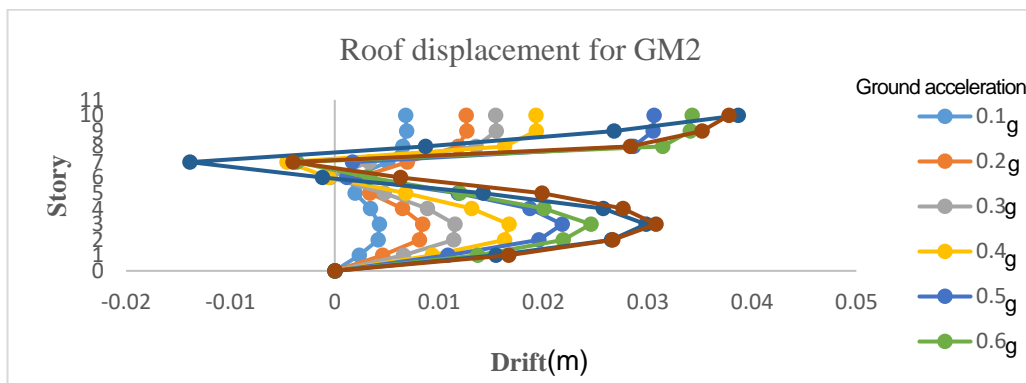
**C) Inter-Story drift ratio of all the MRFSW models**

The models from Figures 40 to 42 that have been investigated demonstrate that the narrative drift ratios are irregular, particularly in the GM2 when a negative multi-curvature plot is shown. The higher mode effect, which refers to the notion that the structure can vibrate in numerous modes and that when it follows the second mode, it can result in greater sway, may also be related to how the cross sections of columns altered based on the building's elevation during the design. The highest narrative drift ratio is also found in the top stories. This has to do with the placement of the shear wall, which is not only affecting the design property but also how well the reinforcement performs. It can also be seen that at PGA 0.6g with GM4, the drift is facing a sudden softening and hardening for MRFSW with 6m and 7m. The support

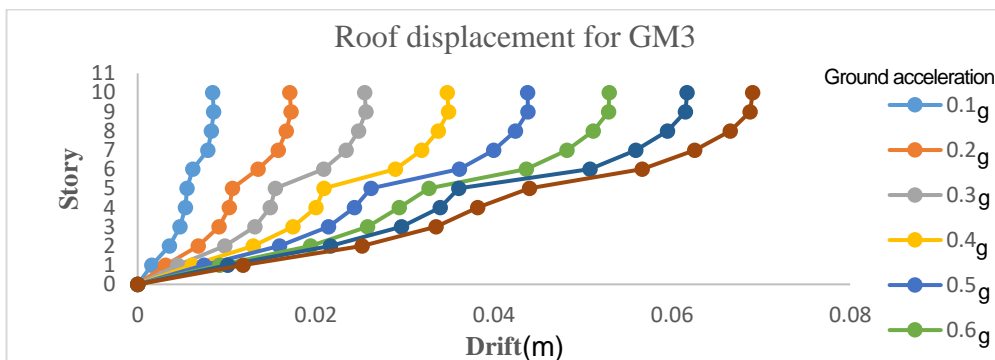
fixities are what give rise to the low-story drift at the base. The increase of the span length results also in the increment of the ISDR.

Figure 40

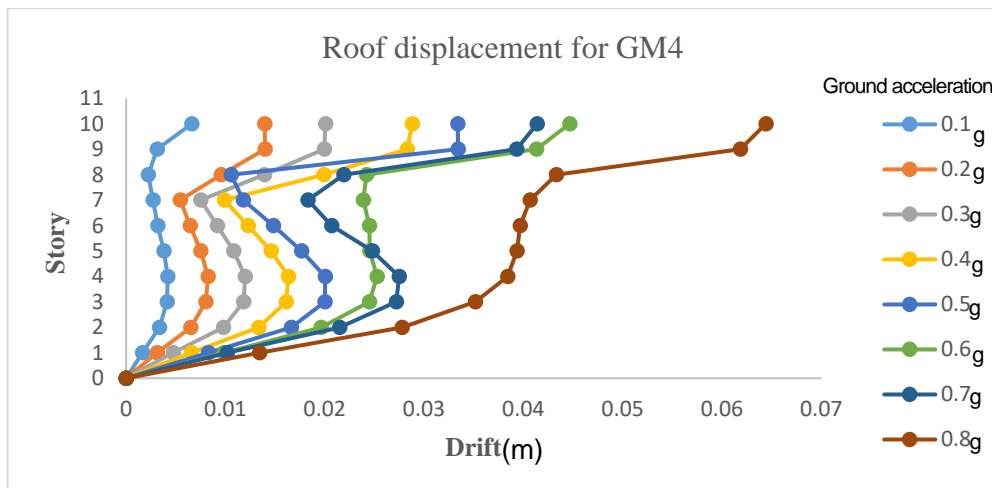
Roof displacement for MRFSW with 5m span length: a) GM2, b) GM3, c) GM4



a)



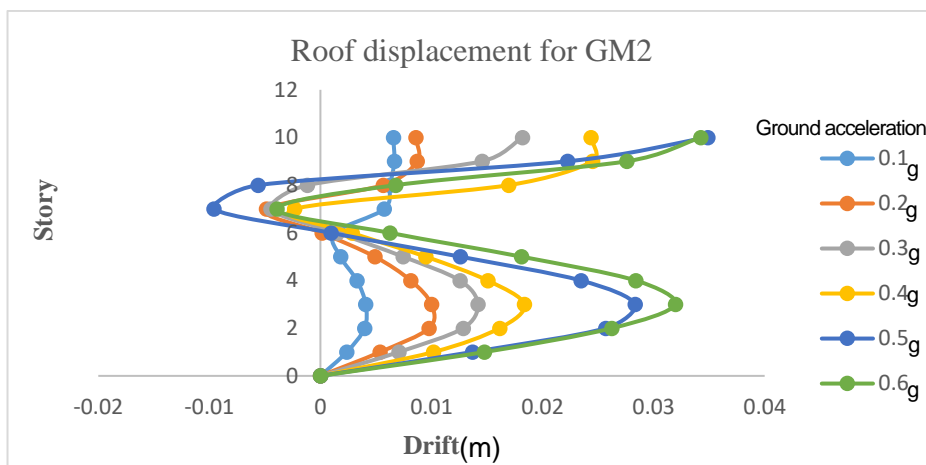
b)



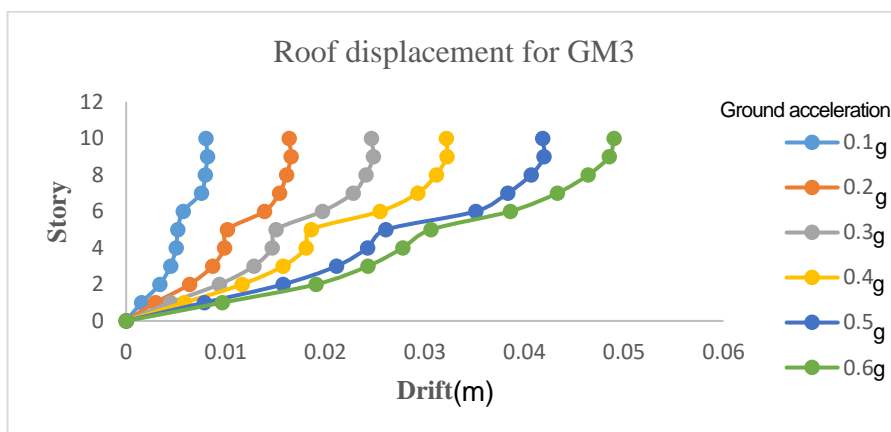
c)

Figure 41

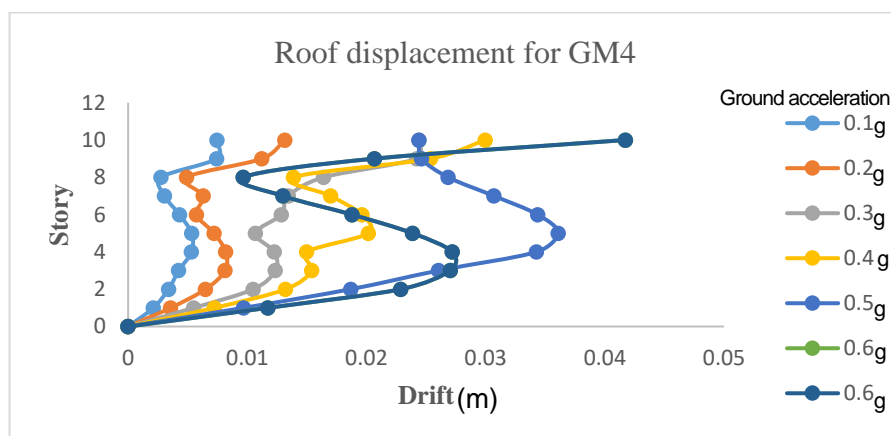
Roof displacement for MRFSW with 6m span length: a) GM2, b) GM3, c) GM4



a)



b)

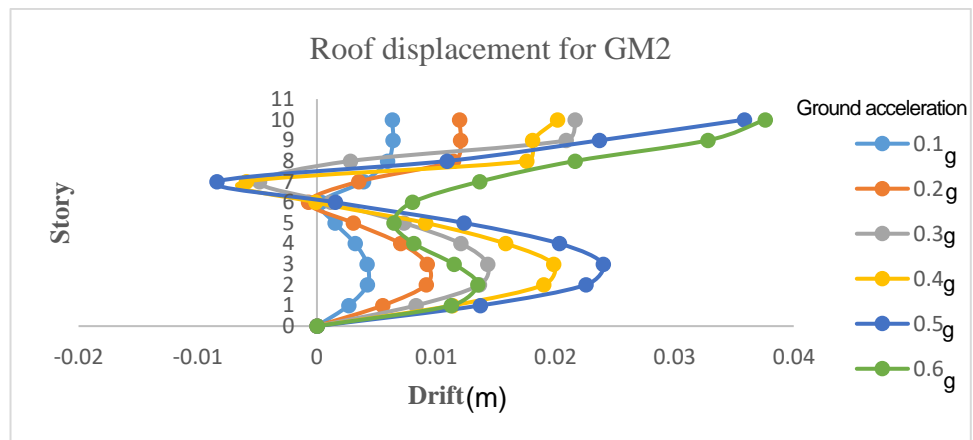


c)

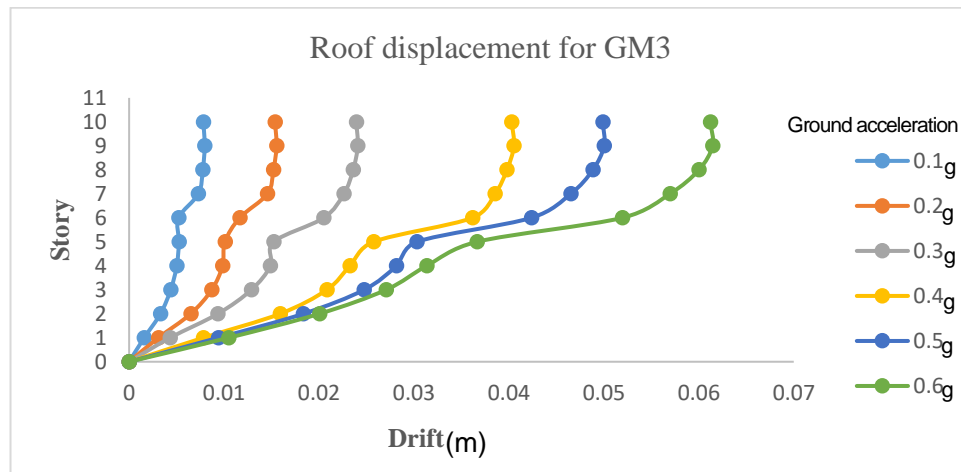


Figure 42

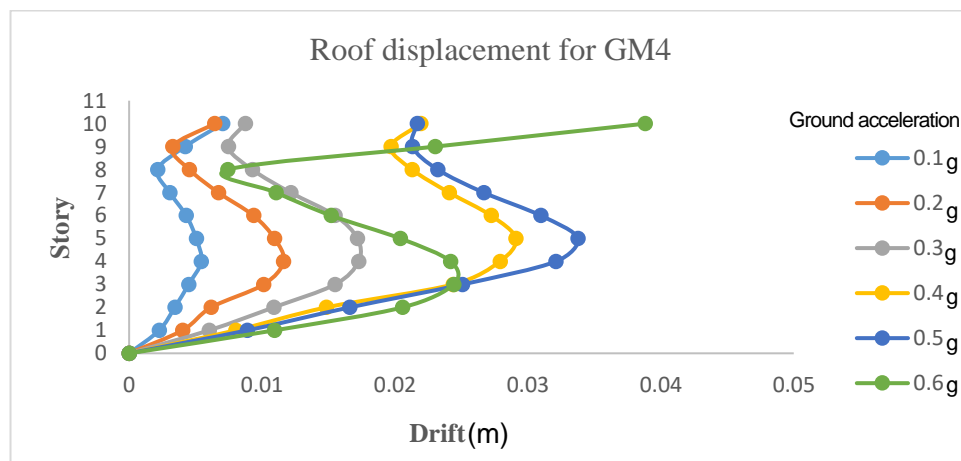
Roof displacement for MRFSW with 7m span length: a) GM2, b) GM3, c) GM4



a)



b)



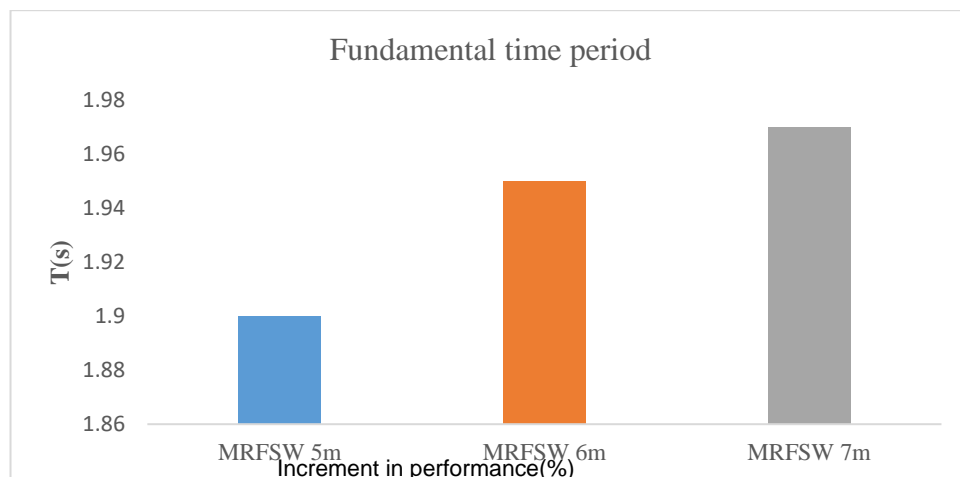
c)

*d) Fundamental time period effect of all the MRFSW models*

The MRFSW first mode period is shown in Figure 43, and it increases as the span length does. The MRFSW with 5m clearly has a lower mode when contrasted with the other frames. The graph shows that the MRFB with 5m mode has expanded by 26.3% and 36.8% when compared to the MRFSW with 6m and 7m, respectively. Because the longer spans are more flexible, the vibration lasts longer, which is due to the influence of the span length. Shear walls typically enhance a structure's performance by stiffening it up.

Figure 43

*The fundamental time period of all the MRFSW models*



#### **4.5 Comparison among all the 3 different framing systems**

##### *4.5.1 Comparison based on the fragility curve with respect to the CP limit state*

Table 16 provides the fragility curve data that can be used as powerful information in order to make the contrast among the 3 different systems that have been investigated in this study that are: MRFs, MRFB and MRFSW. As it has been shown above, the probability of exceeding the Collapse Prevention (CP) limit state has been assessed by means of the minimum PGA which is 0.5g and the results show that the Shear Wall provides better performance under seismic loads because the rate of damage state has increased significantly compared to the Bracing which is stiffer than the normal Frame.

In the Figure 41, Contrasting with the MRFs with 5m there is a decrease in the CP value that is around 51% and 63% to MRFB 5m and MRFSW 5m respectively. For the MRFs with 6m, 54% and 65% are the rate of increment compared to the MRFB and MRFSW both with 6m correspondingly. 51% and 65% are the raise up of the damage state of the MRFs with 7m compared to the other systems.

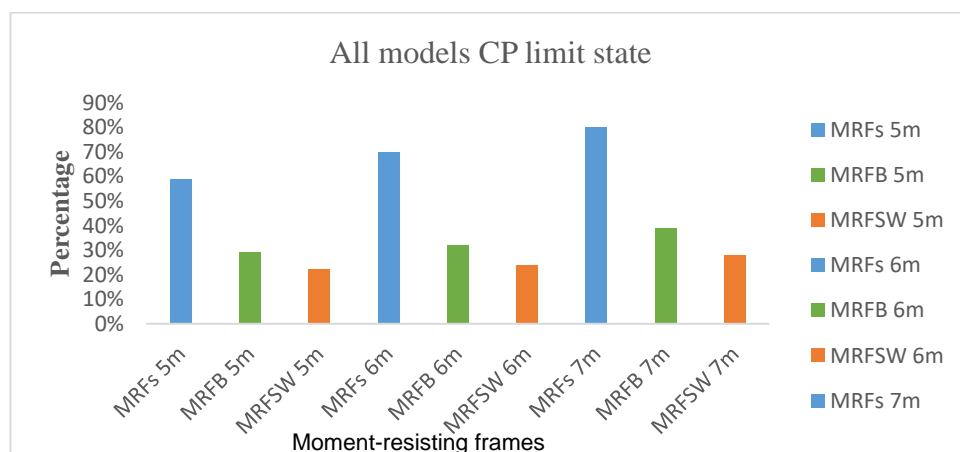
Table 16

*Percentage of the CP limit state of all the models*

Models	CP
MRFs 5m	59%
MRFB 5m	29%
MRFSW 5m	22%
MRFs 6m	70%
MRFB 6m	32%
MRFSW 6m	24%
MRFs 7m	80%
MRFB 7m	39%
MRFSW 7m	28%

Figure 41

*All models CP limit state percentages*



#### 4.5. 2 Comparison based on the fundamental time period of all the models

Figure 42 and Table 16 shed light on the fundamental time period of all the frames that have been analysed in this study and the MRFSW as stated above has performed better

because the period is lowest compared to the MRFs and MRFB. The bracing system has also considerably decreased the time compared to the normal frame. It is observed that contrasting with the 5m span length models, the MRFs value has been lowered by 22% and 51% with MRFB and MRFSW respectively. For the 6m, 26% and 59% are the decreased values of MRFB and MRFSW compared to MRFs. Taking into account the 7m length, compared to the MRFs, the MRFB and MRFSW has lowered by 29% and 65%.

Basically, the use of lateral reinforcement has increased the stiffness of the structure to resist more of the GMs that have been used to analyze the systems. Among all the systems, a shear wall is found to be more efficient compared to bracing and a normal frame. MRFs are found to be a really weak framing system that exposes the structure to severe damage.

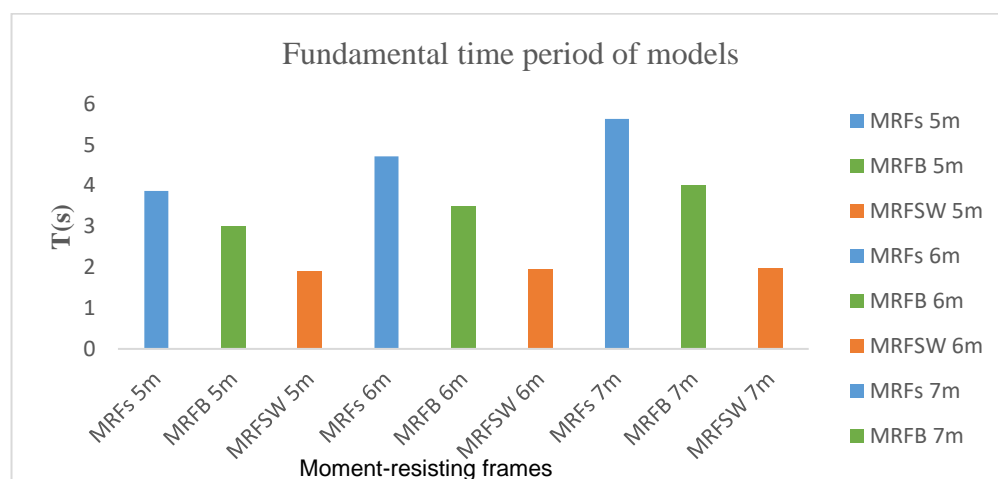
Table 16

*The fundamental time period for all the analyzed models*

Models	T(s)
MRFs 5m	3.87
MRFB 5m	3
MRFSW 5m	1.9
MRFs 6m	4.71
MRFB 6m	3.49
MRFSW 6m	1.95
MRFs 7m	5.63
MRFB 7m	4.01
MRFSW 7m	1.97

Figure 42

*All Models fundamental time period values*



## CHAPTER V

### Discussion

This chapter discusses the aforementioned findings in relation to the literature reviews.

#### 5.1 Overview

According to Tiwari and Kasnale (2017) study, IDA is carried out on an RC building to figure out its vulnerability. They discovered that; 7-story frame yields at PGA 0.29g in both directions. At PGA 0.37g in the X-axis and 0.38g in plane of Y, a collapse occurs. Building with 11 floors produces yielding at 0.61g in X and 0.58g in Y. While, 0.73g in X direction and 0.71g in the path of Y, a collapse is produced. Since it reduces the structure's stiffness as discovered, boosts yielding and collapse PGA, increasing the span length of the structure has the same impact as increasing its height.

Tran et al., (2017), three 2D RC frames—4-, 6-, and 8-story—were constructed using the Open Sees software with varying heights to assess how height affects construction behavior. Each frame's floor is the same height, measuring 3.3 meters in elevation and 1 bay by 6.0 meters in the plan. Four-story, six-story, and eight-story buildings, respectively, have first mode periods of 0.479s, 0.609s, and 0.771s. In order to simulate the structure, nonlinear Beam-Column elements are used. The Fiber Section technique is used to represent the cross section, which includes layers of reinforcement and rectangular patches of concrete. 10 strong ground motion databases with Large Magnitude characteristics between 6.5 and 7 have been compiled by PEER database. The likelihood for each RC frame to exceed CP level is found to be 16.52%, 33.92%, and 40.76% when peak ground motion increases by 0.5g for 4-6 and 8 story. For the case of our study, it is found that with 6m span length, there is 70% probability of exceeding CP limit state and this is due to the geometry of our frame. But in overall they came to the same conclusion as us that the MRFs is really weak under seismic loads.

Rimal & Maskey, (2019), 126 distinct imaginary buildings are chosen for the sensitivity analysis in this study of the factors influencing the basic period of RC moment resistant frames, following which they are modelled and created using finite

element software. The structures under consideration are uniform and have an equal number of bays in both horizontal directions. The Rayleigh approach is then used to analyze each building model and determine the building's fundamental time period. The impact of various parameters on the basic time period is then examined. Last but not least, a rough formulation of the fundamental time scale based on the chosen structural factors is suggested. It is found that the mass of the building increases with an increase in length while maintaining a constant number of bays, but the stiffness of the columns against lateral force does not. As a result, the structure is made more flexible, increasing the building's fundamental lifespan. Similar findings have been drawn from our analysis because the increase in the length from 5-6 to 7m had great effect on the stiffness of our frames.

## **CHAPTER VI**

## Conclusion and recommendations

This chapter delivers suggestion based on the analysis drawn from the research findings in accordance with the main purpose and any supporting objectives.

### 6.1 Conclusion

The seismic response of 3-dimensional framing systems under 7 ground motion was evaluated throughout this work using incremental dynamic analysis. A total number of 9 frames have been modelled and analyse by means of SAP 2000 software. The framing systems that have been adopted are: Moment Resisting Frame, Moment Resisting Frame with X Bracing and Moment Resisting Frame with Shear Wall with an increment of the span length 5-6 and 7m. After the analysis was performed, based on the IDA curve, the Fragility curve, the Storey Drift and Fundamental Time Period, all the frames have been assessed and compared. The following conclusion have been drawn from this study:

➤ *Based on the IDA curve results*

The accelerogram and structural models used in the IDA study are unique; when subjected to various ground motions, a model frequently produces highly distinct reactions that are challenging to predict beforehand. Take frame as an example, which displays reactions that range from a slow decline towards collapse to a quick, non-monotonic, back-and-forth twisting activity. Each graph shows the demands that each ground motion record places on the structure at various intensities, and they are rather intriguing in both their parallels and differences.

The MRFs with 5m span length is found to be stiffer compare to the MRFs with 6m and 7m owing to the increase of the length that makes the structure more flexible. It was observed that the MRFs with 6m and 7m based on the GM3 have 20% and 50% for IO, 17% and 55.5% for LS, 25% and 59.4% for CP respectively less than the MRFs with 5m. According to the GM4, compared to the rate of the MRFs with 5m PGA, there is a decrease in the value of the MRFs with 6m and 7m respectively which is about 12.5% and 85.7% for IO, 88.9% for LS, 26.67% and 86.4% for CP.

The MRFB with 5m from the GM3 and GM4, has a higher rigidity, which enabled the structure to withstand more. Based on the GM3, the MRFB with 6m and 7m have, respectively, 17% and 50% for IO, 23.1% and 46.1% for LS, and 34.6% and 40.38%

for CP less than the MRFB with 5m, as shown by the graphs that showed the pace of the drop in the performance of the structure. The value of the MRFB with 6m and 7m, which is roughly 20% and 40% for IO, 12.5% and 42% for LS, as well as 6% and 25.5% for CP, respectively, is lower than the rate of the MRFB with 5m PGA, per the GM4.

According to the GM3, the MRFSW with 6m and 7m had, respectively, 12.5% and 31.25% less for IO, 22% and 28% for LS, and 5% and 22% less for CP than the MRFSW with 5m, as evidenced by the analysis that showed the speed of the decline in the structure's performance. The rate of the MRFSW with 5m, according to the GM4, is higher than the value of the MRFSW with 6m and 7m, which is around 7% and 14% for IO, 13.3% and 23.3% for LS, as well as 7% and 28.6% for CP, respectively.

➤ *Following the findings of the ISDR curve*

Since IDA graph is function of the inter-story drift ratio, it can be concluded that the MRF with 5m for all the system has higher stiffness that allowed the structure to resist more to the seismic load.

➤ *Based on the fragility curve results*

The results demonstrate that the Shear Wall offers better performance under seismic loads because the rate of damage state has increased significantly compared to the Bracing, which is stiffer than the normal Frame. The probability of exceeding the Collapse Prevention (CP) limit state has been assessed using the minimum PGA, which is 0.5g. In contrast to the MRFs with 5m, the CP value for the MRFB 5m and MRFSW 5m, respectively, has decreased by about 51% and 63%. The rate of increase for the MRFs with 6m is 54% and 65%, respectively, in comparison to the MRFB and MRFSW, both of which have 6m. In comparison to the other systems, the damage state of the MRFs increased by 51% and 65% with 7m.

➤ *Based on the Fundamental Time Period Results*

It is observed that contrasting with the 5m span length models, the MRFs value has been lowered by 22% and 51% with MRFB and MRFSW respectively. For the 6m, 26% and 59% are the decreased values of MRFB and MRFSW compared to MRFs. Taking into account the 7m length, compared to the MRFs, the MRFB and MRFSW has lowered by 29% and 65%.



In overall, the analysis show that, the MRFs system is weaker since the lateral forces have great effect on the performance of the structure compared to the MRFB and MRFSW;

The Shear Wall increase considerably the stiffness of the structure that make the structure more capable to dissipate the force that acting on the structure under seismic event;

The increase in the span length makes the structure more flexible therefore less efficient under seismic loads because longer span induced to longer deflection of the structure;

Each Ground Motion affects the structure differently because of the frequency and amplitude that varies from one to another GM.

## **6.2 Recommendations**

Future works might include these following recommendations:

- Shear walls were without openings, the openings in the shear walls can be considered in future studies.
- The number of spans that are used are 5 spans and the same length, so a greater number of spans and different length in X and Y direction also should be used in future researches.
- A combine system can be assessed with the use of shear wall and bracing in the future work.
- This study focused essentially on X direction therefore taking into account Y direction can provide thorough understanding.
- PGA have been used as EDPs in the study, so the use of Sa (Spectral Acceleration) can be used and compared the results.

## **Références**

- El-Maissi, A. M., Argyroudis, S. A., & Nazri, F. M. (2020). Seismic vulnerability assessment methodologies for roadway assets and Networks: A state-of-the-art review. *Sustainability*, 13(1), 61. <https://doi.org/10.3390/su13010061>
- Kang, C., Kwon, O.-S., & Song, J. (2021). Evaluation of correlation between engineering demand parameters of structures for seismic system reliability analysis. *Structural Safety*, 93, 102133. <https://doi.org/10.1016/j.strusafe.2021.102133>
- Rasol, M. A. (2014, January 1). Seismic Performance Assessment and strengthening of a multi-story RC building through a case study of "Seaside hotel". Handle Proxy. Retrieved March 26, 2023, from <http://hdl.handle.net/11129/1305>
- Celarec, D., & Dolšek, M. (2013). The impact of modelling uncertainties on the seismic performance assessment of reinforced concrete frame buildings. *Engineering Structures*, 52, 340–354. <https://doi.org/10.1016/j.engstruct.2013.02.036>
- Liao, W.-C., & Goel, S. C. (2012). Performance-based plastic design and energy-based evaluation of seismic resistant RC moment frame. *Journal of Marine Science and Technology*, 20(3). <https://doi.org/10.51400/2709-6998.1808>
- Maniyar, M. M., Khare, R. K., & Dhakal, R. P. (2009). Probabilistic seismic performance evaluation of non-seismic RC Frame Buildings. *Structural Engineering and Mechanics*, 33(6), 725–745. <https://doi.org/10.12989/sem.2009.33.6.725>
- Chopra, A. K., & Goel, R. K. (2004). A modal pushover analysis procedure to estimate seismic demands for unsymmetric-plan buildings. *Earthquake Engineering & Structural Dynamics*, 33(8), 903–927. <https://doi.org/10.1002/eqe.380>
- Vamvatsikos, D., & Cornell, C. A. (2002). Incremental dynamic analysis. *Earthquake Engineering & Structural Dynamics*, 31(3), 491–514. <https://doi.org/10.1002/eqe.141>
- Wang, J., & Zhao, H. (2018). High performance damage-resistant seismic resistant structural systems for sustainable and Resilient City: A Review. *Shock and Vibration*, 2018, 1–32. <https://doi.org/10.1155/2018/8703697>
- Chaulagain, H., Rodrigues, H., Spacone, E., & Varum, H. (2015). Seismic response of current RC buildings in Kathmandu Valley. *Structural Engineering and Mechanics*, 53(4), 791–818. <https://doi.org/10.12989/sem.2015.53.4.791>
- DİLMAÇ, H., ULUTAŞ, H., TEKELİ, H., & DEMİR, F. (2018). Türkiye'Deki Mevcut betonarme Binaların Deprem performansları üzerine Bir Değerlendirme. *Mehmet Akif Ersoy Üniversitesi Fen Bilimleri Enstitüsü Dergisi*, 9(Ek (Suppl.) 1), 224–237. <https://doi.org/10.29048/makufebd.443126>

- Baikerikar, A., & Kanagali, K. (2014). Study of Lateral Load Resisting Systems of Variable Heights in all Soil types of High Seismic Zone. *International Journal of Research in Engineering and Technology*, 3(10).
- Vargas, Y. F., Pujades, L. G., Barbat, A. H., & Hurtado, J. E. (2013). Incremental dynamic analysis and pushover analysis of buildings. A probabilistic comparison. *Computational Methods in Stochastic Dynamics*, 293–308. [https://doi.org/10.1007/978-94-007-5134-7\\_17](https://doi.org/10.1007/978-94-007-5134-7_17)
- Journal, I. R. J. E. T. (2018, November 15). IRJET- comparison of incremental dynamic analysis curve with pushover curve. *Academia.edu*. Retrieved March 28, 2023, from [https://www.academia.edu/37784650/IRJET\\_COMPARISON\\_OF\\_INCREMENTAL\\_DYNAMIC\\_ANALYSIS\\_CURVE\\_WITH\\_PUSHOVER\\_CURVE](https://www.academia.edu/37784650/IRJET_COMPARISON_OF_INCREMENTAL_DYNAMIC_ANALYSIS_CURVE_WITH_PUSHOVER_CURVE)
- Seyedkazemi, A., & Rofooei, F. (2019). Comparison of static pushover analysis and Ida-based probabilistic methods in assessing the seismic performance factors of diagrid structures. *Scientia Iranica*. <https://doi.org/10.24200/sci.2019.51555.2250>
- Maniyar, M. M., Khare, R. K., & Dhakal, R. P. (2009). Probabilistic seismic performance evaluation of non-seismic RC Frame Buildings. *Structural Engineering and Mechanics*, 33(6), 725–745. <https://doi.org/10.12989/sem.2009.33.6.725>
- Brunesi, E., Nascimbene, R., Parisi, F., & Augenti, N. (2015). Progressive collapse fragility of reinforced concrete framed structures through incremental dynamic analysis. *Engineering Structures*, 104, 65–79. <https://doi.org/10.1016/j.engstruct.2015.09.024>
- El-Betar, S. A. (2018). Seismic vulnerability evaluation of existing R.C. Buildings. *HBRC Journal*, 14(2), 189–197. <https://doi.org/10.1016/j.hbrcj.2016.09.002>
- Inel, M., Cayci, B. T., & Meral, E. (2018). Nonlinear static and dynamic analyses of RC Buildings. *International Journal of Civil Engineering*, 16(9), 1241–1259. <https://doi.org/10.1007/s40999-018-0285-0>
- Baros, D. K., & Dritsos, S. E. (2008). A simplified procedure to select a suitable retrofit strategy for existing RC buildings using pushover analysis. *Journal of Earthquake Engineering*, 12(6), 823–848. <https://doi.org/10.1080/13632460801890240>
- Ricci, P., Manfredi, V., Noto, F., Terrenzi, M., De Risi, M. T., Di Domenico, M., Camata, G., Franchin, P., Masi, A., Mollaioli, F., Spacone, E., & Verderame, G. M. (2019). RINTC-E: Towards seismic risk assessment of existing residential reinforced concrete buildings in Italy. *Proceedings of the 7th International Conference on Computational Methods in Structural Dynamics and Earthquake Engineering (COMPdyn 2015)*. <https://doi.org/10.7712/120119.6939.20040>

- Sadjadi, R., Kianoush, M. R., & Talebi, S. (2007). Seismic performance of reinforced concrete moment resisting frames. *Engineering Structures*, 29(9), 2365–2380. <https://doi.org/10.1016/j.engstruct.2006.11.029>
- Seo, J., Hu, J., & Davaajamts, B. (2015). Seismic performance evaluation of multistory reinforced concrete moment resisting frame structure with shear walls. *Sustainability*, 7(10), 14287–14308. <https://doi.org/10.3390/su71014287>
- Bisht, S. (2020, September 6). Types of bracing systems. *Civil Wale*. Retrieved March 30, 2023, from <https://civilwale.com/types-of-bracing-systems/>
- Leng, J., Buonopane, S. G., & Schafer, B. W. (2020). Incremental Dynamic Analysis and FEMA P695 seismic performance evaluation of a cold-formed steel-framed building with gravity framing and architectural sheathing. *Earthquake Engineering & Structural Dynamics*, 49(4), 394–412. <https://doi.org/10.1002/eqe.3245>
- S.R. Thorat., & P.J. Salunke. (2014). Seismic behaviour of multi-storey shear wall frame versus braced ... Retrieved April 9, 2023, from [https://www.ripublication.com/ijame-spl/ijamev4n3spl\\_12.pdf](https://www.ripublication.com/ijame-spl/ijamev4n3spl_12.pdf)
- A. Dharanya, S. Gayathri, and M. Deepika(2017) “Comparison Study of Shear Wall and Bracings under Seismic Loading in Multi- Storey Residential Building,” vol. 10, no. 8, pp. 417–424, 2017, <https://www.academia.edu/40390130>
- Atif, M., Nair, V., & Vairagade, L. (2015). Comparative study on seismic analysis of Multistorey building stiffened with bracing and shear wall *International Research Journal of Engineering and Technology (IRJET)* . Retrieved April 9, 2023, from <https://mail.irjet.net/archives/V2/i5/IRJET-V2I5192.pdf>
- AZAD, M. D. S. A. M. D. A. N. I., & HAZNI, S. Y. E. D. (2016). (PDF)" Comparative Study of seismic analysis of multistory buildings with shear wall and bracing system " *International Journal of Advanced Structures and Geotechnical Engineering*. Retrieved April 9, 2023, from [https://www.researchgate.net/publication/308777769\\_Comparative\\_study\\_of\\_seismic\\_analysis\\_of\\_multistory\\_buildings\\_with\\_shear\\_walls\\_and\\_bracing\\_systems](https://www.researchgate.net/publication/308777769_Comparative_study_of_seismic_analysis_of_multistory_buildings_with_shear_walls_and_bracing_systems)
- Pavel, F., & Pricopie, A. (2015). Prediction of engineering demand parameters for RC Wall Structures. *Structural Engineering and Mechanics*, 54(4), 741–754. <https://doi.org/10.12989/sem.2015.54.4.741>
- Bhatt, A. D. (2020). Comparison of Interstorey Drift in general RC buildings in pounding and no pounding case. *Technical Journal*, 2(1), 40–47. <https://doi.org/10.3126/tj.v2i1.32828>

Kristiawan, S., Hapsari, I., Purwanto, E., & Marwahyudi, M. (2021). Evaluation of damage limit state for RC frame based on Fe Modeling. *Buildings*, 12(1), 21. <https://doi.org/10.3390/buildings12010021>

A comprehensive study on the seismic behavior of double-layer space ... (n.d.). Retrieved April 22, 2023, from

[https://www.researchgate.net/publication/261171164\\_A\\_Comprehensive\\_Study\\_on\\_the\\_Seismic\\_Behavior\\_of\\_Double-Layer\\_Space\\_Structure\\_Domes](https://www.researchgate.net/publication/261171164_A_Comprehensive_Study_on_the_Seismic_Behavior_of_Double-Layer_Space_Structure_Domes)

Tiwari, V., & Kasnale, A. (2017). Incremental Dynamic Analysis of RC frames. *www.irjet.net*. Retrieved April 28, 2023, from <https://www.irjet.net/archives/V4/i6/IRJET-V4I6127.pdf>

Tran, T. T., Nguyen, T. H., Park, J., & Kim, D. (2017). Nonlinear behaviour of reinforced concrete structures using incremental ...ResearchGate. [https://www.researchgate.net/profile/Thanh-Tuan-Tran/publication/326802247\\_Nonlinear\\_Behaviour\\_of\\_Reinforced\\_Concrete\\_Structures\\_Using\\_Incremental\\_Dynamic\\_Analysis\\_Considering\\_Height\\_Effects/links/5b64089fa6fdcc45b30c9e8d/Nonlinear-Behaviour-of-Reinforced-Concrete-Structures-Using-Incremental-Dynamic-Analysis-Considering-Height-Effects.pdf?origin=publication\\_detail](https://www.researchgate.net/profile/Thanh-Tuan-Tran/publication/326802247_Nonlinear_Behaviour_of_Reinforced_Concrete_Structures_Using_Incremental_Dynamic_Analysis_Considering_Height_Effects/links/5b64089fa6fdcc45b30c9e8d/Nonlinear-Behaviour-of-Reinforced-Concrete-Structures-Using-Incremental-Dynamic-Analysis-Considering-Height-Effects.pdf?origin=publication_detail)

Rimal, J. C., & Maskey, P. N. (2019). Fundamental time period of Rc moment resisting frames. *Proceedings of IOE Graduate Conference*,. <http://conference.ioe.edu.np/publications/ioegc2019-summer/IOEGC-2019-Summer-073.pdf>

## APPENDICES

### Appendix A

### Input tables for fragility curve of remaining moment resisting frames

Table A.1

a) *Input table for MRFs with 5m for developing the fragility curve*

Acceleration (g)	Drift (%)	Ln(Drift)
0.1	0.58	-0.5447272
0.1	0.84	-0.1743534
0.1	0.96	-0.040822
0.1	2.18	0.7793249
0.1	1.47	0.3852624
0.1	0.43	-0.8439701
0.1	0.11	-2.2072749
0.2	0.76	-0.2744368
0.2	1.56	0.4446858
0.2	2.27	0.8197798
0.2	3.8	1.3350011
0.2	2.35	0.8544153
0.2	0.67	-0.4004776
0.2	0.22	-1.5141277
0.3	1.14	0.1310283
0.3	2.23	0.8020016
0.3	3.5	1.252763
0.3	99	4.5951199
0.3	1.85	0.6151856
0.3	0.95	-0.0512933
0.3	0.33	-1.1086626
0.4	1.58	0.4574248
0.4	2.79	1.0260416
0.4	7.94	2.0719133
0.4	100	4.6051702
0.4	3.05	1.1151416
0.4	1.21	0.1906204
0.4	0.45	-0.7985077
0.5	2.27	0.8197798
0.5	3.34	1.2059708
0.5	100	4.6051702
0.5	100	4.6051702
0.5	4.52	1.508512
0.5	1.57	0.4510756
0.5	0.57	-0.5621189

b) *Input table for MRFs with 6m for developing the fragility curve*

Acceleration (g)	Drift (%)	Ln(Drift)
0.1	0.41	-0.891598
0.1	0.87	-0.139262
0.1	1.21	0.1906204
0.1	1.12	0.1133287
0.1	0.9	-0.105361
0.1	0.4	-0.916291
0.1	0.17	-1.771957
0.2	0.82	-0.198451
0.2	1.5	0.4054651
0.2	2.52	0.9242589
0.2	4	1.3862944
0.2	1.82	0.5988365
0.2	0.76	-0.274437
0.2	0.34	-1.07881
0.3	1.47	0.3852624
0.3	2.11	0.7466879
0.3	18.8	2.9338569
0.3	32.1	3.468856
0.3	13.93	2.6340448
0.3	1.14	0.1310283
0.3	0.51	-0.673345
0.4	2.29	0.8285518
0.4	2.58	0.9477894
0.4	21.4	3.0633909
0.4	36.7	3.6027768
0.4	15.08	2.7133694
0.4	1.75	0.5596158
0.4	0.67	-0.400478
0.5	3.24	1.1755733
0.5	16	2.7725887
0.5	34.19	3.5319332
0.5	100	4.6051702
0.5	20.21	3.0061775
0.5	2.49	0.9122827
0.5	0.84	-0.174353

*c) Input table for MRFs with 7m for developing the fragility curve*

Acceleration (g)	Drift (%)	Ln(Drift)
0.1	0.47	-0.755023
0.1	0.86	-0.150823
0.1	2.73	1.0043016
0.1	20.89	3.0392706
0.1	1.73	0.5481214
0.1	0.59	-0.527633
0.1	0.2	-1.609438
0.2	1.1	0.0953102
0.2	3.75	1.3217558
0.2	13.8	2.6246686
0.2	12.31	2.5104119
0.2	15.38	2.733068
0.2	1.26	0.2311117
0.2	0.4	-0.916291

Table A.2

a) Input table for MRFB with 5m for developing the fragility curve

Acceleration (g)	Drift (%)	Ln(Drift)
0.1	0.11	-2.2072749
0.1	0.77	-0.2613648
0.1	0.82	-0.1984509
0.1	0.98	-0.0202027
0.1	0.95	-0.0512933
0.1	0.32	-1.1394343
0.1	0.14	-1.9661129
0.2	0.19	-1.6607312
0.2	1.47	0.3852624
0.2	1.53	0.4252677
0.2	1.66	0.5068176
0.2	1.95	0.6678294
0.2	0.51	-0.6733446
0.2	0.29	-1.2378744
0.3	1.15	0.1397619
0.3	2.17	0.7747272
0.3	2.22	0.7975072
0.3	2.43	0.8878913
0.3	2.76	1.0152307
0.3	0.64	-0.4462871
0.3	0.44	-0.8209806
0.4	1.35	0.3001046



0.4	2.87	1.054312
0.4	3.03	1.1085626
0.4	3.08	1.1249296
0.4	4.16	1.4255151
0.4	0.78	-0.2484614
0.4	0.57	-0.5621189
0.5	1.73	0.5481214
0.5	3.56	1.2697605
0.5	3.89	1.3584092
0.5	3.91	1.3635374
0.5	4.65	1.5368672
0.5	0.94	-0.0618754
0.5	0.69	-0.3710637
0.6	2.13	0.756122
0.6	4.24	1.4445633
0.6	4.8	1.5686159
0.6	4.95	1.5993876
0.6	6.52	1.8748744
0.6	1.16	0.14842
0.6	0.8	-0.2231436
0.7	2.22	0.7975072
0.7	4.43	1.4883996
0.7	5.64	1.7298841
0.7	6.38	1.8531681
0.7	7.62	2.0307764
0.7	1.37	0.3148107
0.7	0.9	-0.1053605
0.8	2.58	0.9477894
0.8	5.59	1.7209793
0.8	6.54	1.8779372
0.8	8.03	2.0831845
0.8	7.9	2.0668628
0.8	1.61	0.4762342
0.8	1.01	0.0099503

*b) Input table for MRFB with 6m for developing the fragility curve*

Acceleration (g)	Drift (%)	Ln(Drift)
0.1	0.46	-0.7765288

0.1	0.87	-0.1392621
0.1	0.93	-0.0725707
0.1	2	0.6931472
0.1	1.36	0.3074847
0.1	0.41	-0.8915981
0.1	0.2	-1.6094379
0.2	0.8	-0.2231436
0.2	1.57	0.4510756
0.2	1.78	0.5766134
0.2	2.83	1.0402767
0.2	2.5	0.9162907
0.2	0.73	-0.3147107
0.2	0.39	-0.9416085
0.3	1.06	0.0582689
0.3	2.36	0.8586616
0.3	2.71	0.9969486
0.3	2.83	1.0402767
0.3	3.8	1.3350011
0.3	1.07	0.0676586
0.3	0.6	-0.5108256
0.4	1.5	0.4054651
0.4	3.14	1.1442228
0.4	3.75	1.3217558
0.4	3.1	1.1314021
0.4	6.02	1.7950873
0.4	1.28	0.2468601
0.4	0.76	-0.2744368
0.5	1.8	0.5877867
0.5	3.89	1.3584092
0.5	4.95	1.5993876
0.5	4.23	1.442202
0.5	6.85	1.9242487
0.5	1.61	0.4762342
0.5	0.99	-0.0100503
0.6	2.21	0.7929925
0.6	4.61	1.5282279
0.6	6.15	1.8164521
0.6	7.61	2.0294632
0.6	7.21	1.975469
0.6	2.08	0.7323679
0.6	1.11	0.10436

*c) Input table for MRFB with 7m for developing the fragility curve*

Acceleration (g)	Drift (%)	Ln(Drift)
0.1	0.61	-0.4942963

0.1	0.91	-0.0943107
0.1	1.02	0.0198026
0.1	1.25	0.2231436
0.1	1.34	0.2926696
0.1	0.47	-0.7550226
0.1	0.12	-2.1202635
0.2	0.83	-0.1863296
0.2	1.62	0.4824261
0.2	2.03	0.7080358
0.2	2.48	0.9082586
0.2	2.36	0.8586616
0.2	0.89	-0.1165338
0.2	0.24	-1.4271164
0.3	1.22	0.1988509
0.3	2.43	0.8878913
0.3	3.55	1.2669476
0.3	4.5	1.5040774
0.3	4.48	1.499623
0.3	1.07	0.0676586
0.3	0.36	-1.0216512
0.4	1.66	0.5068176
0.4	3.15	1.1474025
0.4	4.63	1.5325569
0.4	4.43	1.4883996
0.4	4.82	1.5727739
0.4	1.35	0.3001046
0.4	0.47	-0.7550226
0.5	2.16	0.7701082
0.5	4.06	1.401183
0.5	5.91	1.7766458
0.5	6.67	1.8976199
0.5	6.47	1.8671761
0.5	1.85	0.6151856
0.5	0.59	-0.5276327
0.6	2.74	1.0079579
0.6	4.97	1.6034198
0.6	7.24	1.9796212
0.6	9.26	2.225704
0.6	4.02	1.3912819
0.6	2.15	0.7654678
0.6	0.68	-0.3856625

Table A.3

*a) Input table for MRFSW with 5m for developing the fragility curve*

Acceleration (g)	Drift (%)	Ln(Drift)
0.1	0.29	-1.2378744
0.1	0.69	-0.3710637
0.1	0.85	-0.1625189
0.1	0.66	-0.4155154
0.1	0.5	-0.6931472
0.1	0.6	-0.5108256
0.1	0.19	-1.6607312
0.2	0.57	-0.5621189
0.2	1.26	0.2311117
0.2	1.72	0.5423243
0.2	1.4	0.3364722
0.2	0.96	-0.040822
0.2	1.01	0.0099503
0.2	0.39	-0.9416085
0.3	0.9	-0.1053605
0.3	1.55	0.4382549
0.3	2.56	0.9400073
0.3	2.01	0.6981347
0.3	1.49	0.3987761
0.3	1.44	0.3646431
0.3	0.58	-0.5447272
0.4	1.23	0.2070142
0.4	1.93	0.65752
0.4	3.49	1.2499017
0.4	2.88	1.0577903
0.4	1.99	0.6881346
0.4	1.94	0.662688
0.4	0.77	-0.2613648
0.5	1.58	0.4574248
0.5	3.06	1.1184149
0.5	4.38	1.4770487
0.5	3.34	1.2059708
0.5	2.47	0.9042182
0.5	2.42	0.8837675
0.5	0.95	-0.0512933
0.6	1.96	0.6729445
0.6	3.42	1.2296406
0.6	5.29	1.6658182
0.6	4.47	1.4973884
0.6	3.01	1.1019401
0.6	2.92	1.0715836
0.6	1.12	0.1133287
0.7	2.25	0.8109302

0.7	3.87	1.3532545
0.7	6.17	1.8196988
0.7	4.14	1.4206958
0.7	3.56	1.2697605
0.7	3.39	1.2208299
0.7	1.28	0.2468601
0.8	2.69	0.9895412
0.8	3.78	1.329724
0.8	6.91	1.9329696
0.8	6.44	1.8625285
0.8	4.25	1.446919
0.8	4	1.3862944
0.8	1.44	0.3646431

*b) Input table for MRFSW with 6m for developing the fragility curve*

Acceleration (g)	Drift (%)	Ln(Drift)
0.1	0.3	-1.2039728
0.1	0.66	-0.4155154
0.1	0.7	-0.3566749
0.1	0.81	-0.210721
0.1	0.49	-0.7133499
0.1	0.61	-0.4942963
0.1	0.11	-2.2072749
0.2	0.6	-0.5108256
0.2	1	0
0.2	1.31	0.2700271
0.2	1.65	0.5007753
0.2	1.1	0.0953102
0.2	1.13	0.1222176
0.2	0.23	-1.469676
0.3	1.06	0.0582689
0.3	1.82	0.5988365
0.3	2.44	0.891998
0.3	2.48	0.9082586
0.3	1.63	0.48858
0.3	1.48	0.3920421
0.3	0.34	-1.0788097
0.4	1.24	0.2151114
0.4	2.45	0.896088
0.4	3	1.0986123
0.4	3.22	1.1693814
0.4	2.25	0.8109302
0.4	1.95	0.6678294

0.4	0.46	-0.7765288
0.5	1.66	0.5068176
0.5	3.49	1.2499017
0.5	3.61	1.2837078
0.5	3.8	1.3350011
0.5	3	1.0986123
0.5	2.4	0.8754687
0.5	0.58	-0.5447272
0.6	2.03	0.7080358
0.6	3.42	1.2296406
0.6	4.17	1.427916
0.6	4.9	1.5892352
0.6	3.59	1.2781522
0.6	2.74	1.0079579
0.6	0.7	-0.3566749

*c) Input table for MRFSW with 7m for developing the fragility curve*

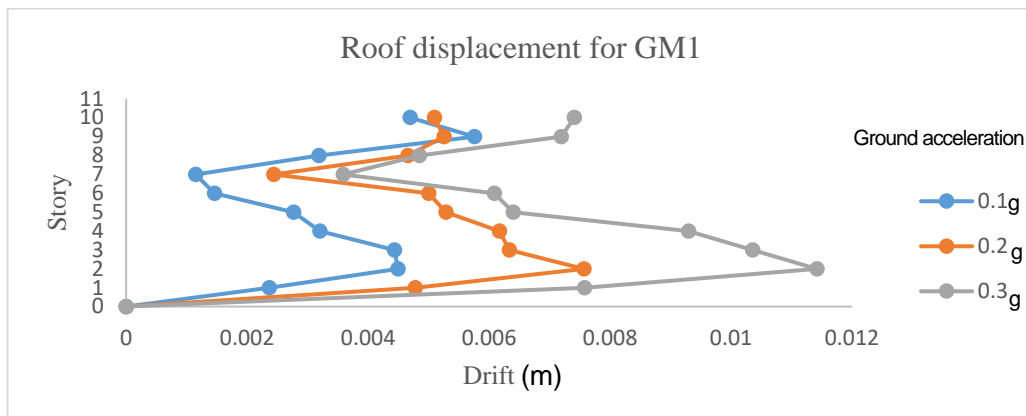
Acceleration (g)	Drift (%)	Ln(Drift)
0.1	0.35	-1.0498221
0.1	0.64	-0.4462871
0.1	0.7	-0.3566749
0.1	0.79	-0.2357223
0.1	0.49	-0.7133499
0.1	0.59	-0.5276327
0.1	0.2	-1.6094379
0.2	0.65	-0.4307829
0.2	1.2	0.1823216
0.2	1.16	0.14842
0.2	1.55	0.4382549
0.2	1.08	0.076961
0.2	1.21	0.1906204
0.2	0.37	-0.9942523
0.3	1.13	0.1222176
0.3	2.16	0.7701082
0.3	1.72	0.5423243
0.3	2.41	0.8796267
0.3	1.66	0.5068176
0.3	1.42	0.3506569
0.3	0.6	-0.5108256
0.4	1.2	0.1823216
0.4	2	0.6931472
0.4	2.91	1.0681531

0.4	4.05	1.3987169
0.4	2.13	0.756122
0.4	1.83	0.604316
0.4	0.81	-0.210721
0.5	1.93	0.65752
0.5	3.58	1.2753628
0.5	3.38	1.2178757
0.5	5	1.6094379
0.5	2.84	1.0438041
0.5	2.31	0.8372475
0.5	1.02	0.0198026
0.6	1.93	0.65752
0.6	3.76	1.324419
0.6	3.88	1.3558352
0.6	6.14	1.8148247
0.6	3.58	1.2753628
0.6	3.08	1.1249296
0.6	1.06	0.0582689
0.7	2.58	0.9477894
0.7	4.63	1.5325569
0.7	5.9	1.7749524
0.7	6.62	1.8900954
0.7	4.07	1.403643
0.7	3.39	1.2208299
0.7	1.24	0.2151114

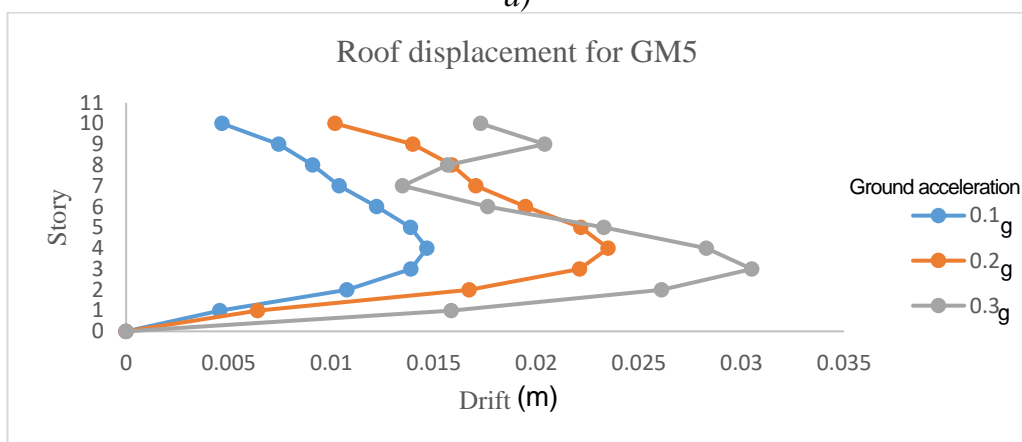
## Appendix B

### Roof displacement of the remaining frames

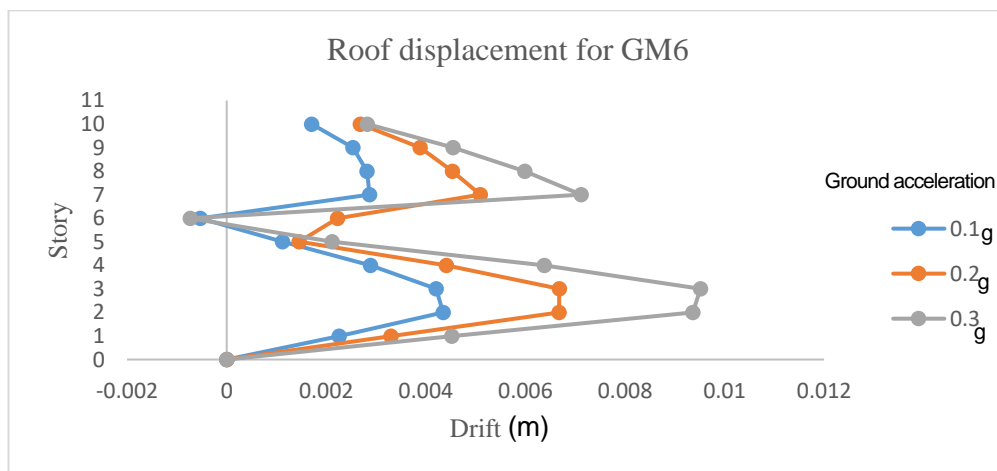
Figure B.1  
 Roof displacement for MRFs with 5m for: a) GM1, b) GM5, c) GM6, d) GM7



a)

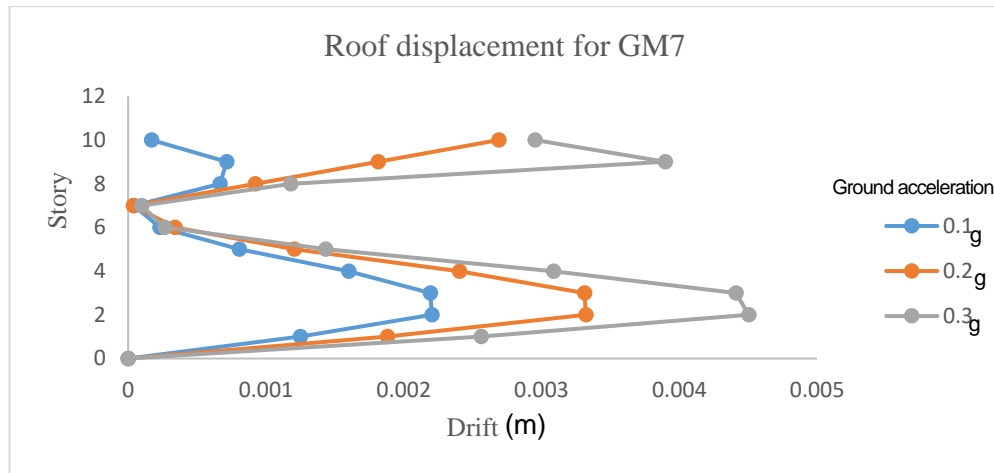


b)



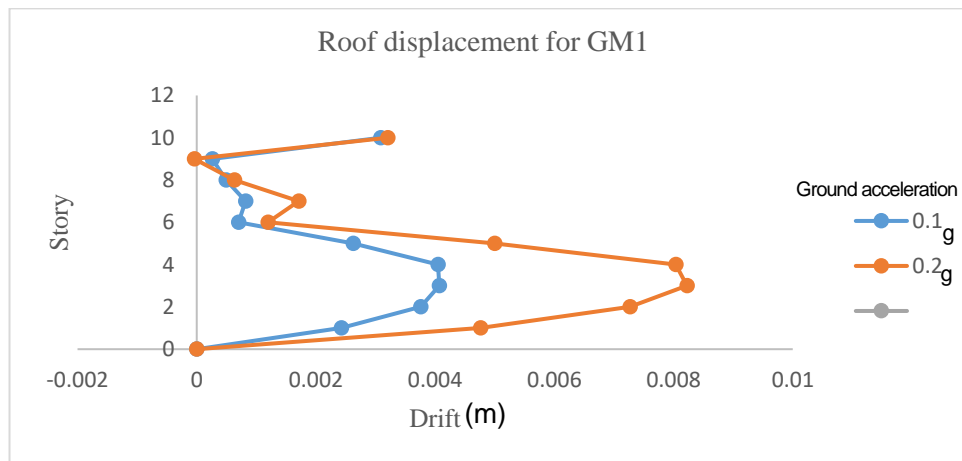
c)



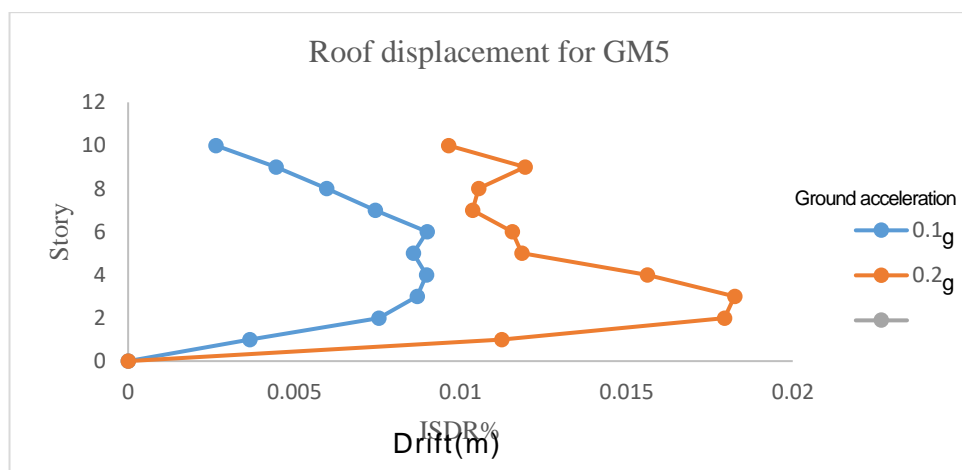


d)

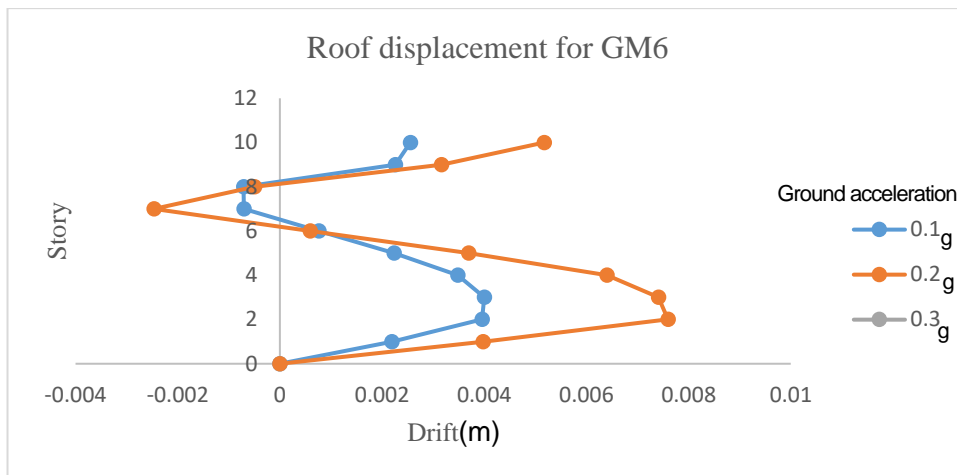
Figure B.2  
Roof displacement for MRFs with 6m for: a) GM1, b) GM5, c) GM6, d) GM7



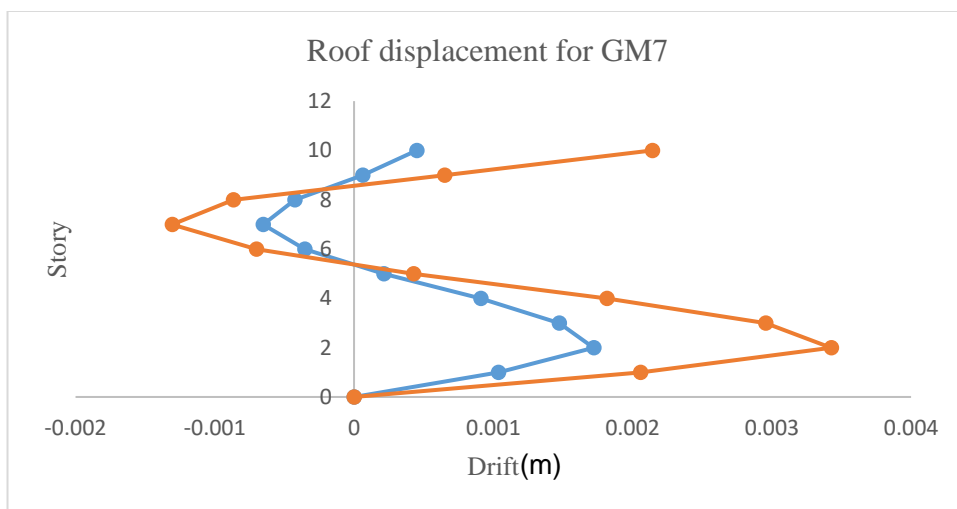
a)



b)

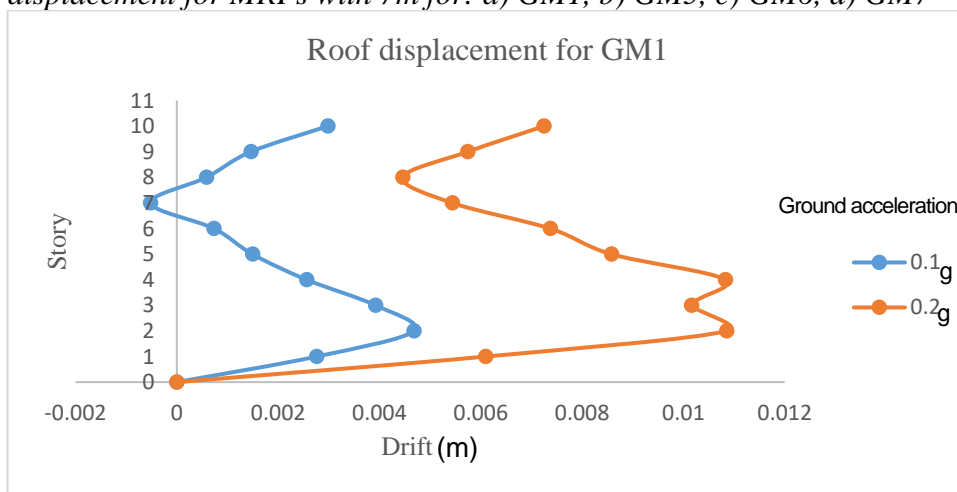


c)

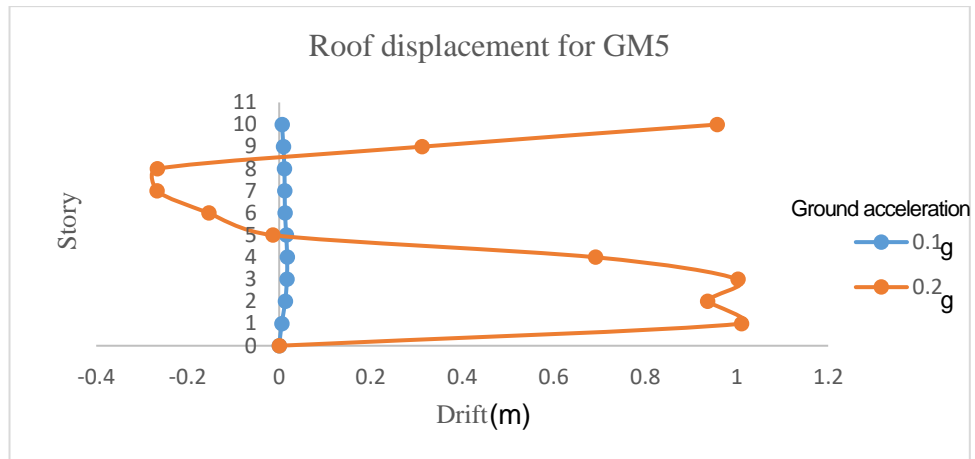


d)

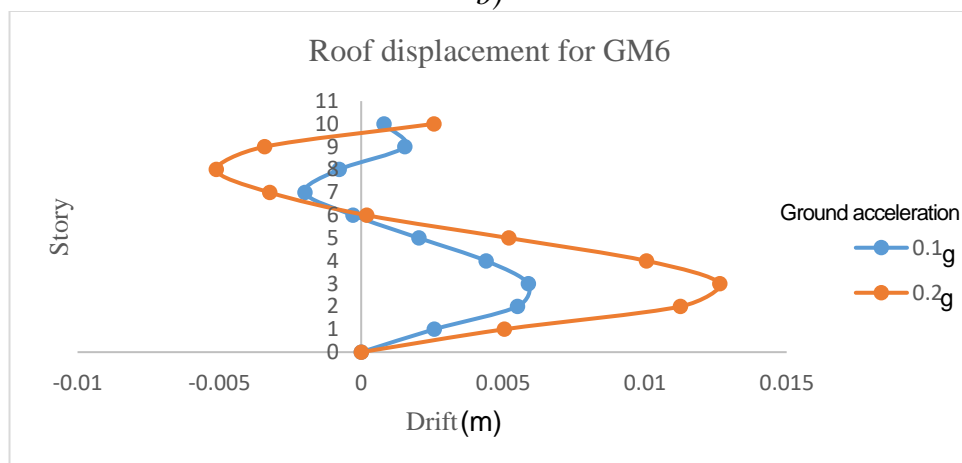
Figure B.3  
Roof displacement for MRFs with 7m for: a) GM1, b) GM5, c) GM6, d) GM7



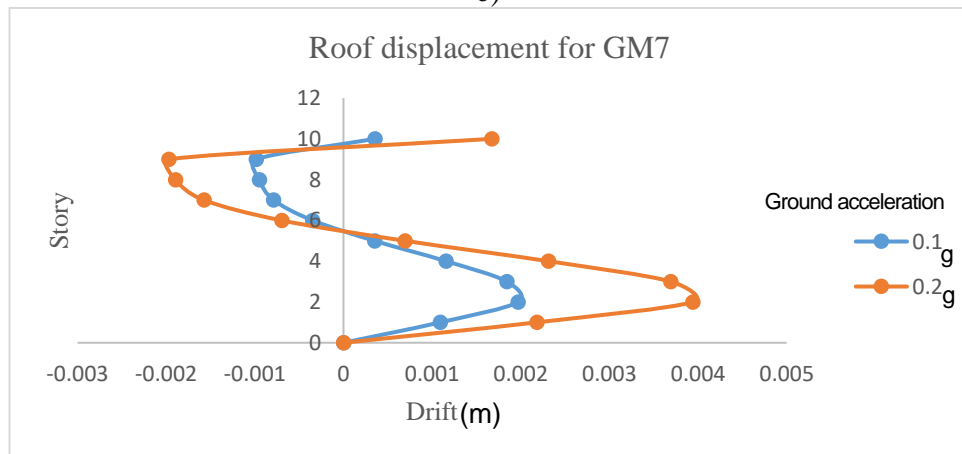
a)



b)



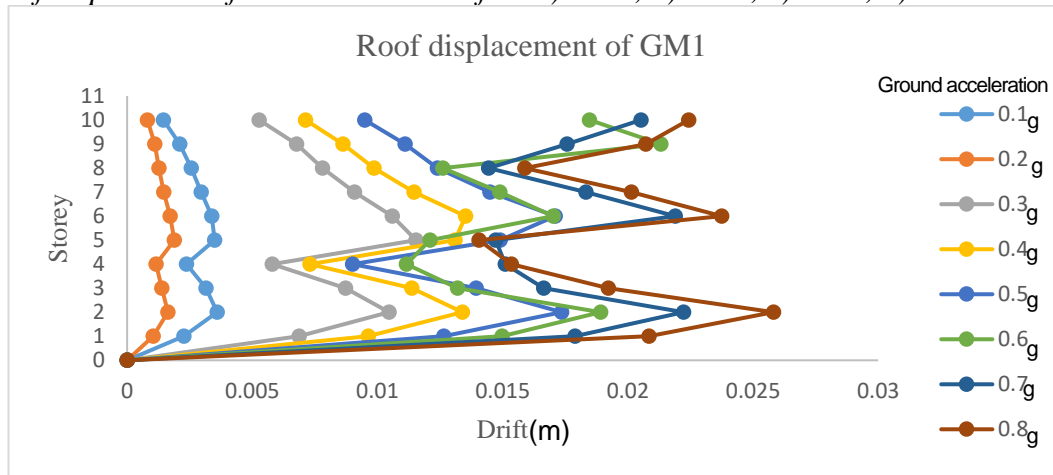
c)



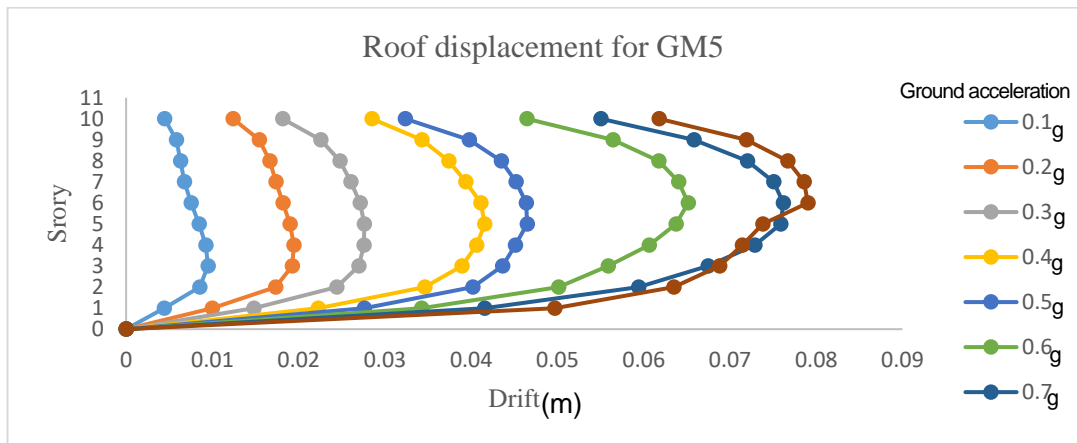
d)

Figure B.4

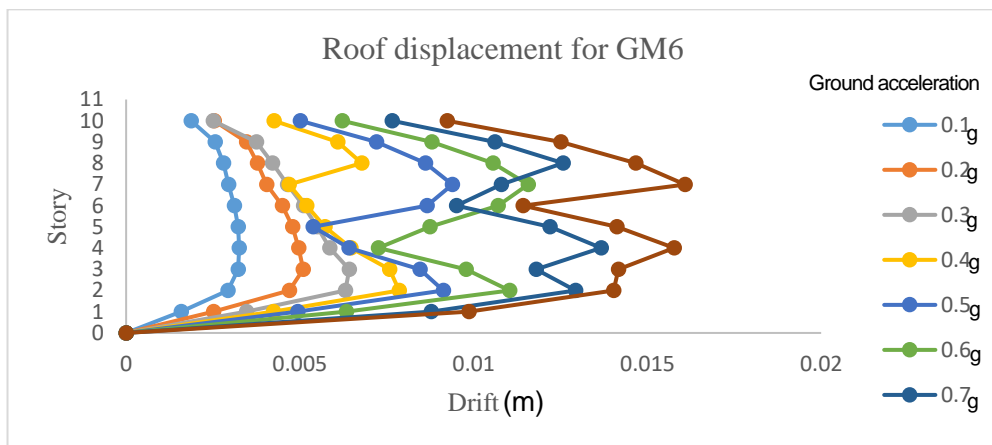
Roof displacement for MRFB with 5m for: a) GM1, b) GM5, c) GM6, d) GM7



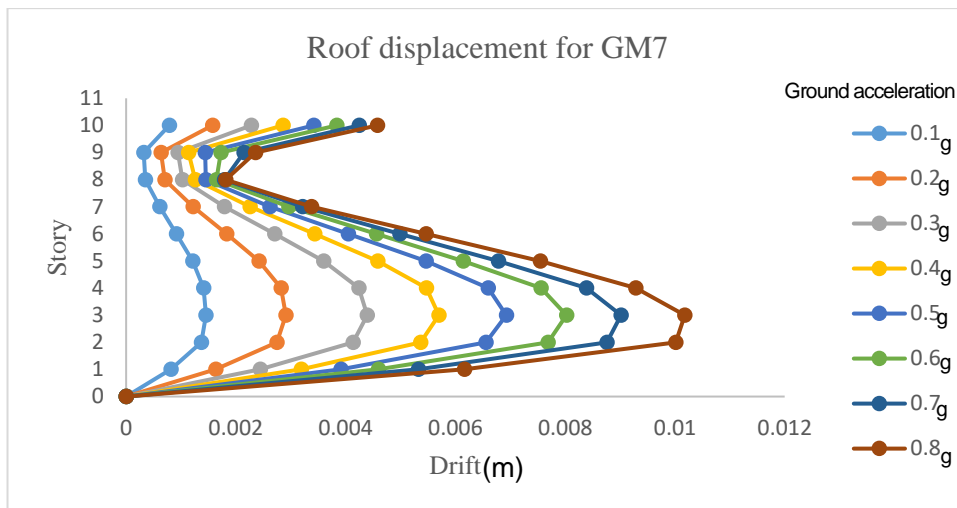
a)



b)

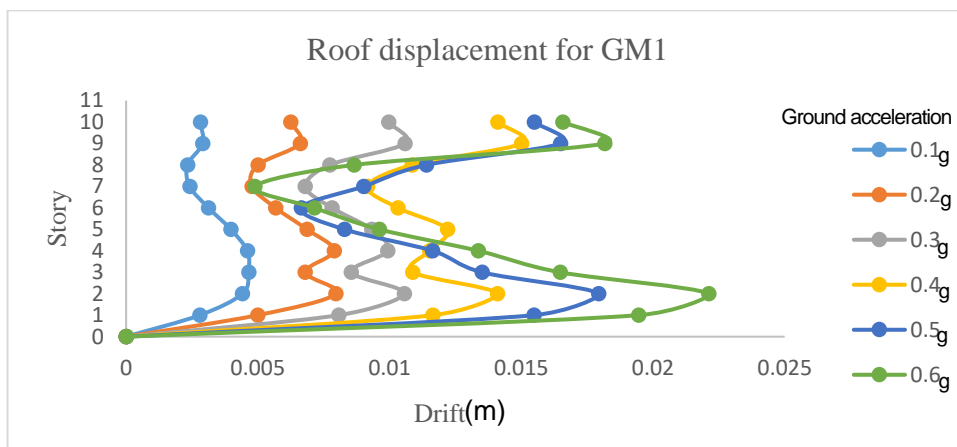


c)

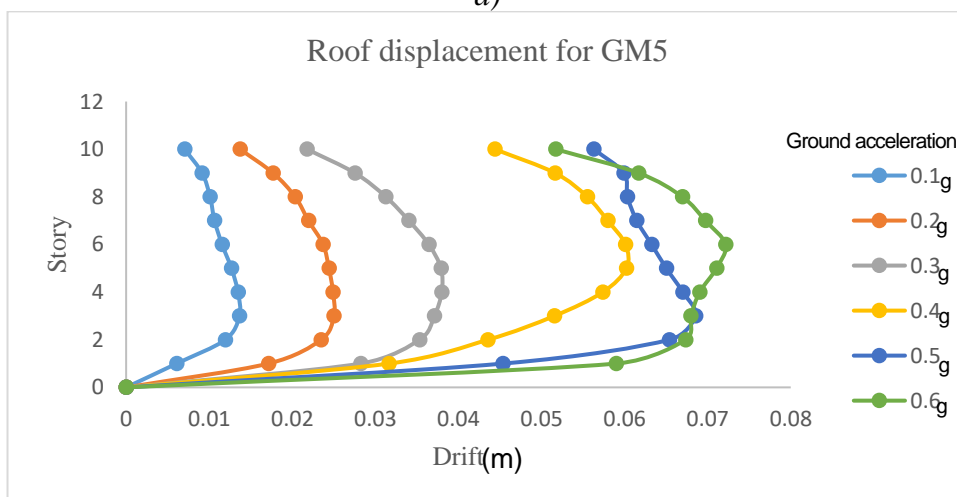


d)

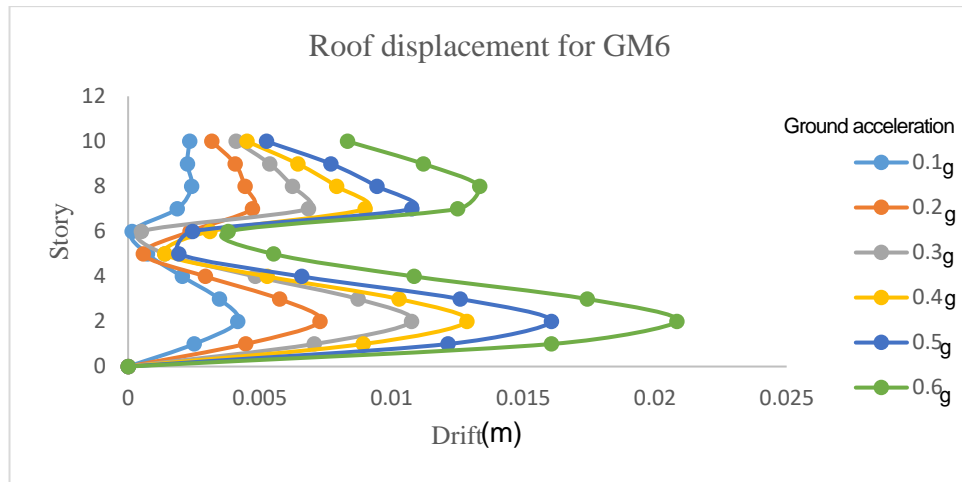
Figure B.5  
Roof displacement for MRFB with 6m for: a) GM1, b) GM5, c) GM6, d) GM7



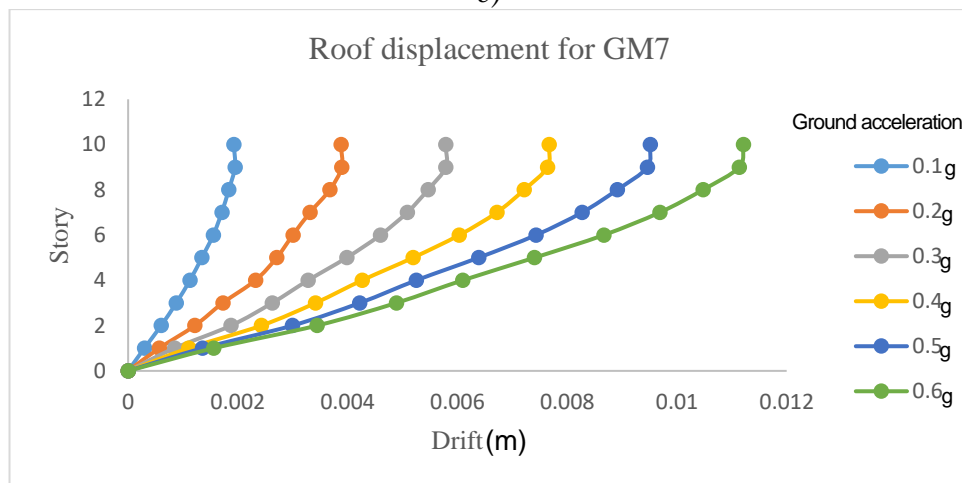
a)



b)

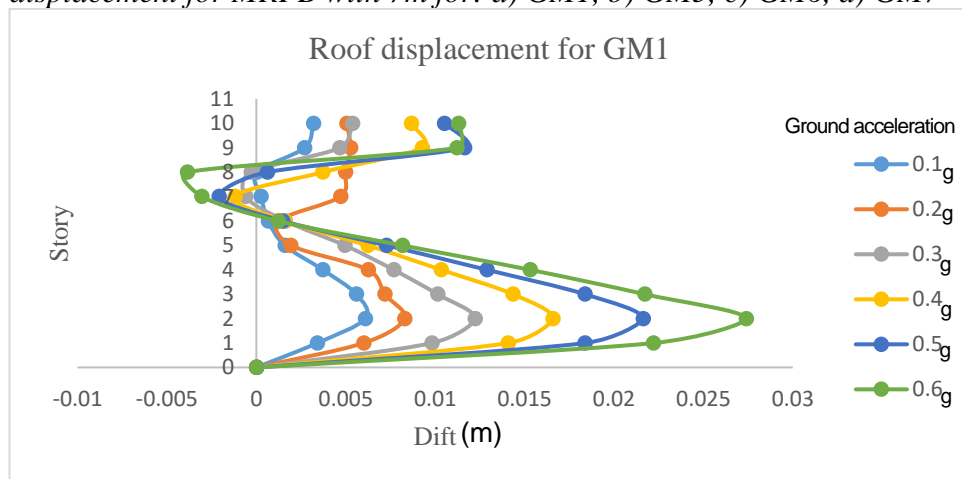


c)

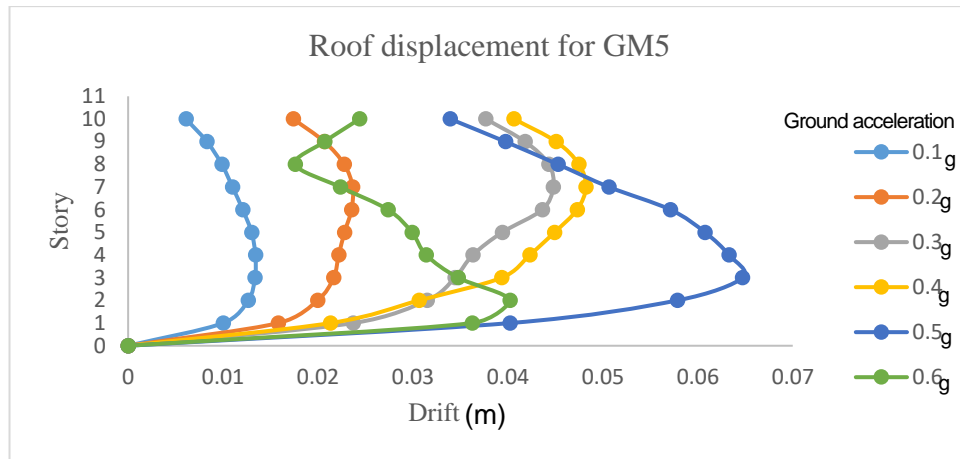


d)

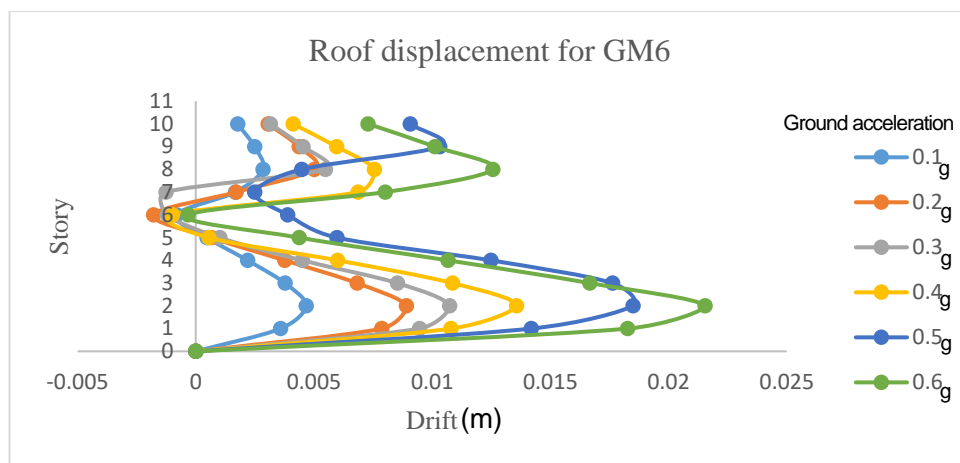
Figure B.6  
Roof displacement for MRFB with 7m for: a) GM1, b) GM5, c) GM6, d) GM7



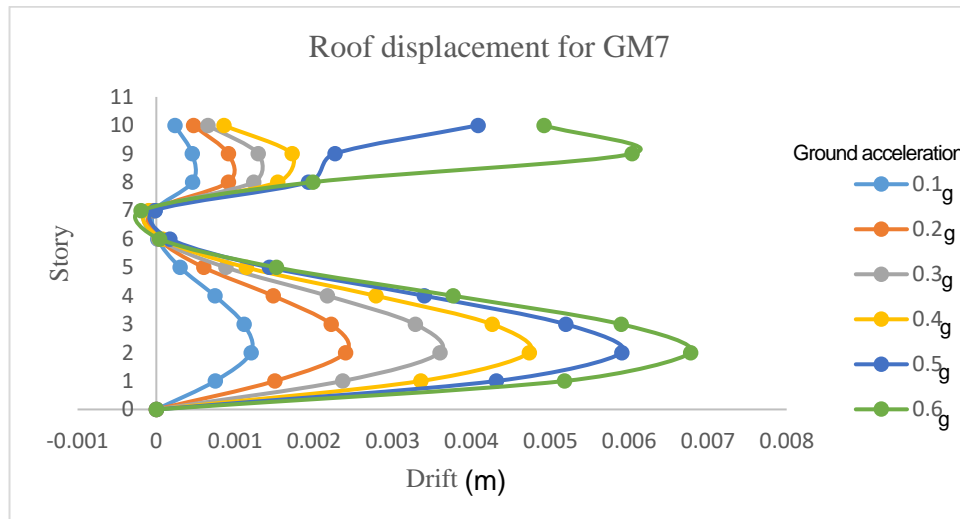
a)



b)

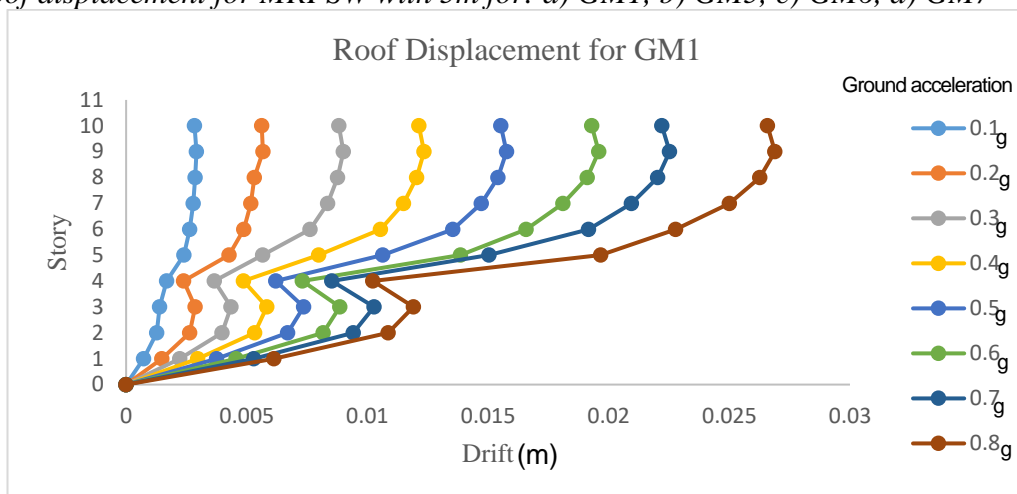


c)

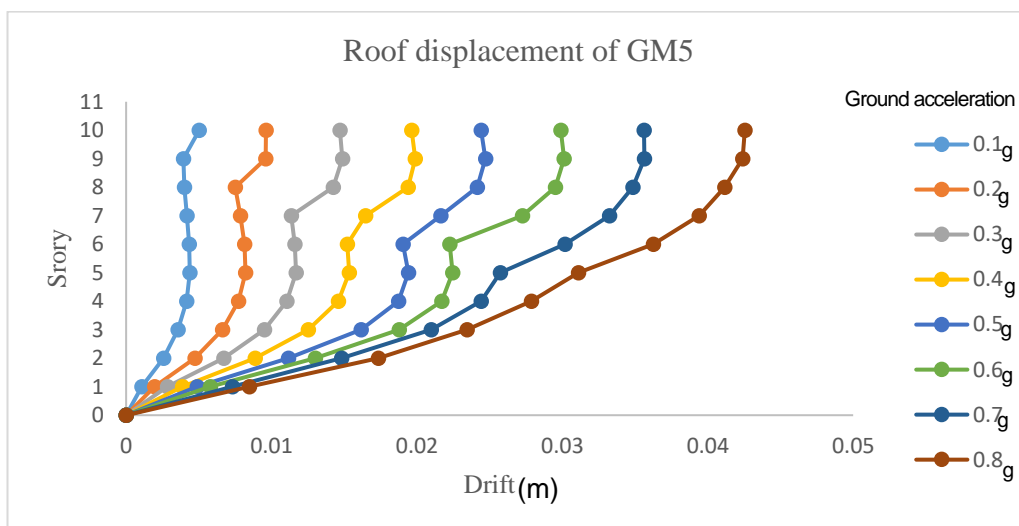


d)

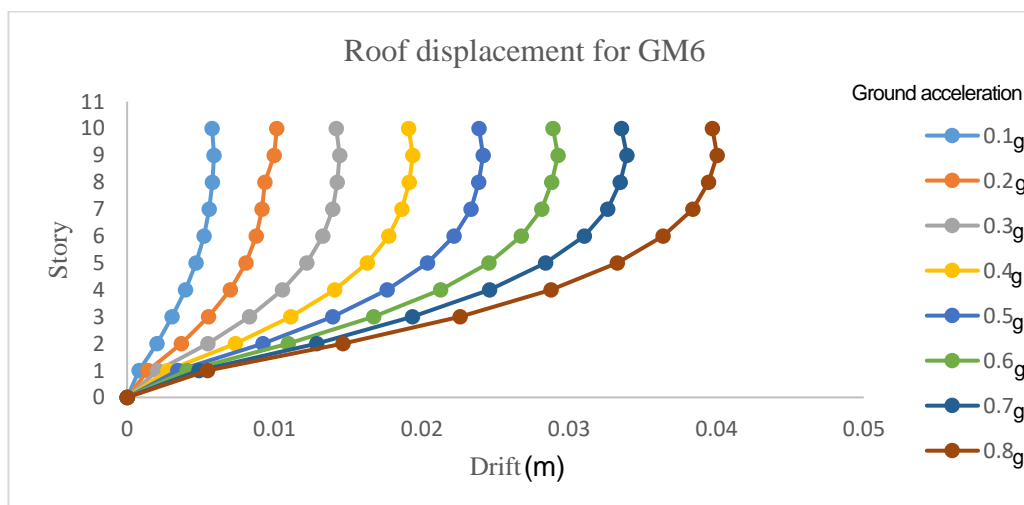
Figure B.7  
 Roof displacement for MRFSW with 5m for: a) GM1, b) GM5, c) GM6, d) GM7



a)

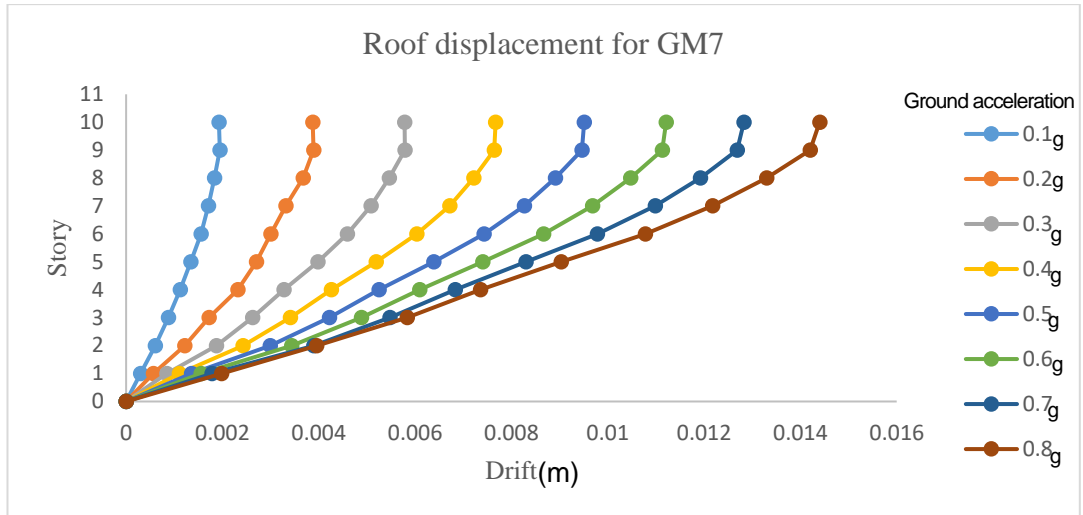


b)



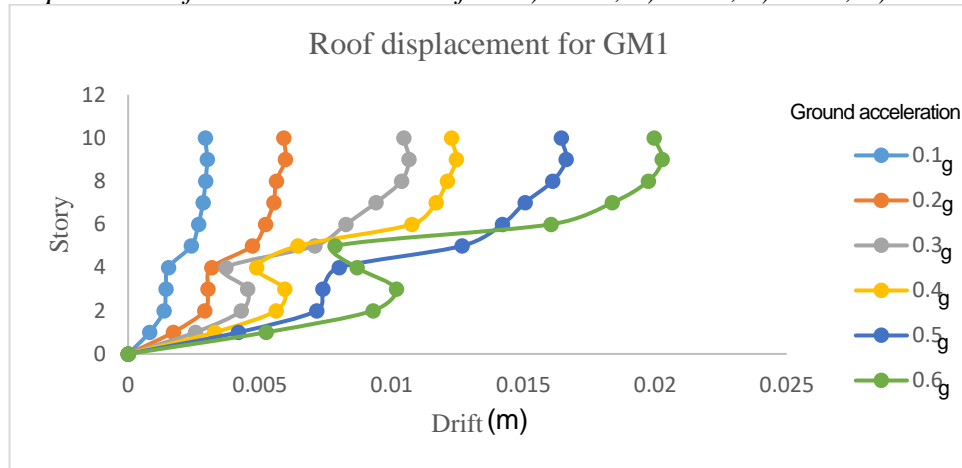
c)



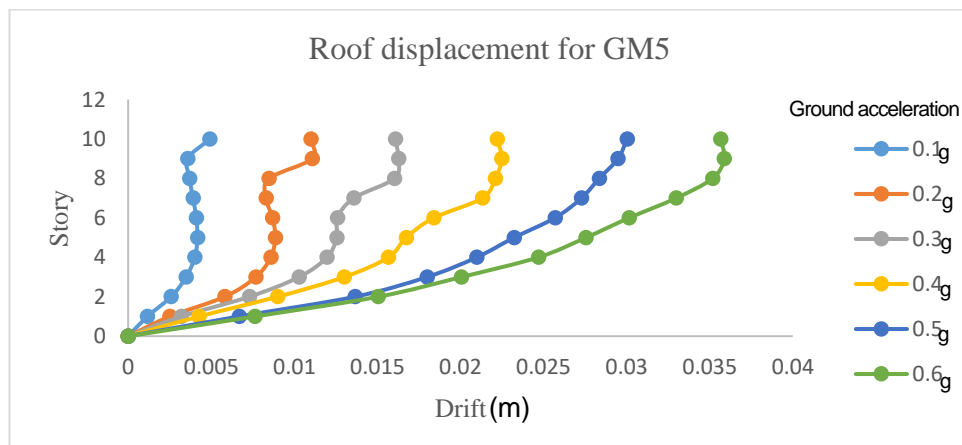


d)

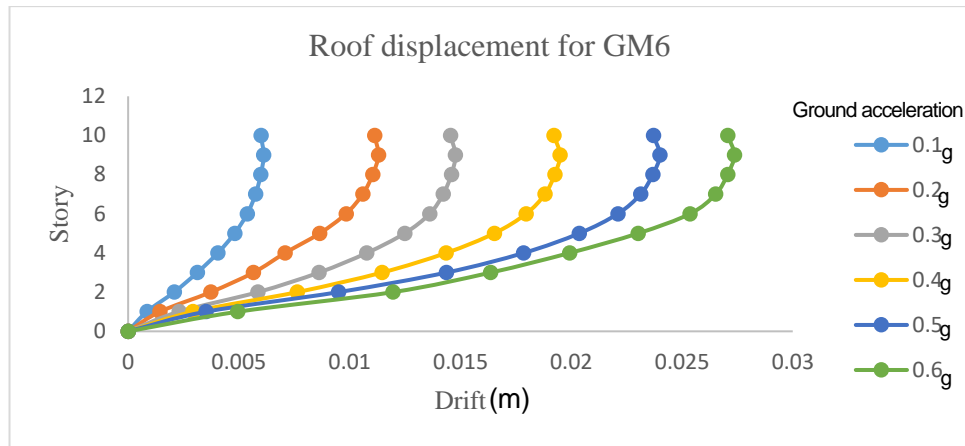
Figure B.8  
Roof displacement for MRFSW with 6m for: a) GM1, b) GM5, c) GM6, d) GM7



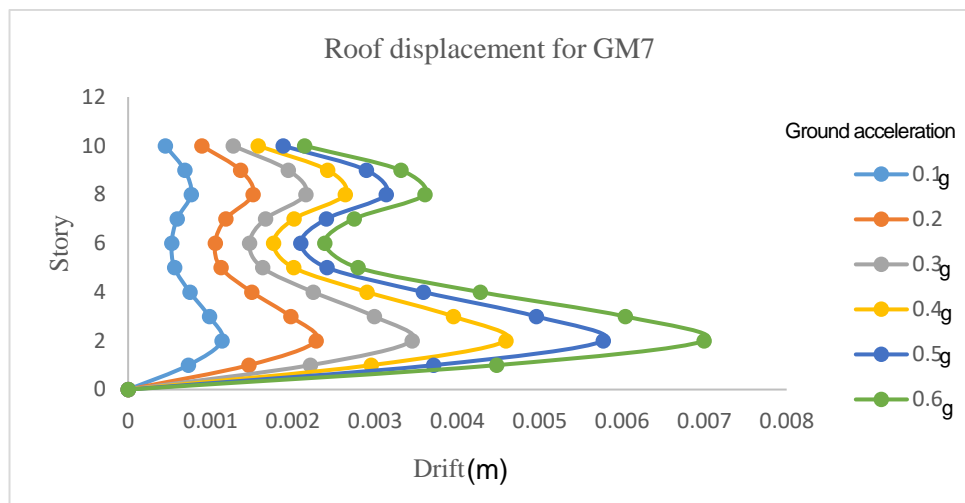
a)



b)

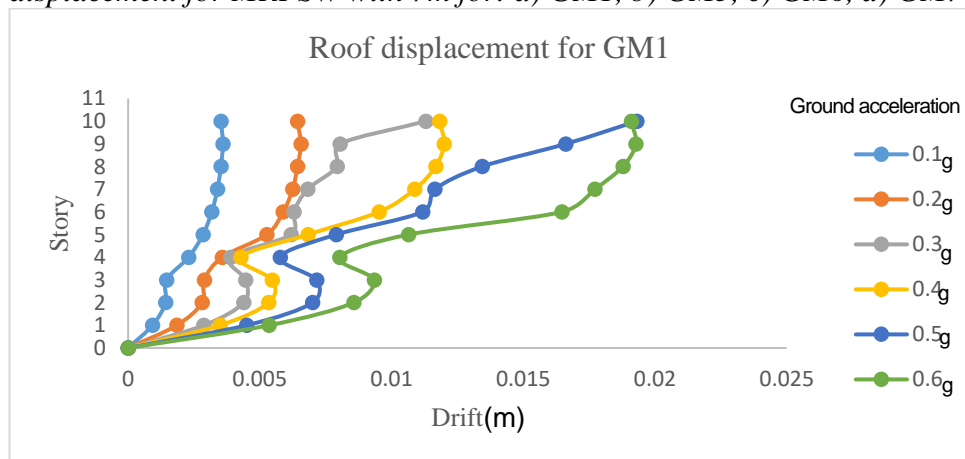


c)

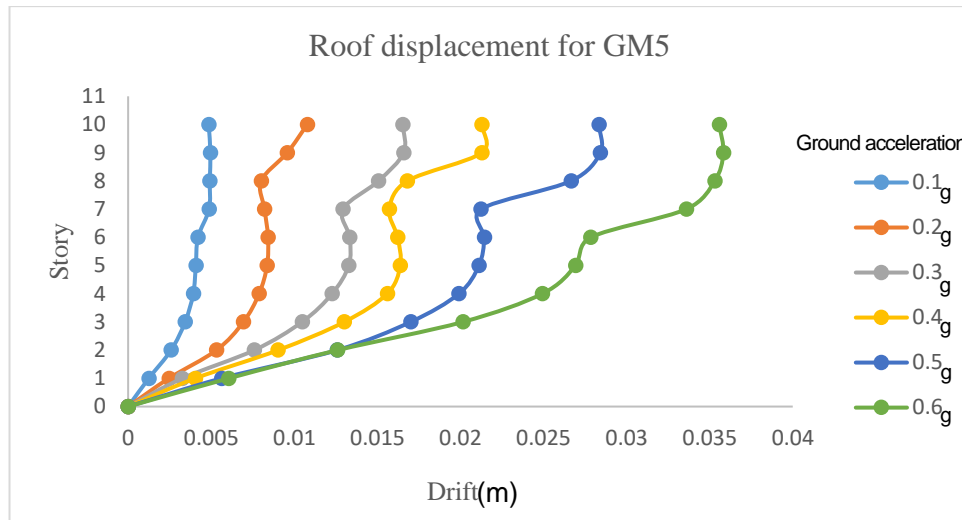


d)

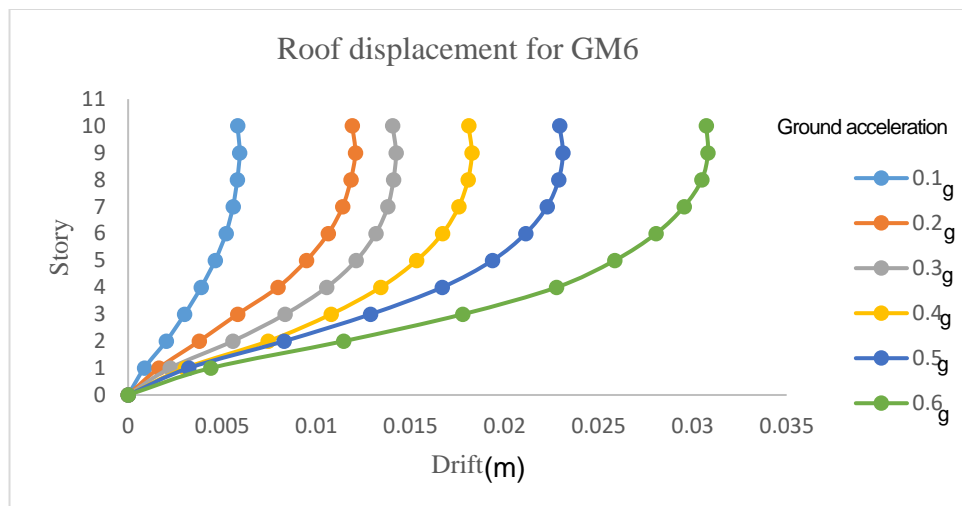
Figure B.9  
Roof displacement for MRFSW with 7m for: a) GM1, b) GM5, c) GM6, d) GM7



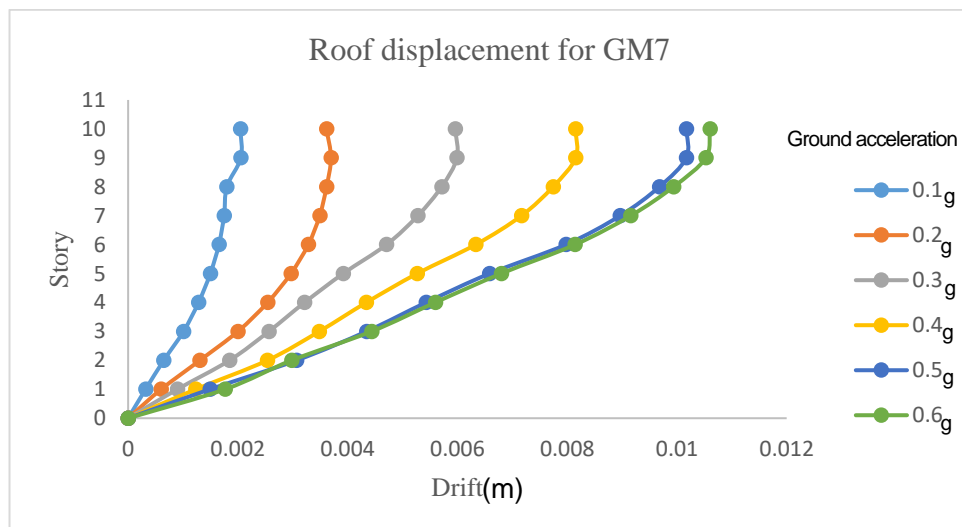
a)



b)



c)



d)

## Appendix C

### Uniform and concentrated loads from UBC-1997 code

1997 UNIFORM BUILDING CODE

TABLE 16-A

TABLE 16-A—UNIFORM AND CONCENTRATED LOADS

USE OR OCCUPANCY		UNIFORM LOAD <sup>1</sup> (psf)	CONCENTRATED LOAD (pounds)
Category	Description	× 0.0479 for kN/m <sup>2</sup>	× 0.004 48 for kN
1. Access floor systems	Office use	50	2,000 <sup>2</sup>
	Computer use	100	2,000 <sup>2</sup>
2. Armories		150	0
3. Assembly areas <sup>3</sup> and auditoriums and balconies therewith	Fixed seating areas	50	0
	Movable seating and other areas	100	0
	Stage areas and enclosed platforms	125	0
4. Cornices and marquees		60 <sup>4</sup>	0
5. Exit facilities <sup>5</sup>		100	0 <sup>6</sup>
6. Garages	General storage and/or repair	100	<sup>7</sup>
	Private or pleasure-type motor vehicle storage	50	<sup>7</sup>
7. Hospitals	Wards and rooms	40	1,000 <sup>2</sup>
8. Libraries	Reading rooms	60	1,000 <sup>2</sup>
	Stack rooms	125	1,500 <sup>2</sup>
9. Manufacturing	Light	75	2,000 <sup>2</sup>
	Heavy	125	3,000 <sup>2</sup>
10. Offices		50	2,000 <sup>2</sup>
11. Printing plants	Press rooms	150	2,500 <sup>2</sup>
	Composing and linotype rooms	100	2,000 <sup>2</sup>
12. Residential <sup>8</sup>	Basic floor area	40	0 <sup>6</sup>
	Exterior balconies	60 <sup>4</sup>	0
	Decks	40 <sup>4</sup>	0
	Storage	40	0
13. Restrooms <sup>9</sup>			
14. Reviewing stands, grandstands, bleachers, and folding and telescoping seating		100	0
15. Roof decks	Same as area served or for the type of occupancy accommodated		
16. Schools	Classrooms	40	1,000 <sup>2</sup>
17. Sidewalks and driveways	Public access	250	<sup>7</sup>
18. Storage	Light	125	
	Heavy	250	
19. Stores		100	3,000 <sup>2</sup>
20. Pedestrian bridges and walkways		100	

## Appendix D

### Similarity check report

<input type="button" value="Submit File"/>		Online Grading Report   <a href="#">Edit assignment settings</a>   <a href="#">Email non-submitters</a>						
<input type="checkbox"/>	AUTHOR	TITLE	SIMILARITY	GRADE	RESPONSE	FILE	PAPER ID	DATE
<input type="checkbox"/>	Hama Issa Moctar	Modified Full Thisis	9% <span style="color: green;">■</span>	--	--		2133241247	18-Jul-2023
<input type="checkbox"/>	Hama Issa Moctar	CHAPTER VI	0% <span style="color: blue;">■</span>	--	--		2133240502	18-Jul-2023
<input type="checkbox"/>	Hama Issa Moctar	CHAPTER V	0% <span style="color: blue;">■</span>	--	--		2133240061	18-Jul-2023
<input type="checkbox"/>	Hama Issa Moctar	CHAPTER IV	2% <span style="color: green;">■</span>	--	--		2133239690	18-Jul-2023
<input type="checkbox"/>	Hama Issa Moctar	CHAPTER III	4% <span style="color: green;">■</span>	--	--		2133239208	18-Jul-2023
<input type="checkbox"/>	Hama Issa Moctar	CHAPTER II	6% <span style="color: green;">■</span>	--	--		2133238779	18-Jul-2023
<input type="checkbox"/>	Hama Issa Moctar	CHAPTER I	1% <span style="color: green;">■</span>	--	--		2133237743	18-Jul-2023
<input type="checkbox"/>	Hama Issa Moctar	Abstract	0% <span style="color: blue;">■</span>	--	--		2133237308	18-Jul-2023

Prof. Dr. Kabir Sadeghi



## Ethical approval letter

February 2, 2023,  
Nicosia

YAKIN DOĞU ÜNİVERSİTESİ



NEAR EAST UNIVERSITY

**ETHICS EVALUATION**

Dear Hama Issa Moctar

Your application titled “Seismic performance risk analysis of moment resisting RC frame structure” has been evaluated by me (instead of the Scientific Research Ethics Committee) and granted approval. You can start your research on the conditions that you will abide by the information provided in your application.

This evaluation has been done by me because you have not to use a questionnaire and no need for data collection from the people, and your work will be based on analytical calculations and application of the software.

Sincerely yours

Prof. Kabir Sadeghi, Ph.D., P.E.

Head of Civil Engineering Department-Postgraduate Program

Faculty of Civil and Environmental Engineering

Near East University, Near East Boulevard, ZIP: 99138, Nicosia/TRNC, Mersin 10 - Turkey